Title

THEORETICAL AND EXPERIMENTAL ASPECTS OF THE ENERGY LOSS OF RELATIVISTIC HEAVILY IONIZING PARTICLES

Author

Ahlen, S.P.

Publication Date

1979-06-01

LBL-9353 c.2
Preprint

Lawrence Berkeley Laboratory
UNIVERSITY OF CALIFORNIA, BERKELEY, CA

Submitted to Review of Modern Physics

THEORETICAL AND EXPERIMENTAL ASPECTS OF THE ENERGY LOSS OF RELATIVISTIC HEAVILY IONIZING PARTICLES

Steven P. Ahlen

June 1979

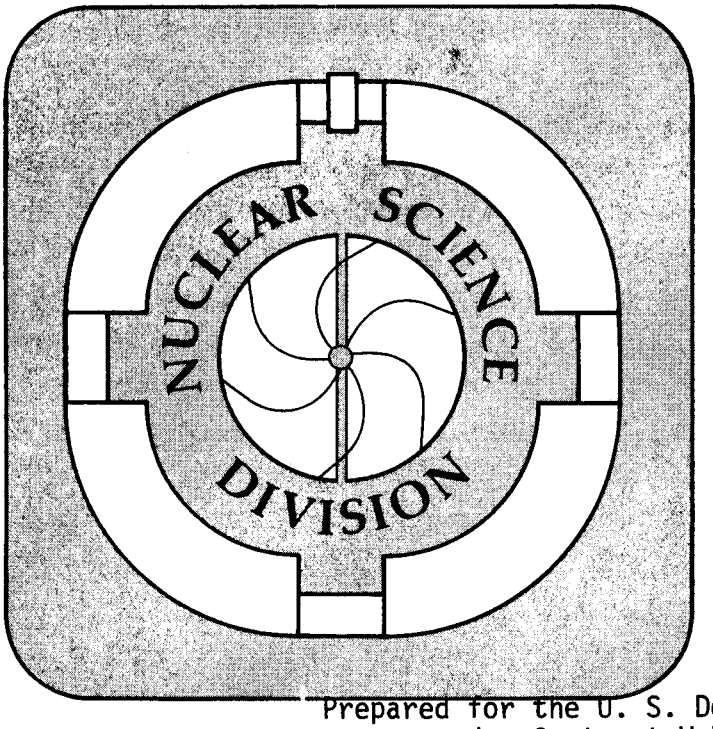

Prepared for the U. S. Department of Energy
under Contract W-7405-ENG-48

DISCLAIMER

TABLE OF CONTENTS

Theoretical and Experimental Aspects of the Energy Loss of Relativistic Heavily Ionizing Particles

Steven P. Ahlen[†]

Lawrence Berkeley Laboratory and Space Sciences Laboratory,
University of California, Berkeley, California 94720

We review the theory of the electromagnetic interactions between rapidly moving charged particles and the matter through which they pass. The emphasis will be on very massive electric ($-100 \leq Z_1 \leq 100$) and magnetic ($|g| = 137e$ and $137e/2$) particles moving with relativistic velocities ($\beta > 0.2$, $\gamma < 100$). Consideration will be given to both the stopping power of the projectile and to the response of the absorbing medium to the excitation caused by the projectile.

[†]Mailing Address: Department of Physics, University of California
Berkeley, California 94720

I. INTRODUCTION

Various aspects of the penetration of charged particles in matter have occupied the thoughts of some of the finest physicists of this century (Thomson, 1903; Rutherford, 1911; Bohr, 1913, 1915, 1948a; Bethe, 1930, 1932; Mott, 1931; Bloch, 1933a, 1933b; Fermi, 1940; and Landau, 1944). The theoretical and experimental investigations of this problem have, in fact, played a very important role in the development of modern physics. The distinction between large and small angle Coulomb scattering led to the discovery of the nuclear atom. The manner in which α and β rays were influenced by the matter through which they were allowed to pass enabled their identification as stripped helium nuclei and energetic electrons respectively and provided important information on nuclear transmutations. Particle track detectors (cloud chambers, bubble chambers, nuclear emulsions, etc.) have been directly responsible for the discovery of most of the known elementary particles, and charged particle detectors in general have been at least indirectly responsible for all of the experimental results in high, medium, and low energy physics. Research in astrophysics, nuclear physics, atomic physics, molecular physics, biophysics, and many other fields relies on experimental techniques utilizing high energy radiation and theoretical knowledge regarding the subsequent interaction between the radiation and matter. Many review articles have been written on the subject of charged particle penetration in matter. Among these are those by Bethe (1933), Livingston and Bethe (1937), Bohr (1948a), Bethe and Ashkin (1953), Allison and Warshaw (1953), Uehling (1954), Fano (1963), Northcliffe (1963), Bichsel (1968),

and Bichsel (1972). Many textbooks and monographs contain discussions of the stopping power and range of charged particles. Those by Rossi (1952), Landau and Lifshitz (1960), and Jackson (1975) are particularly recommended for an introduction to the subject.

Being based on either semi-classical physics or a first order quantal perturbation approach, most of the above works yield a result for the stopping power of a projectile[1] which is proportional to the square of the projectile charge and to a function of the projectile velocity.[2] In this Review we will be concerned primarily with the limitations of these results. Corrections to the stopping power formula due to higher order terms will be enumerated and evaluated. These corrections are most important at very low energies, at very high energies, and for very large charges. Severe complications are encountered in the low energy regime so we will devote most of our attention to heavily ionizing particles moving at large velocities. These particles will include familiar species, such as stripped heavy nuclei, and hypothetical particles, such as heavy anti-nuclei and magnetic monopoles.

In addition to being intrinsically interesting in itself with regard to atomic, molecular, and solid state physics, this problem is quite important due to its intimate connection with a variety of research and development programs in quite diverse fields. The development and application of high energy heavy ion accelerators[3] (see White et al., 1971; Grunder et al., 1971; and Grunder and Selph, 1977) is enhanced by a good understanding of how these fast heavy ions interact with the matter through which they pass. The correct interpretation

of the ultra-heavy cosmic ray data (Israel et al., 1975; Fowler et al., 1977; Shirk and Price, 1978), which is quite important in order to understand various high energy astrophysical phenomena, depends on accurate knowledge of both the manner in which very heavy nuclei slow in matter and the manner in which particle detectors respond to these nuclei. One of the most effective means of treating cancer is to apply high energy radiation to the tumor. For a very readable review of this technique, see Bleehen, 1972. Practical considerations have thus far limited the radiation sources so utilized to sources of x-rays and γ-rays. Fowler (1965) has emphasized the advantages of charged particle beams over electromagnetic radiation for cancer therapy. In addition to having a more favorable dose distribution for selective cell destruction, charged particles have more favorable RBE (relative biological effectiveness) and OER (oxygen enhancement ratio) characteristics than their electromagnetic counterparts. Tobias and Todd (1966) have advocated the use of fast heavy ions for cancer therapy. Experimental results along this line can be found in Todd et al. (1971) and Tobias et al. (1971). It is clearly desirable to achieve as good an understanding as possible of the interactions of fast heavy ions with matter in order to optimize these techniques. Another very exciting program which requires an understanding of heavy ion interactions with matter is that of heavy ion fusion (Bangerter et al., 1976). The use of intense, energetic, heavy ion beams to ignite deuterium pellets has attracted a great deal of attention in recent years (PT, 1978). There are still unresolved problems involving the interactions of these heavy ion beams with the pellets. Some of the theory summarized here should be useful in addressing these problems.

Finally, we should mention that successful searches for exotic, heavily ionizing particles[4] depend on a thorough knowledge of detector response and energy loss rates of the exotic particles. Price et al. (1978) summarize the status of the peculiar cosmic ray event which has variously been interpreted as being a magnetic monopole (Price et al., 1975) and a heavy anti-nucleus (Hagstrom, 1977). They point out the difficulties involved with the experiment and essentially conclude that the event was unlike anything yet observed, although they do not know what caused it. The early excitement caused by this event can be attributed to a lack of sufficient knowledge of the behavior of the nuclear track detectors employed in the experiment.[5] It will be impossible for us to delve too deeply into any of these particular problems involving heavily ionizing particles. However, we hope to present a sufficiently clear and concise summary of the state of our understanding of the electromagnetic interactions of these particles with matter so that the above mentioned problems can be easily attacked.

II. SCOPE

We will be solely concerned with the electromagnetic interactions of very massive, heavily ionizing particles with matter. For these particles, multiple Coulomb scattering is quite small and it is a very good approximation to assume that the particles travel in straight trajectories. Large angle Coulombic nuclear scattering is a rare occurrence and it will not be considered. The subject of multiple scattering is reviewed in detail by Scott (1963). We will also neglect the effects of inelastic nuclear collisions. Again, these occur relatively rarely and are only a serious consideration in the context of the range of high energy particles for which the probability of at least one inelastic collision in the total pathlength can approach unity.

With regard to the range of velocities to be considered, we will limit ourselves from below by the velocity at which shell corrections become important for singly charged particles ($\beta \sim 0.2$ depending on the atomic weight of the absorber) and from above by $\gamma \sim 100$ at which point radiative corrections and spin effects, among other things (to be discussed in detail at a later point), start becoming significant.

The conclusions reached in this Review can be meaningful only if the words negligible, insignificant, etc., are complemented by firm numerical estimates of the error incurred by the exclusion of the effects so qualified. We will, therefore, endeavor to make such estimates whenever the need should arise. The importance of the effects mentioned in the above paragraphs of this section will be so quantified in subsequent sections.

In the next section we will present key results from the first order treatment of energy loss. These will include a discussion of shell corrections, the density effect, energy loss and range straggling, and the mean ionization potential. In section IV we will systematically consider the various approximations involved with the results of section III and we will present algorithms for correcting for these approximations should they fail. We will consider the energy loss of magnetic monopoles in section V. General characteristics of energy deposition in matter will be described in section VI. In this section we will briefly discuss the response of various particle detectors to heavily ionizing charged particles. The notation to be employed in this work is given in Table II-1.

III. STOPPING POWER OF ELECTRICALLY CHARGED PARTICLES IN THE FIRST BORN APPROXIMATION

In this section we will summarize the status of stopping power theory from the point of view of semi-classical physics or a first order quantal perturbation treatment. In doing so we will draw heavily from the work of Fano (1963), Bichsel (1972), and Jackson (1975).

A. Statement of the Problem and the Nature of the Interaction Between Particle and Medium

A particle of mass M_1 and electric charge Z_1e penetrates a material composed of atoms of atomic number Z_2 and atomic mass $M_2 (M_2 = A_2$ amu).[6] The projectile interacts with the medium via the electromagnetic force with the electrons and protons and via the strong nuclear force with the nuclei of the absorber. For the moment we will completely disregard the nuclear force due to the vanishingly small ratio of the nuclear to atomic cross sections ($\sim 10^{-10}$). The projectile slows down by losing energy to the atoms of the absorbing medium. The collisions responsible for this energy transfer may be elastic (i.e., the atom is displaced but its internal state remains unchanged) or inelastic (the atom is both displaced and internally excited). In his classic paper on the theory of the passage of fast charged particles through matter, Bethe (1930) showed that for inelastic collisions the ratio of the atomic excitation energy to that due to atomic displacement is larger than M_2/m where m is the mass of the electron. It can also be shown, by using an expression for the elastic cross section obtained by Bethe (1930), that the ratio of energy lost in elastic collisions

to that lost in inelastic collisions is of the order mZ_2/M_2 (or smaller than this if realistic multi-electron wave functions are employed). Hence, less than 0.1% of the projectile energy goes into atomic displacement. In calculating the stopping power we merely need to sum over the various atomic excitation energies weighted by the cross section for excitation (by excitation, we mean to include ionization processes). Bethe (1930) showed that this cross section is independent of the mass of the atom provided $M_1 >> m$. Consequently, negligible error is incurred in the calculation of stopping power by assuming the target atom to be infinitely heavy.[7]

The problem is then successfully reduced to one involving the interaction between the projectile and atomic electrons bound to infinitely heavy nuclei. As we have seen, the interaction between the projectile and the target nucleus results in negligible energy loss. Large angle Coulomb scattering off of the nucleus is a rare but possible occurrence. In this sense it is in the same category as inelastic nuclear collisions. As such it will be considered in more detail in a later section. We will also consider at a later point the small angle multiple Coulomb scattering off of nuclei and electrons experienced by a projectile in passing through matter. For the heavy particles considered in this Review, this scattering is quite small and results in very small corrections (<1%) which need to be applied to energy loss and range calculations. For the duration of this section, we will assume that the incident particle trajectory is very closely approximated by a straight line.

In the following subsections we will briefly review the calculations of stopping power as performed by Bohr (1913), Bethe (1930), and Bloch (1933a). In addition to adding a sense of completeness to this Review, it is important to consider this earlier work so that we can isolate various features of these different treatments which are relevant to very recent experimental and theoretical work on stopping power.

B. The Bohr Solution

Bohr (1913, 1915) realized that binding effects are crucial for a proper treatment of energy loss. Earlier workers (Thomson, 1912 and Darwin, 1912) had treated the problem as one involving collisions with free electrons for which a maximum impact parameter was imposed in order to prevent the result from diverging. This divergence is due to the fact that the integrated Rutherford cross section is infinite. The limiting impact parameters chosen by the early workers were ad hoc in nature. Darwin (1912) assumed that the maximum impact parameter should correspond to the atomic radius, outside of which the force on a passing charged particle is zero and Thomson (1912) suggested that the limiting impact parameter should correspond to the mean inter-electronic spacing. Bohr (1913) pointed out the flaws with these selections and proposed that the effective maximum impact parameter should be that distance b for which the collision time $\sim b/v$ is comparable to the atomic orbital time = $1/\nu$. Bohr justified this proposition with a rigorous calculation which was based on the following assumption:

There exists an intermediate impact parameter b_1 (impact parameters

being defined to be the distance of closest approach to the assumed infinitely massive nucleus) for which collisions with $b > b_1$ can be treated as electromagnetic excitations of charged harmonic oscillators in a spatially uniform electric field due to the passing particle and for which collisions with $b < b_1$ can be treated as free electron scattering by the projectile in the center of momentum frame.

The justification of the assumption of an infinitely massive nucleus was provided by Darwin (1912). Needless to say, it was implicitly assumed that collisions could be legitimately characterized by impact parameters since the advent of wave mechanics was still ten years in the future. With the assumption that $M_1 >> m$ and expressed in the notation of this Review, Bohr obtained the following results:

$$\Delta E(b) = \frac{2Z_1^2 e^4}{mv^2 b^2} [\xi^2 K_1^2(\xi) + \xi^2 K_o^2(\xi)/\gamma^2], \quad b > b_1 \qquad \text{III.1}$$

where $\xi = (\omega b)/(\gamma v)$, ω is the circular frequency of the oscillator and $K_o(\xi)$, $K_1(\xi)$ are modified Bessel functions of order 0 and 1 respectively (see Abramowitz and Stegun, 1970). $\Delta E(b)$ is the energy lost to one electron, initially at rest at the nucleus. Eq. III.1 is obtained with the assumption that only the electric force acts on the electron and that the electron sees a spatially uniform field. This latter assumption is often referred to as the impulse approximation. Various integral representations of the Bessel functions establish the link between eq. III.1 and the electric force on the electron:

$$2aK_1(a) = \int_{-\infty}^{\infty} \frac{e^{iax}}{(1+x^2)^{3/2}}\, dx \qquad \text{III.2a}$$

$$2iaK_o(a) = \int_{-\infty}^{\infty} \frac{xe^{iax}}{(1+x^2)^{3/2}}\, dx \qquad \text{III.2b}$$

$$2K_o(a) = \int_{-\infty}^{\infty} \frac{e^{iax}}{(1+x^2)^{1/2}}\, dx \qquad \text{III.2c}$$

A derivation of eq. III.1 can be found in Jackson (1975).

For $b < b_1$, Bohr assumed that the electrons could be treated as if they were free with the result:

$$\Delta E(b) = \frac{2Z_1^2e^4}{mv^2} \frac{1}{b^2+(\frac{Z_1e^2}{mv^2\gamma})^2}, \quad b < b_1 \qquad \text{III.3}$$

Equation III.3 is valid classically for arbitrary impact parameters for $\beta << 1$ and is valid for $\beta \sim 1$ for those values of b for which the CM (which denotes the center of momentum frame for the electron-nucleus system) scattering angle is small. In any case, this expression reduces to the correct one for $b = 0$ as long as $m\gamma << M_1$.

The energy lost in collisions with $b > b_1$ is found by integrating eq. III.1 from $b = b_1$ to $b = \infty$ (Jackson, 1975):

$$S_{>b_1} = \frac{4\pi NZ_1^2e^4}{mv^2} [\xi_1 K_1(\xi_1)K_o(\xi_1) - \frac{\beta^2}{2} \xi_1^2(K_1^2(\xi_1) - K_o^2(\xi_1))] \qquad \text{III.4}$$

$S = - dE/dx$, N is the number of electrons per unit volume and $\xi_1 = \xi(b_1)$. Similarly, the close collision energy loss is found by integrating eq. III.3 from $b = 0$ to $b = b_1$:

$$S_{<b_1} = \frac{2\pi N Z_1^2 e^4}{mv^2} \ln\left[1 + \left(\frac{mv^2\gamma b_1}{Z_1 e^2}\right)^2\right] \qquad \text{III.5}$$

Equation III.4 diverges as $b_1 \to 0$ and eq. III.5 diverges as $b_1 \to \infty$, indicating the failure of the respective approximations in these limits. By choosing $b_1 \ll \gamma v/\omega$ (which corresponds to the adiabatically limited impact parameter beyond which energy transfer is inefficient; this is due to the exponential decay of the Bessel functions for large arguments) and $b_1 \gg |Z_1|e^2/(mv^2\gamma)$ (which may be thought of as the "size" of the scattering center) one obtains the total energy loss by adding eq. III.4 and eq. III.5:

$$S = \frac{4\pi N Z_1^2 e^4}{mv^2}\left[\ln\frac{1.123mv^3}{|Z_1|e^2\omega} - \ln(1-\beta^2) - \beta^2/2 + R_1\right] \qquad \text{III.6}$$

where:

$$R_1 = \frac{1}{2}\left(\frac{Z_1 e^2}{mv^2\gamma b_1}\right)^2 + \frac{1}{4}\xi_1^2\left[1-2\left(0.577+\ln\frac{\xi_1}{2}\right)^2/\gamma^2 - 2\beta^2\left(0.077+\ln\frac{\xi_1}{2}\right)\right] \qquad \text{III.7}$$

The small argument limits for the Bessel functions have been used. For $\hbar\omega = 100$ eV, $\beta = 0.5$, $b_{ad} \equiv \gamma v/\omega = 11$ Å and $b_s \equiv |Z_1|e^2/(mv^2\gamma)$ $= 9.7\ F|Z_1|$ where $1F = 10^{-13}$ cm. If $b_1 = 10^{-9}$ cm and $|Z_1| = 10$ then the remainder term, R_1, is of the order -7×10^{-4}. The other terms in the bracket add up to give a number of the order of 10 which means that R_1 provides a correction of -0.01%. This gives an indication of the insensitivity of the classical stopping power formula to the choice of b_1.

C. The Bethe, Fano Solution

Several attempts were made to incorporate quantum effects into the energy loss problem in the 1920's. Henderson (1922) applied the concept of discrete energy levels to the problem by limiting the possible energy transfer to an atom from below by the ionization potential. In this manner he obtained an expression for the stopping power which is roughly half of the correct one (Henderson essentially ignored the distant collision contribution to the energy loss which accounts for the other half). The original classical result of Bohr was recreated in a quantum mechanical treatment by Gaunt (1927), who treated the perturbation of an atom by the passage of a heavy charged particle moving with constant velocity. Bethe (1930) solved the problem quantum mechanically in the first Born approximation whereby the entire system (charged particle + atom) is considered within the framework of quantum theory. His result differed from that of Bohr (1913) and Gaunt (1927) and he attributed the deviation between his and Gaunt's results as being due to the failure of Gaunt to take the recoil of the heavy particle into account. However, it was shown by Mott (1931) that it is completely legitimate to do as Gaunt did, provided the electron mass is much less than that of the incident particle. Mott pointed out that Gaunt had made an error in one of his approximations which led to the erroneous result. The extension of the Bethe formula to relativistic velocities for the incident particle was accomplished by Bethe (1932) and Møller (1932).

In this subsection we will outline the Bethe-Born technique as reviewed by Fano (1963). Fano's article is highly recommended as a

lucid summary of the penetration of protons and mesons in matter.

The significant difference between Bethe's approach and that of Bohr is the use by Bethe of momentum transfer rather than impact parameter to characterize collisions. The principles of wave mechanics prohibit the formation of an infinitely localized wave packet for a particle with well defined momentum. For very close collisions the classical treatment, which presupposes the ability to use such wave packets, must break down. Hence, there exists a class of collisions for which a classical calculation is illegitimate. Bethe (1930) attacked the problem with the lowest order fully quantal approximation developed by Born (1926) and subsequently referred to as the Born approximation. This is essentially equivalent to Fermi's Golden Rule (see Merzbacher, 1970 or any textbook on quantum mechanics) whereby the transition rate per unit time from state $|s\rangle$ to state $|k\rangle$ under the action of a perturbation V_1 is:

$$\frac{dP}{dt} = \frac{2\pi}{\hbar}\left|\langle k|V_1|s\rangle + \sum_m \frac{\langle k|V_1|m\rangle\langle m|V_1|s\rangle}{E_s - E_m}\right|^2 \rho_f(E_s) \qquad \text{III.8}$$

E_s and E_m are the unperturbed energy eigenvalues for states $|s\rangle$ and $|m\rangle$ respectively and $\rho_f(E_s)$ is the energy density of final states evaluated at the initial energy. If $E_k \neq E_s$ $dP/dt = 0$ which must be regarded as an auxiliary condition to eq. III.8. It is important to realize that the matrix elements in eq. III.8 do not assure energy conservation.

In accord with the discussion of section III.A the target atom is assumed to be infinitely massive. If $\vec{p}(\vec{p}')$ denotes the initial (final) momentum of the projectile and if $|0\rangle(|n\rangle)$ denotes the initial

(final) atomic states, $|k\rangle$ and $|s\rangle$ are given by:

$$|k\rangle = V^{-\frac{1}{2}} \exp(i\vec{p}'\cdot\vec{R}/\hbar)|n\rangle \qquad \text{III.9a}$$

$$|s\rangle = V^{-\frac{1}{2}} \exp(i\vec{p}\cdot\vec{R}/\hbar)|0\rangle \qquad \text{III.9b}$$

V is the volume of a large box in which the system is placed and $\vec{R}$ is the position vector of the projectile. Note that we are neglecting internal degrees of freedom of the projectile (such as spin) in describing its quantum state. This is permissible due to the assumed large projectile mass. The perturbation V_1 is taken to be the interaction between the incident particle and the atomic electrons. The particle-nucleus interaction does not lead to atomic excitation and hence is neglected. V_1 is most conveniently expressed in the Coulomb gauge in which the interactions amongst a system of charged particles are given by the instantaneous Coulomb interactions plus the interactions of the particle currents with the transverse vector potential which describes the free photon field (see Sakurai, 1967). By quantizing the transverse vector potential one achieves a fully relativistic, quantum mechanical formalism. Sakurai (1967) gives the quantized vector potential:

$$\vec{A}(\vec{x}) = (4\pi/V)^{\frac{1}{2}} \sum_{\vec{k}\alpha} c\sqrt{\frac{\hbar}{2\omega}} \left[a_{\vec{k}\alpha}\hat{\varepsilon}^{\alpha}e^{i\vec{k}\cdot\vec{x}} + a^{\dagger}_{\vec{k}\alpha}\hat{\varepsilon}^{\alpha}e^{-i\vec{k}\cdot\vec{x}}\right] \qquad \text{III.10}$$

where $a_{\vec{k}\alpha}$ ($a^{\dagger}_{\vec{k}\alpha}$) is the annihilation (creation) operator for a photon with momentum $\hbar\vec{k}$ and linear polarization $\hat{\varepsilon}^{\alpha}$ ($\vec{k}\cdot\hat{\varepsilon}^{\alpha} = 0$ since $\vec{\nabla}\cdot\vec{A} = 0$ in the Coulomb gauge). The perturbation is:

$$V_1 = -\sum_{j=1}^{Z_2} \frac{Z_1 e^2}{|\vec{R}-\vec{r}_j|} - Z_1 e\vec{\alpha}\cdot\vec{A}(\vec{R}) + \sum_j e\vec{\alpha}_j\cdot\vec{A}(\vec{r}_j) \qquad \text{III.11}$$

where $\vec{R}$ and $\vec{r}_j$ are the coordinates of the projectile and the jth atomic electron respectively and $\vec{\alpha}$ and $\vec{\alpha}_j$ are the corresponding Dirac velocity operators. Since the Dirac formalism is utilized for the interaction, the spin and magnetic moment of the electrons are properly treated. By imposing the small scattering angle approximation Fano (1963) shows that the above considerations lead to the conclusion that the cross section for excitation to the atomic state $|n\rangle$ is, to lowest order in Z_1:

$$d\sigma_n = \frac{2\pi Z_1^2 e^4}{mv^2} Z_2 \left[\frac{|F_n(\vec{q})|^2}{Q^2(1+Q/2mc^2)^2} + \frac{|\vec{\beta}_t\cdot\vec{G}_n(\vec{q})|^2}{[Q(1+Q/2mc^2)-E_n^2/2mc^2]}\right](1+\frac{Q}{mc^2})\,dQ \qquad \text{III.12}$$

where $\vec{q} = \vec{p} - \vec{p}'$, $Q(1+Q/2mc^2) = q^2/2m$ (Q is the energy transferred to an unbound electron for momentum transfer $\vec{q}$) and

$$F_n(\vec{q}) = Z_2^{-\frac{1}{2}} \sum_j \langle n|e^{i\vec{q}\cdot\vec{r}_j/\hbar}|0\rangle\,, \qquad \text{III.13a}$$

$$\vec{G}_n(\vec{q}) = Z_2^{-\frac{1}{2}} \sum_j \langle n|\vec{\alpha}_j e^{i\vec{q}\cdot\vec{r}_j/\hbar}|0\rangle\,, \qquad \text{III.13b}$$

and $\vec{\beta}_t = \vec{\beta} - (\vec{\beta}\cdot\vec{q})\vec{q}/q^2$. The stopping power is given by:

$$S = N_a \sum_n \int E_n d\sigma_n \qquad \text{III.14}$$

where N_a is the number of atoms per unit volume.[8] It has been assumed here and above that the ground state energy, E_o, is zero. In order to evaluate eq. III.14 Fano (1963) considers three regions for Q:

1. For Q very small it is assumed that $\vec{q} \cdot \vec{r}_j/\hbar << 1$ so that eqs. III.13a,b reduce to dipole matrix elements. This is assumed valid for $Q < Q_1$.

2. For $Q_1 < Q < Q_2$ only the first term in eq. IV.12 is assumed to contribute. This is the so called longitudinal term which arises from the instantaneous Coulomb interaction (the other term is called the transverse term; it arises from the coupling to the photon field). Q_2 is assumed to be much less than mc^2.

3. For $Q > Q_2$ it is assumed that the electrons can be considered to be free.

By imposing the above approximations Fano (1963) obtains the relativistic Bethe formula:

$$S = \frac{4\pi N Z_1^{\,2} e^4}{mv^2}\left[\ell n \frac{2mv^2}{I} - \ell n(1-\beta^2) - \beta^2\right] \qquad \text{III.15}$$

where I is the logarithmic mean excitation potential per electron and is given by:

$$\ell n I = \sum_n f_n \ell n E_n \qquad \text{III.16}$$

where $f_n = \frac{2mE_n}{\hbar^2 Z_2}\left|\sum_j \langle n|x_j|0\rangle\right|^2$ is the dipole oscillator strength for the

nth energy level (a sum over degenerate states is implied). The Thomas-Reiche-Kuhn sum rule gives the result that $\Sigma f_n = 1$.

D. The Bloch Solution

The difference between eq. III.6 and eq. III.15[9] prompted Bloch (1933a) to investigate the manner in which the classical and quantum mechanical formulae complemented one another. He began by showing that Bohr's distant collision energy loss formula was completely valid quantum mechanically for a bound system provided that $\Delta E(b)$ was interpreted as a mean energy loss, summed over all possible atomic transitions. Bloch needed to impose the dipole approximation (i.e. $b >> r_o$, where r_o is a typical "radius" of the atom) to show this and in this approximation he noted that the higher order corrections to the energy loss at impact parameter b vanished for odd powers of Z_1 and that the Z_1^4 term was a factor $(Z_1e^2r_o)^2/(b\hbar v)^2$ smaller than the Z_1^2 term. This corresponds to a fractional correction of order $(Z_1\alpha/\beta)^2 \frac{r_o^2}{2b_1^2}/\ell n(\frac{r_o v}{b_1 v_o})$ (v_o is a typical atomic electron velocity) for energy loss in collisions with impact parameter greater than b_1.

Bloch then proceeded to analyze the close collisions quantum mechanically. He considered an intermediate impact parameter b_1, just as Bohr had done, inside of which the electrons could be treated as if they were free. However, unlike Bethe, Bloch did not assume that it was valid to consider the electrons to be representable by plane waves in the center of momentum frame. The confinement of the electrons to the interior of the cylinder of radius b_1 introduces transverse momentum components which interfere with one another under the influence of the scattering potential. This interference leads to a scattering

cross section which can be quite different from the quantum mechanical Coulomb cross section for plane wave scattering. Of course, for a very weak scattering center the confinement size b_1 should be large enough to permit the use of plane wave quantum mechanical results in which limit the Bethe formula should obtain. At the other extreme the effective size of the scattering center should be large enough to permit the construction of wave packets which scatter as classical objects in which case the Bohr formula should result. This in fact is the result that Bloch obtained. In the non-relativistic limit the Bloch formula is:

$$S = \frac{4\pi N Z_1^2 e^4}{mv^2}\left[\ell n \frac{2mv^2}{I} + \psi(1) - \mathrm{Re}\,\psi\left(1+i\frac{Z_1\alpha}{\beta}\right)\right] \qquad \text{III.17}$$

where $\psi(z)$ is the logarithmic derivative of $\Gamma(z)$, the gamma function.[10] In the limit of weak scattering, $|Z_1|\alpha/\beta \ll 1$ and the non-relativistic Bethe formula results. For $|Z_1|\alpha/\beta \gg 1$, $\mathrm{Re}\,\psi(1+iZ_1\alpha/\beta) \to \ell n(|Z_1|\alpha/\beta)$ and $\psi(1) = \ell n(1.123/2)$ and the non-relativistic Bohr formula results. Bloch's relativistic formula,

$$S = \frac{4\pi N Z_1^2 e^4}{mv^2}\left[\ell n \frac{2mv^2}{I} - \frac{1}{2}\ell n(1-\beta^2) - \beta^2/2 + \psi(1) - \mathrm{Re}\,\psi(1+iZ_1/\beta)\right] \qquad \text{III.18}$$

does not reduce to the Bethe formula as $Z_1\alpha/\beta \to 0$. This is due to the fact that Bloch used an incorrect close collision cross section for the scattering of free, infinitely broad electron wave packets by the projectile. It does not necessarily imply that the non-relativistic correction term, $\psi(1) - \mathrm{Re}\,\psi(1+iZ_1\alpha/\beta)$, is incorrect in the relativistic limit. There is, however, some question as to the

validity of this correction for relativistic velocities. One might expect to shed some light on this by considering the relevant parameter, $Z_1\alpha/\beta$, which determines the magnitude of the correction. $Z_1\alpha/\beta$ can be thought of as the ratio of the classical size of the scattering center, $Z_1e^2/(mv^2)$ to the deBroglie wavelength of the scattered electron in the CM frame. Each of these quantities would be reduced by a factor of order γ in a relativistic situation which would leave the ratio unchanged. Hence, one would expect the size of the correction to approach a constant value as $\beta \to 1$. By accurately measuring the range of 600 MeV/amu ^{56}Fe nuclei, Tarlé and Solarz (1978) have found that the results are slightly less than two standard deviations away from being consistent with the Bloch corrections, when other effects are taken into account. They find that the magnitude of the observed Bloch correction is less than that given by the non-relativistic term. On the other hand, Andersen et al. (1977) find that the observed Bloch correction is about one standard deviation larger than the calculated value. The former measurement was made at $\beta = 0.8$ and the latter at 0.08. Thus, it seems that further theoretical and experimental work is required to clarify the role of the Bloch correction.

E. Summary of the Bohr-Bethe-Bloch Results

In this sub-section we will summarize the assumptions and approximations ultilized by the various authors in the derivation of the above formulae and we will illustrate the effect of some of these assumptions by comparing the different results. Although it is difficult to pin down precisely the assumptions made by the various authors, particularly when one assumption may involve several effects,

the following list emphasizes the most crucial points:

1. The projectile velocity is much smaller than that of light in vacuum (Bohr, Bloch).[11]

2. The projectile velocity is much larger than characteristic orbital electron velocities (Bohr, Bethe, Bloch).

3. The absorber is a dilute, cold gas (Bohr, Bethe, Bloch).

4. $M_1 >> m\gamma$ (Bohr, Bethe, Bloch).

5. Internal structure of the projectile is neglected (Bohr, Bethe, Bloch).

6. Projectile bremsstrahlung is neglected (Bohr, Bethe, Bloch).

7. Radiative corrections are neglected (Bohr, Bethe, Bloch).

8. Close collisions are considered to be interactions of the projectile with free electrons (Bohr, Bethe, Bloch).

9. The close collisions take place between the projectile and electrons which follow classically well defined trajectories (Bohr).

10. The close collisions take place between a very heavy projectile and electrons which are characterized by plane wave initial states in the CM frame of reference (Bethe).[12]

11. Distant collisions are treated as first order dipole excitations (Bethe, Bloch).

12. Distant collisions are treated as classical energy transfer to a charged harmonic oscillator in the impulse approximation (Bohr).

13. The validity of the first Born approximation is assumed (Bethe).

14. The projectile charge state is constant (Bohr, Bethe, Bloch).

15. The spin of the electron is neglected in all types of collisions (Bohr, Bloch).

There is considerable overlap and interplay between the assumptions listed above. For example, it was shown by Bloch (1933a) that in the dipole approximation, there are no corrections to the stopping power which contain odd powers of Z_1. However, Hill and Merzbacher (1974) showed that for a harmonic oscillator model of the atom, there is a Z_1^3 correction term which arises from the quadrupole term which is considered as a perturbation. Bloch's conclusion was not incorrect but it did place more emphasis on the validity of the dipole approximation than was deserved. The lesson to be learned from this example is that one must be quite careful in correcting lowest order approximate results. All assumptions must be isolated and accounted for with equal weight. If this is done improperly the corrected version could be in greater error than the lowest order approximation. The stopping-power problem is particularly susceptible to this effect. One has distant and close collisions (as well as means of connecting the two) and one has large and small projectile velocity and charge. Many approximations are involved, some of which start breaking down at the same point. This hinders experimental clarification and one must rely to a considerable extent on very careful analysis of data.

Assumption 1 poses no particular difficulties since the Bethe theory is generally chosen as that which is most readily amenable to correction for failure of the above assumptions. Assumption 2 can be corrected for in the case of singly charged particles with the use of the semi-empirical shell corrections described in the following section. Failure of assumption 3 is taken into account by channeling theory and the density effect corrections described in sub-section III.G. Although

the density effect corrections are effectively performed to lowest order, one would not expect higher order terms to significantly affect the results. Assumptions 4 through 7 rely on the projectile moving with non-ultra-relativistic velocities. These will be discussed in some detail in sub-section IV.A. Assumptions 8 through 12 involve the coupling of the close to the distant collisions. These will be discussed in sub-section IV.C following the treatment in sub-section IV.B of higher order Born terms (assumption 13). Electron capture and loss processes (assumption 14) will be discussed in sub-section IV.D. Assumption 15 is essentially a consequence of assumption 1. Furthermore, neglect of the electron spin affects only the close collisions as evidenced by agreement of Bloch's relativistic distant collision stopping power result with that of Bethe.[13]

Aside from details associated with physical processes of only secondary importance, the most crucial assumptions are those involving the validity of the Born approximation and the validity of a classical description. It is these features which cause the main differences between the Bohr, Bethe and Bloch formulae. We now turn our attention to the quantitative comparison of these expressions.

To simplify notation we note that each of eqs. III.6, III.15 and III.18 can be written as:

$$S = (Z_1^2 \omega_p^2 e^2/v^2)L \qquad \text{III.19.}$$

where $\omega_p^2 = 4\pi Ne^2/m$ is the bulk plasma frequency and L is defined by eq. III.19 according to the particular stopping power formula which is chosen. The comparison of the models of Bohr, Bethe and Bloch is

simplified if we adopt as a standardized "atom," one which consists of a single harmonically bound electron. It can then be easily shown that $I = \hbar\omega$ where ω is the circular frequency of the electron. Then:

$$L_{BETHE} = \ell n \frac{2mv^2}{\hbar\omega} - \ell n\ (1-\beta^2) - \beta^2 \qquad \text{III.20a}$$

$$L_{BLOCH} = \ell n \frac{2mv^2}{\hbar\omega} - \frac{1}{2}\ell n(1-\beta^2) - \beta^2/2$$
$$+ \psi(1) - \text{Re}\ \psi(1+iZ_1\alpha/\beta) \qquad \text{III.20b}$$

$$L_{BOHR} = \ell n \frac{1.123mv^3}{|Z_1|e^2\omega} - \ell n(1-\beta^2) - \beta^2/2 \qquad \text{III.20c}$$

It is noted that the relativistic corrections are similar but not identical for the three models. Careful analysis shows that exactly one half of Bethe's relativistic correction is due to distant collisions and the other half is due to close collisions. Both Bloch and Bohr obtain distant collision relativistic corrections which agree with those of Bethe (namely $-\frac{1}{2}\ell n(1-\beta^2) - \beta^2/2$). Their close collision corrections are incorrect since incorrect physics involving these collisions was utilized. It should be noted that Bethe's close collision relativistic corrections are valid only within the first Born approximation. This confuses comparison with Bohr's and Bloch's calculation which are not restricted in applicability in an identical way with those of Bethe. For the moment then we neglect all relativistic corrections, noting only that they amount to about -7% at $\beta = 0.5$ in Bethe's model.

In Fig. III.1 we plot the non-relativistic forms of L_{BETHE}, L_{BLOCH} and L_{BOHR} as a function of $\ell n\beta$ for $\hbar\omega = 100$ eV and for $Z_1 = 1$,

10 and 92. Note that $L_{BLOCH} = L_{BETHE}$ for $Z_1 = 1$. Note also that for $Z_1 = 92$ L_{BLOCH} is nearly equal to L_{BOHR} from $\beta = 0.05$ to $\beta = 0.5$. For $Z_1 = 10$ $L_{BLOCH} \rightarrow L_{BETHE}$ as $\beta \rightarrow 0.5$ and $L_{BLOCH} \rightarrow L_{BOHR}$ as $\beta \rightarrow 0.05$. It is interesting and important to note that although $L_{BETHE} = L_{BOHR}$ at $\beta = 0.13$ for $Z_1 = 10$, they differ from L_{BLOCH} by 5%. This is indicative of the general situation in which a classical calculation yields a result which equals that of a first order quantal calculation. One may not on this basis conclude that either calculation is correct. Rather one is forced to conclude that they are both in error by the same amount. In each of the models considered L becomes negative for small values of β. This is clearly unphysical and indicates failure of each of the models at low velocities. We will discuss this feature in the next subsection in the context of Bethe's quantal treatment.

It is appropriate at this point to comment on the underlying physical principles which give rise to the differences between the various solutions as indicated in Fig. III.1. At the very heart of the matter is the distinction between quantal and classical physics.

The First Born Approximation is equivalent to any lowest order quantal perturbation approach. Bethe's theory utilized this approximation for all classes of collisions while Bloch's treatment required a first order approximation only for the distant collisions which were considered in the dipole approximation. The close collisions were treated (in the non-relativistic limit) by Bloch with the use of the exact asymptotic form of the scattering amplitude for Coulomb scattering with a suitable approximation of the structure of the electron wave packets in the CM frame imposed to allow for the finite lateral extent

of the projectile scattering center in this frame. It has been seen that in the limit $|Z_1|\alpha/\beta << 1$ the non-relativistic Bloch result approaches the non-relativistic Bethe result. This corresponds to the oft quoted regime of validity of the first Born approximation which is simply the limiting case of a very small perturbation compared to the unperturbed energies and forces. The opposite limit, $|Z_1|\alpha/\beta >> 1$, is the limit of very strong interactions and corresponds to the regime of validity for Bohr's result. Mott and Massey (1965) discuss the range of validity of the Born and classical approximations; for a classical treatment to hold there are two conditions: a) the orbit of the particle must be well defined in relation to other relevant distances and b) the angular deflection due to the collision must also be well defined. For unscreened Coulomb scattering, these two requirements determine the above criterion, namely $|Z_1|\alpha/\beta << 1$ (>>1) for Born approximation (classical approximation) validity. This is the condition which characterizes the appropriate approach to close collision energy loss. The distant collisions are more difficult to characterize due to the interference of the dipole with the Born approximation. However, since the treatment of the distant collisions by Bloch and by Bethe rely on essentially the same assumptions and since Bloch's distant collision result is identical to that of Bohr even up to relativistic corrections, we see that any differences between the three theories must involve the close and/or immediate collisions.

This contention is supported by the simple plausibility arguments given by several authors (Rossi, 1952 and Jackson, 1975) for construction of the Bethe formula from semi-classical considerations. The

usual trick is to proceed as Bohr did for $b > b_1$. For $b < b_1$, one recognizes that the exact result of Bohr can be obtained by setting b_1 equal to $(Z_1e^2)/(mv^2\gamma)$ and using only the "distant collision" energy loss. Physically, this amounts to cutting off the impact parameter at the value for which the kinematically limited energy transfer obtains with a simplified $1/b^2$ function for energy transfer. However, as the argument goes, if the deBroglie wavelength of the electron in the CM frame exceeds $(Z_1e^2)/(mv^2\gamma)$, it must be used in place of the classical minimum impact parameter because smearing of the wave packet of the electron eliminates energy transfer for the close collisions. Hence, if $Z_1\alpha/\beta < 1$, the quantal value of b_1 leads to Bethe's formula and if $Z_1\alpha/\beta > 1$, Bohr's result is obtained. These conditions are precisely the same as those given by the criteria for the validity of the first Born approximation and the classical approximation respectively. One must be careful not to attribute too much significance to the above argument. It is in fact little more than dimensional analysis where characteristic classical and quantal distances are inserted into $\ell n(b_{ad}/b_{min})$ where b_{ad} is the adiabatically limited impact parameter (see Lindhard, 1976). One should realize that there is actually no division of validity between the close and intermediate collisions as might be guessed from the simple plausibility argument. In fact, the derivation of the criterion for Born (classical) validity is independent of impact parameter and applies equally to intermediate and close collisions.

It is important to appreciate the importance of binding in assessing the validity of the different formulae. Mott and Massey (1965),

following Williams (1945), discuss the connection between the Bohr and Bethe theories by assuming free electron scattering. In terms of the scattering angle of an incident electron, they find that the stopping power is proportional to $\ell n(\theta_{max}/\theta_{min})$ with $\theta_{max} \sim 1$ and $\theta_{min} = \hbar/(mvb_{ad})$ for $\alpha/\beta << 1$ and $\theta_{min} = e^2/(mv^2 b_{ad})$ for $\alpha/\beta >> 1$. It seems then that the distinction between classical and quantal stopping power lies in the distant collisions, which correspond to small scattering angles. The apparent paradox is resolved when one realizes that $\theta_{min} = 0$. This is so since energy transfer is possible without scattering by means of having the atomic nucleus absorb any transverse momentum which is necessary. Thus a more careful analysis is actually required. The success of the above approach in obtaining the correct answers is again due to the usefulness of dimensional analyses.

It is amusing to consider yet one more way of obtaining the Bethe formula for stopping power. As will be described in more detail in sub-section III.G, Landau and Lifshitz (1960) calculate the distant collision energy loss by a semi-classical method where-in the wave vector $\vec{k}$ of the Fourier transforms of the classical fields is interpreted as the wave vector of an exchanged photon. By adding this to the close collision energy loss obtained with the use of the classical Rutherford cross section in terms of momentum transfer one may obtain the exact Bethe formula in the non-relativistic limit. Thus, the only quantum mechanics required has been the interpretation of small momentum transfer processes in electromagnetic interactions as being mediated by discrete, exchanged quanta. It is interesting to speculate

on the course of events had someone taken what was known in 1910 and added the notion of virtual photons to correctly derive the Bethe formula twenty years ahead of time. For very large values of Z_1, this treatment would break down due to the need to include multi-photon exchange processes, in which case the impact parameter approach of Bohr would be valid. Lest one become too enamored with the semi-classical physics embodied in the Landau approach, we should point out that it may merely be fortuitous that the correct answers are obtained due to the equality of the classical and quantal Coulomb scattering cross section. Indeed, it is clearly untenable to adopt the position that electrons follow well defined trajectories and that it is merely in a statistical observational sense that the uncertainty principle applies. Otherwise, the Bohr formula would be correct, which it is known not to be for $Z_1\alpha/\beta < 1$.

F. Low Velocities: Shell Corrections From the Bethe Theory

In the remainder of this section we will concentrate our attention on the first order quantal treatment of Bethe. Most of the experimental and theoretical work on stopping power has been confined to a regime where this theory is most appropriate. In section IV we will indicate how this theory must be modified in order to remain applicable in other regimes.

It was remarked in the previous subsection that L becomes negative at very low velocities. As Fano (1963) emphasizes, the validity of the Bethe formula relies on the assumption that the speed of the incident particle is much greater than that of the electrons bound to the absorbing medium. Only in this case can one cleanly separate low

momentum transfer collisions from intermediate momentum transfer collisions and in such a way apply the generalized sum rule first derived by Bethe (1930). In principle one can correctly calculate the stopping power within the framework of the first Born approximation without recourse to the generalized sum rule. The formal expression for this is given by:

$$L = \ell n \frac{2mv^2}{I} - \ell n(1-\beta^2) - \beta^2 - C/Z_2 \qquad \text{III.21}$$

C/Z_2 is referred to as the shell correction term. Bichsel (1972) indicates how the theoretical work of Walske (1952, 1956) and Bonderup (1967) are incorporated with experimental work in order to obtain a semi-empirical expression for C/Z_2 which is valid for $Z_1 = 1$. The fitting procedure described by Bichsel yields experimental values for I in addition to the shell corrections. Since higher order Born terms are probably included in C/Z_2, Bichsel cautions the reader that the shell corrections are only valid for particles with $Z_1 = 1$.
Figure III.2a is a reproduction of the results obtained by Bichsel (1972) for C/Z_2. In Fig. III.2b we reproduce the figure given by Fano (1963) for the shell corrections which were obtained by techniques similar to those employed by Bichsel (1972). In each of these figures the shell corrections are plotted as a function of proton kinetic energy. To apply them to other singly charged particles it is necessary to use that proton energy which corresponds to the same velocity of the other particle type under consideration.

A comparison of Fig. III.2a and Fig. III.2b reveals significant differences between the results of Fano and Bichsel. For example, at

a proton energy of 8 MeV in lead, the Fano shell correction is 0.30 and the Bichsel shell correction is 0.25. The difference between these two corrections amounts to a difference in stopping power of about 2%. Since this is roughly the magnitude of the error of stopping power measurements at these energies, such differences should be regarded as being a measure of the uncertainty of these semi-empirical estimates of the size of the shell corrections.

For the purpose of this Review, the shell corrections are intended to serve as a cushion to soften the transition into the complex low velocity region. For this reason we anticipate some of the discussion to appear in section IV regarding the extraction of the true shell corrections, apart form higher order Born terms. Andersen et al. (1977) have empirically determined the Z_1^3 and Z_1^4 corrections to the stopping power. They have used these measured corrections to separate the shell corrections from the higher order Born terms. In Fig. III.2c to 2f these corrections, (C/Z_2), are compared with those which include higher order corrections (C/Z_2') and those calculated by Bonderup (1967) $(C/Z_2)_{Th}$. Good agreement is obtained between (C/Z_2) and $(C/Z_2)_{Th}$. Note that (C/Z_2) becomes quite close to $(C/Z_2)'$ at large velocities (the difference amounts to less than 1% in stopping power above 5 MeV/amu). This is due to the small higher order corrections to proton stopping power at these velocities. Hence, if one adopts the reasonable point of view that the shell corrections can be looked upon as a purely velocity dependent contribution which corrects for the failure of the generalized sum rule, then one is in error by less than 1% in stopping power if he

uses the Fano or Bichsel shell corrections above 10 MeV/amu for any charge.

G. Condensed Matter Effects

1. Channeling

In all of the preceding discussion it has been tacitly assumed that the medium through which the charged particle passed was a very dilute gas. Only for such a situation is it legitimate to incoherently add the energy lost to individual atoms to obtain the total stopping power.[14] In condensed media one encounters several problems not present for gaseous absorbers. If, for example, the solid possesses symmetry with respect to spatial displacement (i.e. it is a crystal) one would not expect a priori that its stopping power relative to an impinging beam of charged particles would be independent of the crystal orientation. One might expect that any such orientation dependence would be negligible for absorbers of finite thickness and for beams with non-zero divergence. However, as was first predicted by Stark and Wendt (1912) and was first observed by Piercy et al. (1963) and Lutz and Sizmann (1963), charged particles which enter a crystal lattice at small angles relative to the crystal rows or planes undergo a set of correlated small angle scattering events which tend to force them to move down crystal "channels." Lindhard (1964) derived the following expression for the critical angle between the incident particle trajectory and the crystal axis for channeling:

$$\psi_c = C\left(\frac{2Z_1Z_2e^2}{Ed}\right)^{\frac{1}{2}} \qquad \text{III.22}$$

where C is a number between 1.5 and 2 and d is the interatomic spacing along the direction of the channel. As it stands, eq. III.22 is applicable for non-relativistic velocities. It is easily modified to be generally applicable by replacing E with $\frac{1}{2}pv$ (p is the momentum of the projectile; see Esbensen et al. 1977). If $\psi > \psi_c$ the penetration into the crystal is essentially the same as for a random medium. If we take C = 1.75 then:

$$\psi_c = (Z_1 Z_2/A_1)^{\frac{1}{2}} (a_o/d)^{\frac{1}{2}}/(1670\beta\gamma^{\frac{1}{2}}) \qquad \text{III.23}$$

where a_o is the Bohr radius. If we assume $Z_1/A_1 = 0.5$, then $\psi_c \sim 1°$ for $Z_2 = 79$ (gold) at $\beta = 0.1$. This is clearly a manageable alignment angle (i.e. one must be aware of the alignment conditions so that channeling can either be avoided or achieved, depending on the experimental goals.) At higher velocities it becomes much more difficult to meet the channeling criterion. For this reason and due to the absence of sufficiently thick crystals to match the penetration depth of high energy particles we will subsequently assume that solid absorbers are amorphous.[15] For a more complete treatment of charged particle penetration in crystals, including a discussion of channeled particle stopping power and how this differs from that in amorphous absorbers, the reader is referred to the review articles by Datz et al. (1967) and by Gemmell (1974). A discussion of relativistic channeling of positive and negative pions, kaons and protons is to be found in Esbensen et al. (1978).

2. The Density Effect

The neglect of the channeling effect is implicit in the Bohr formulation by the prescription:

$$S = N\int_0^\infty \Delta E(b)\, 2\pi b\, db \qquad \text{III.24}$$

and in the Bethe formulation by:

$$S = N_a \sum_n \int E_n \, d\sigma_n \qquad \text{III.14}$$

In each case, a thin slab of absorber of thickness dx is assumed to contain atoms distributed randomly across the slab. Another implicit assumption reflected by eq. III.14 and eq. III.24 is that the total energy lost is that given by an incoherent sum of energy lost to individual atoms (or molecules). If the absorber is a gas, the intermolecular separation is equal to 33 Å at STP (standard temperature and pressure: $T = 273^\circ$ K and $p = 1$ atm). For $\hbar\omega = 100$ eV the adiabatically limited impact parameter is equal to:[16]

$$b_{ad} = 20\ \beta\gamma \text{Å} \quad \text{for} \quad \hbar\omega = 100 \text{ eV} \ . \qquad \text{III.25}$$

For typical gases at energies less than those at extreme relativistic velocities, it is seen that at any given time the projectile is interacting with no more than one gas molecule. The incoherent sums eq. III.24 and eq. III.14 are thus valid for gases except at extreme relativistic velocities. For solids, the density is increased relative to gases by about a factor of 1000 so that the interatomic spacing is reduced by a factor of order 10. In this case it is no longer true that the projectile interacts only with one atom at a time. Nor is

it legitimate to think of the atoms as independent of each other. A correct theory would be based on eq. III.14 where the "atoms" would be considered to be aggregates of matter which were essentially complete in themselves, i.e. they don't interact strongly with the remainder of the absorbing medium. If this is done properly the dielectric screening of the macroscopic electric field, i.e. the longitudinal interaction, is automatically accounted for. Dielectric screening is, after all, nothing more than the effect of electrons interacting with each other in response to the electric field of the projectile. Another modification which is required in order to extend the Bethe theory of energy loss to condensed media involves the use of the quantized vector potential (eq. III.10) to describe the transverse interaction. Neamtan (1953) has pointed out that the strength of the interaction between the electrons of a medium and the photon field is characterized by the index of refraction $n = [\varepsilon(\omega)]^{\frac{1}{2}}$. If n is significantly different from unity it is no longer legitimate to think in terms of free photons propagating with the speed of light through the medium. Alternatively one must consider the propagation of combined electronic-electromagnetic excitations with the group velocity c/n through the medium. It is thus inappropriate to use eq. III.10 as a basis for the description of the transverse interaction.

Fano (1956a, 1956b, 1963) has discussed how the quantal theory of Bethe is to be modified to take into consideration the "density effect" discussed in the preceding paragraph. It is to be emphasized that Fano's theory treated the entire problem within the framework of quantum mechanics, without recourse to classical macroscopic electro-

dynamics as was the case with early treatments of the density effect by Swann (1938) and Fermi (1940). Crispin and Fowler (1970) have reviewed the theoretical and experimental aspects of the density effect in the ionization energy loss of fast charged particles in matter. They indicate the degree of equivalence between the quantal and classical techniques and conclude that, although the quantal approach is in principle capable of giving higher order corrections, the classical approach of Fermi (1940) as modified and refined by Sternheimer (1952, 1956, 1961), should be used as a "theoretical yardstick for comparison with experiment." The quantal approach will become more desirable as more detailed information on photo-ionization cross sections and form factors, which serve as input to the theory, become available. For these reasons we will henceforth consider the density effect from the classical macroscopic point of view. This should be satisfactory, at least in the regime of energies where consideration of the density effect can be thought of as giving rise to a correction to the stopping power, rather than being the dominant effect.

A very fine presentation of the classical density effect can be found in Landau and Lifshitz (1960). Their approach can be more properly called semi-classical in that distant collisions are considered from the point of view of classical macroscopic electrodynamics but are characterized by momentum transfer rather than impact parameter, as was done by Fermi and Sternheimer. This characterization is made possible by interpretation of the vector $\vec{k}$ which appears in the Fourier transforms of the classical fields as the wave vector of an exchanged photon. Landau and Lifshitz calculate the work done on the particle

by the electric field produced by this particle. This is the energy lost by the particle in distant collisions. Their result can be summarized by the expression:

$$S_{<q_o} = \frac{4\pi N Z_1^2 e^4}{mv^2} \left[\ell n \frac{\gamma\beta c q_o}{\Omega} - \beta^2/2 + \rho^2/(2\omega_p^2\gamma^2)\right] \qquad \text{III.26}$$

where $\hbar q_o$ is the maximum momentum transfer for which the above treatment is valid and $\rho = \omega(0)/i$ where $\omega(q)$ is defined by:

$$\omega^2(q)[\varepsilon(\omega(q)) - 1/\beta^2] = c^2q^2 \qquad \text{III.27}$$

where $\varepsilon(\omega)$ is the complex dielectric constant of the medium. The quantity Ω plays the role of the mean excitation frequency and is defined by:

$$\ell n\Omega = \frac{2}{\pi\omega_p^2} \int_0^\infty \omega \, \mathrm{Im}\left[-\frac{1}{\varepsilon(\omega)}\right] \ell n(\omega^2+\rho^2)^{\frac{1}{2}} \, d\omega \qquad \text{III.28}$$

In those cases for which there are two roots to eq. III.27 with $q = 0$, that value of $\omega(0)$ with the largest imaginary part is to be used in the definition $\rho = \omega(0)/i$. Hence, if $\beta^2 < 1/\varepsilon_o$ (where $\varepsilon_o = \varepsilon(0)$), $\rho = 0$ and if $\beta^2 > 1/\varepsilon_o$, ρ is defined by $\beta^2\varepsilon(i\rho) = 1$. For conductors $\varepsilon_o = \infty$ so that the latter value of ρ should always be used.

The close collision energy loss is just that from the Bethe theory (Fano, 1963)

$$S_{>q_o} = \frac{4\pi N Z_1^2 e^4}{mv^2} \left[\ell n \frac{2mv}{q_o} - \frac{1}{2}\ell n(1-\beta^2) - \frac{1}{2}\beta^2\right] \qquad \text{III.29}$$

By adding eq. III.26 to eq. III.29 one obtains the total energy loss:

$$S = \frac{4\pi N Z_1^2 e^4}{mv^2} \left[\ell n \frac{2mv^2}{I} - \ell n(1-\beta^2) - \beta^2 - \delta/2\right] \qquad \text{III.30}$$

where the mean ionization potential, I, and the density effect correction, δ, are given by:

$$\ell n I = \frac{2}{\pi\omega_p^2} \int_0^\infty \omega \, \mathrm{Im}\left[-\frac{1}{\varepsilon(\omega)}\right] \ell n \hbar\omega \, d\omega \qquad \text{III.31}$$

and

$$\delta = \frac{2}{\pi\omega_p^2} \left[\int_0^\infty \omega \, \mathrm{Im}\left[-\frac{1}{\varepsilon(\omega)}\right] \ell n\left(1 + \frac{\rho^2}{\omega^2}\right) d\omega - \frac{\pi}{2} \rho^2 (1-\beta^2)\right] \qquad \text{III.32}$$

For the case of a non-conducting absorbing medium, ε_o is finite and there is a sharp dividing velocity below which there is no density effect correction, namely $\beta_o = 1/\sqrt{\varepsilon_o}$. I is then just the experimentally measured mean ionization potential, if the measurements are done at velocities below β_o.[17] Sternheimer (1952, 1956) has expressed I and δ in terms of the oscillator strengths and energy levels of isolated atoms:

$$\ell n I = \sum_n f_n \, \ell n\left[\hbar\omega_n \left(1+\omega_p^2 f_n/\omega_n^2\right)^{\frac{1}{2}}\right] \qquad \text{III.33}$$

and

$$\delta = \sum_n f_n \, \ell n\left(1+\rho^2/\omega_n^2\right) - (1-\beta^2) \, \rho^2/\omega_p^2 \qquad \text{III.34}$$

Note that eq. III.33 does not agree with that from the Bethe theory (eq. III.16), except in the limit $\omega_p \to 0$ as one would have for a gas. There is a low velocity density effect which is caused by the dielectric screening of the longitudinal interaction which reduces the stopping power by a small but finite amount.

By expressing ρ in terms of atomic properties, namely:

$$1/\beta^2 - 1 = \sum_n f_n \omega_p^2/(\omega_n^2+\rho^2) \qquad \text{III.35}$$

Sternheimer (1952, 1956, 1966, 1967) has calculated δ for a number of substances by incorporating optical measurements of f_n, ω_n and experimental determinations of I in a semi-empirical fit. Sternheimer (1952, 1956) used values of I which differ from the presently accepted values (which will be discussed in subsection III.H). For this reason, and in order to extend the calculation of the density effect to substances not previously considered, Sternheimer and Peierls (1971) obtained a general expression for the density effect based on updated information regarding f_n, ω_n and I. The functional form for δ originally proposed by Sternheimer (1952) is still used and is given by:

$$\delta = \begin{cases} 0 & X < X_o \qquad \text{III.36a} \\ 4.606\,X + C + a(X_1-X)^m & X_o < X < X_1 \qquad \text{III.36b} \\ 4.606\,X + C & X_1 < X \qquad \text{III.36c} \end{cases}$$

where

$$X = \log_{10}(\beta\gamma) \qquad \text{III.37}$$

The values for C, a, X_o, X_1 and m to be used are given in Table III.1. The maximum error in stopping power is claimed to be ±2% by Sternheimer and Peierls (1971) while the average error is less than ±1% in stopping power. In Fig. III.3a,b we plot δ as a function of $\log_{10}(\beta\gamma)$ for various solids, liquids and gases, as obtained with the parameters from Table III.1. Table III.2 contains a list of plasma energies for several kinds of substances which were used in computing values for Fig. III.3. The values for I which were used in these computations were

those given by Barkas and Berger (1967). A more complete discussion of these selections follows in subsection III.H.

H. The Mean Ionization Potential I

The central parameter to stopping power theory in the first Born approximation is I, the mean ionization potential. Neglect of the density effect leads to a definition of I which depends only on atomic (or molecular) properties as indicated by eq. III.16. We have seen that inclusion of the density effect in stopping power theory yields an expression for I which depends on the physical state of the absorbing medium (eq. III.33). Since measurements of I are for the most part done with solid absorbers, comparison with theoretical values tends to be clouded by this physical state or atomic aggregation effect. We will delay this comparison until we first separately discuss the experimental and theoretical determinations of I.

1. Experimental Determinations of I

There are several ways in which I can be determined experimentally:

a. One can directly measure the energy lost in thin absorbers by measuring initial and final energies with some configuration of electromagnetic fields. One then requires that:

$$S = \frac{4\pi N Z_1^{\,2} e^4}{mv^2} \left[\ell n \frac{2mc^2\beta^2\gamma^2}{I} - \beta^2 - C/Z_2 - \delta/2 \right] \qquad \text{III.38}$$

Since S is related to the measured value of ΔE in a manner which depends on the thickness of the absorber and on the velocity and charge of the projectile[18] one can measure the

quantity $\ell n\ I + C/Z_2$, provided $\log_{10}(\beta\gamma) < X_o$ so that $\delta = 0$. This velocity is at least that of an 820 MeV proton for all solids and gases (see Table III.1). All of the key experiments related to the determination of I utilized particles with energies less than that at which the density effect "turns on."[19]

b. One measures energy lost by calorimetric techniques (Andersen et al. 1966). Subsequent analysis proceeds as in (a) above.

c. One measures relative stopping powers by determining the amount of matter which causes the same amount of slowing as in a reference absorber.

d. One measures ranges at different energies. I is found from the shape of the range-energy curve or from direct integration of the stopping power formula.

Recommended values of I which are based on experiments such as those above and in Table III.3 can be found in NCRP (1961), Fano (1963), Bichsel (1968), Turner et al. (1970), Bichsel (1972), and Andersen and Ziegler (1977). These values are given in Table III.4. Several comments regarding these values are in order. The remarkable agreement of the various sources on the value of I for aluminum (the average of the 6 values from Table III.4 is 164 ± 1 eV) was achieved by neglecting the early result of 150 eV obtained by Mather and Segrè (1951) on the basis of range measurements of 340 MeV protons. The discrepancy between this measurement and those obtained at low energies was

attributed by Barkas and von Friesen (1961) to an improper deconvolution of the Bragg ionization curve obtained by Mather and Segrè (1951). This explanation was convincingly verified by Zrelov et al. (1974) who went to great pains to include every correction in the deconvolution of their Bragg curve (in most respects this experiment, which utilized 660 MeV protons, was quite similar to that performed by Mather and Segrè). In so doing they obtained a value of I for copper of 320 ± 4 eV which agrees very well with the average value of 317 ± 2 eV from Table III.4. Hence the evidence is quite strong for the conclusion that I is independent of energy, as it must be from the Bethe theory.

It is important to note that the experimental values for I should be independent of whether or not higher order corrections are included in the stopping-power formula. This is so because all velocity dependence (and hence dependence on higher order Born corrections) is included in the shell corrections. Of course, proper evaluation of the shell corrections requires some knowledge of higher order corrections. This will be discussed in more detail in section IV.

2. Theoretical Determinations of I

Bethe (1930) was able to calculate a value of I for atomic hydrogen with the use of the exact hydrogenic wave functions. Of course his results only applied to a gas of atomic hydrogen, a situation not encountered in the laboratory. In any case Bethe obtained that I_H = 15.0 eV. Bethe (1930) attempted to extend his caluclations to heavier atoms through the use of hydrogen-like

wave functions but met with little success. He overestimated the stopping power in gold by about 100%. Bloch (1933b) used the Thomas-Fermi model for atoms to show that I should be proportional to Z_2. This is in fact a good approximation for $Z_2 > 20$ which corresponds to the domain of applicability of the Thomas-Fermi model. Ball et al. (1973) have obtained Bloch's proportionality constant and have found that $I/Z_2 = 4.95$ eV in the Thomas-Fermi model. This is too small by about a factor of 2 to account for the data in Table III.4 and hence rigorous application of the Thomas-Fermi model cannot be accepted as corresponding to reality.[20]

Dehmer et al. (1975) summarize the status of calculations[21] of various moments of dipole oscillator-strength distributions for isolated atoms with $2 \leq Z_2 \leq 18$. Included in these calculations are those for I. Generally speaking, one can divide these calculations into rigorous ones utilizing realistic atomic wave functions and based on eq. III.16 and into those based on the local plasma model of Lindhard and Scharff (1953) as performed by Chu and Powers (1972).

In Fig. III.4 we plot a variation of Fig. 9 from Dehmer et al. (1975). We show the results of the local plasma approximation calculations of Chu and Powers (1972) as open circles. The results of the accurate calculations performed by Dehmer et al. are displayed as solid circles and the mean value of all the accurate calculations summarized by Dehmer et al. are displayed as dots with error bars representing a standard deviation for the mean value. Experimental data have been plotted as solid squares.

These have been obtained by averaging the values of Table III.4 as follows: 1) For solids and liquids we average the tabulated values with equal weight to obtain: I(Li) = 40.0 eV, I(Be) = 63.9 eV, I(C) = 79.0 eV, I(N) = 85.1 eV, I(O) = 98.3 eV, I(Al) = 164 eV, I(Si) = 169.3 eV, I(Cl) = 173 eV; 2) For rare gases we average the tabulated values with equal weight to obtain: I(He) = 42.3 eV, I(Ne) = 133.3 eV, I(Ar) = 188 eV. In all cases the error of the mean is smaller than the solid square.

It can be seen from Fig. III.4 that the shapes of the results of the two types of calculations as a function of Z_2 are quite similar but are offset by a nearly constant amount. Inokuti (1978) suggests that this difference may involve the parameter γ introduced by Lindhard and Scharff (1953) to relate the excitation energy with the local plasma energy via $E = \gamma\hbar\omega_p(r)$. $\omega_p(r)$ is not the same as the bulk plasma frequency we have been using; it is the local plasma frequency of the atom. Intuitive arguments advanced by Lindhard and Scharff suggest that $\gamma = \sqrt{2}$. However, other choices cannot be ruled out.

The general shape of I/Z_2 can be seen to be roughly constant, in qualitative agreement with the Bloch (1933b) theory, modulated by a periodic dependence on Z_2 which is correlated with atomic shell structure. Increased binding for closed shell atoms seems to cause an enhanced value for I/Z_2. There is rather remarkable agreement between those values for I/Z_2 obtained from accurate calculations and from experiments for those cases for which such a comparison is justified, namely for the rare gases. This obser-

vation strengthens the conclusion that the differences between measured value of I for solids and the calculated values for the corresponding atoms represent a real effect, which will now be discussed in the context of the Bragg rule and the low velocity density effect.

3. Suggested Values of I for Gases, Liquids, Solids and Compounds: Bragg's Rule and the Low Velocity Density Effect

Starting with Bragg and Kleeman (1905) it has almost universally been assumed in any application of stopping power theory that chemical and atomic aggregation phenomena affect stopping-power to a very limited extent. This is embodied in the Bragg rule for the evaluation of the mean ionization potential:

$$N \ln I = N_1 \ln I_1 + N_2 \ln I_2 + \ldots \qquad \text{III.39}$$

where N_i is the number density of electrons associated with element i and I_i is the atomic mean ionization potential per electron for that element. The implication of eq. III.39 is that the stopping power in a compound is the sum of the stopping powers of the individual elements.

It is not obvious that Bragg's rule should work at all. When several atoms combine to form a molecule, the energy levels of the valence electrons can change considerably. As an example recall that Bethe calculated that $I(H) = 15.0$ eV.[22] Platzman (1952) has calculated I for molecular hydrogen and has obtained $I(H_2) = 19$ eV.[23] This result, which is corroborated by experimental measurements of H_2 gas (averaging these values from

Table III.4 yields $I(H_2)$ = 18.5 eV), is not surprising in view of the fact that the bond dissociation energy for the hydrogen molecule is 4.52 eV (CRC, 1968). The effect is not so easily seen by comparing $I(N_2)$ and $I(O_2)$ with the corresponding theoretical values I(N) and I(O) from Fig. III.4. The experimental values plotted there are for liquid nitrogen and oxygen. $I(O_2)$ = 99.6 eV from the averaged value for oxygen gas from Table III.4. The value $I(N_2)$ = 87 eV seems to be inconsistent with the fairly well established value of I(Air) = 85 eV. By accepting this latter value we obtain $I(N_2)$ = 80 eV. Dehmer et al. (1975) refer to experimental works which give $I(O_2)$ = 101 eV and 93 eV and $I(N_2)$ = 90 eV and 78 eV. The smaller values are from work by Hanke and Bichsel (1975) on N_2 and O_2. Dehmer et al. (1975) obtain the theoretical values I(N) = 77 eV and I(O) = 82 eV for atomic nitrogen and oxygen respectively. Other theoretical treatments quoted in this reference yield I(N) = 77 eV, 82 eV and I(O) = 99 eV. Treating these measurements and calculations with equal weight we obtain $I(N_2)$ = 83 ± 4 eV, $I(O_2)$ = 98 ± 3 eV and I(N) = 79 ± 2 eV, I(O) = 91 ± 9 eV. Although it is tempting to ascribe these values to binding effects, the measurements and calculations are not accurate enough to convincingly demonstrate this. Indeed, the molecular dissociation energies for N_2 (9.84 eV) and O_2 (5.16 eV) are small enough to be masked by the experimental and theoretical fluctuations.

It seems clear from these observations that chemical binding does affect the mean ionization potential but that the effect

decreases rapidly with increasing atomic charge. This conclusion is consistent with the observations of Thompson (1952), who compared the stopping power of 270 MeV protons in liquid hydrogen, nitrogen and oxygen and in solid carbon with that in condensed compounds containing these elements. Thompson observed that the largest discrepancies from Bragg's law involved hydrogen and were of the order of 2% in stopping power. The deviations were negligible for chlorine (and presumably for heavier elements). Compounds containing carbon, nitrogen and oxygen obeyed Bragg's law to within ~1% in stopping power. For the proton energy utilized by Thompson, a difference of stopping power of 1% in C, N, O corresponds to a difference in I of the order of 10 eV. Similarly a difference of 2% in H corresponds to a difference in I of 4 eV. These energies are comparable in size to those discussed in the preceding paragraph. The increased validity of Bragg's law with increasing Z_2 relies on the increased dependence of I on inner shell electrons which are insensitive to chemical effects. The NCRP (1961) data in Table III.4 on elements from different chemical bond configurations are based on those from Thompson's thesis. They have been renormalized to agree with I(Al) = 164 eV.

Dehmer et al. (1975) interpret the good agreement of their calculations with observations of I for N_2 and O_2 gases as indicating that the larger discrepancy between theoretical values of I and those observed in solids is due to an atomic aggregation effect. Sternheimer (1953b) calculates the ratio I(gas)/I(condensed) based on his low velocity density effect calculations. Brandt

(1956) finds I(gas)/I(condensed) due to the rearrangement of valence electrons in the condensed phase. These ratios are given in Table III.5 along with the "observed" ratio, using the accurate calculations quoted by Dehmer et al. (1975) as a guide to a measure of I(gas). One would supposedly multiply Sternheimer's results by Brandt's to obtain the total effect. This is clearly too small to account for the Dehmer et al. ratios.

Deviations from Bragg's rule should be more apparent at low energies for which the logarithmic term in the Bethe formula becomes a sensitive function of I. This feature has been capitalized on in many recent experiments. Chan et al. (1977) examined the stopping power of low energy He ions (0.06 - 0.5 MeV/amu) in saturated alcohols and ethers in the gas phase. They found that Bragg's rule holds to within 1% in stopping power for single bonds at all energies. This was not the case for double bonds. The stopping power for double bonded oxygen was found to be 6% higher than that expected from application of Bragg's rule to single bond data at 0.5 MeV/amu. Lodhi and Powers (1974) performed a similar experiment with C-H, C-F and C-H-F, C-Br-F compounds. They found that the stopping power of hydrogen compounds was larger than that expected on the basis of experimental data for H_2.

Baglin and Ziegler (1974) tested Bragg's rule in solid compounds with 0.5 MeV/amu He nuclei and found no breakdown within the 2% experimental uncertainty of measurements of stopping power. Langley and Blewer (1976) have tested Bragg's rule in erbium and

erbium oxide with 0.1 - 0.6 MeV/amu He nuclei and protons of the same range of velocities. They observe slight deviations from Bragg's rule below 2 MeV but none at the 1% level above 2 MeV.

Feng et al. (1974) have used Mg, Al, Si, Fe and their oxides to test the Bragg rule with 0.25 - 0.5 MeV/amu He nuclei. They observe no deviations from Bragg's rule at the 2% level. By choosing absolute stopping cross sections from other work, these authors conclude that the stopping power of solid oxygen is from 6 - 22% smaller than would be expected from gas phase stopping power measurements. They conclude that this is a physical state effect which consists of the two separate effects of the sort considered by Sternheimer (1953b) and Brandt (1956).

All of these low energy experiments are consistent in quality with what one would expect on the basis of Thompson's high energy experiments. Detailed quantitative agreement between theory and experiment with regard to deviations from the Bragg rule and to atomic aggregation effects, be they predominantly due to polarization effects (low velocity density effect) or valence electron rearrangements, has not yet been achieved. It seems safe to conclude that experimental determination of I is sufficiently accurate to ensure accurate calculation of stopping power for heavy singly charged particles in the regime between 10 and 1000 MeV/amu. The error in stopping power should be less than 1%.

In Fig. III.5 we plot the data of Table III.4 (excluding those of Andersen and Ziegler) along with two semi-empirical functions which have been advocated for use in calculating I.

Sternheimer (1963) suggests the use of the following formula for the adjusted mean ionization potential I_{adj}:

$$I_{adj}/Z_2 = \begin{cases} 12 + 7/Z_2 \text{ eV}, & Z_2 < 13 \\ 9.76 + 58.8\ Z_2^{-1.19} \text{ eV}, & Z_2 > 13 \end{cases} \qquad \text{III.40}$$

where I_{adj} is defined by:

$$\ln I_{adj} = \ln I + C/Z_2(\beta=1) \qquad \text{III.41}$$

I_{adj} is so defined to avoid the necessity of using the large velocity limit of the shell corrections. I_{adj} differs from I significantly only for very large values of Z_2.

Dalton and Turner (1968) have suggested that the expression:

$$I = \begin{cases} 11.2 + 11.7\ Z_2 \text{ eV}, & Z_2 \lesssim 13 \\ 52.8 + 8.71\ Z_2 \text{ eV}, & Z_2 > 13 \end{cases} \qquad \text{III.42}$$

be used to evaluate I.

The large scatter of experimental points for $Z_2 < 10$ is due primarily to physical and chemical variations rather than experimental error. This emphasizes the fact that it is not legitimate to quote a value of I for such elements. It is crucial to specify whether the element is in a compound or not and to specify if it is in a solid, liquid or gas phase. The scatter of the large Z_2 data is a measure of the experimental error in this regime.

We feel that there are no significant systematic trends present in the 6 sets of recommended I values of Table III.4. For this reason we recommend use of averaged values. We also

would place more emphasis on the unspecified I values of nitrogen than on Fano's molecular value of 88 eV. These give an average value of 82 eV which is consistent with the established value for air, namely 85 eV. Similarly we treat the unspecified values of I for O_2 on an equal basis as the gas values. In Table III.6 we present our recommended values and the corresponding values for I and I_{adj} as given by eq. III.40 and eq. III.42 respectively. The quoted errors for the recommended values are equal to the standard deviation for the mean value of I obtained from the author to author averaging procedure.

In Fig. III.6 we plot the fractional error in stopping power, $|\Delta S/S|$, as a function of fractional error in the mean ionization potential, $|\Delta I/I|$, for various values of I and β. We use the Bethe formula with Bichsel's shell corrections (Fig. III.2a). The energies are small enough so that the density effect corrections are equal to zero.

I. Distributions for Energy Lost in Absorbers: Landau, Vavilov, Bohr and Tschalär Distributions

The entirety of our preceding discussion has involved average values of the stopping power. This leads to no confusion if one is dealing with a regime of projectile charge and velocity and absorber thickness for which the distribution of energy lost in the absorber is Gaussianly distributed, as one might expect would be the case on the basis of the central limit theorem. This theorem states that the probability density function of the sum of a set of commonly distributed random variables approaches a Gaussian distribution in the

limit of an infinite number of random variables. See Feller (1968) for a rigorous discussion of this very important theorem. If we identify our random variable as being the energy lost in a very thin slab of an absorber, then the sum of the energies lost in the complete set of slabs which constitutes an absorber of finite thickness should be determined by a Gaussian distribution, provided the absorber is thick enough to ensure the validity of the central limit theorem.

As is always the case for application of the central limit theorem to a specific problem, it is difficult to estimate how large the number of random variables (in this case, the thickness of an absorber for a given projectile charge and velocity) should be before one can be assured that the probability density fucntion is reasonably approximated by a Gaussian function. Bohr (1915) considered the problem by assuming the absorber to be thick enough so that this criterion is actually satisfied. He then obtained the standard deviation of the resulting distribution by adding in quadrature the standard deviations of the distributions of the thin slabs. The central limit theorem does not require the thin slab distributions to be Gaussian to validate this prescription. This can be written as:

$$\sigma^2 = x \int_{w_{min}}^{w_{max}} \frac{dn}{dwdx} w^2 dw \qquad \text{III.43}$$

where it has been assumed that the projectile velocity is constant throughout the absorber. $\frac{dn}{dwdx} dw$ is the number of collision events per unit pathlength which result in an energy loss between w and w + dw. Bohr assumed that the collision spectrum could be approxi-

mated by the free electron spectrum which is given by a suitable transposition of the Rutherford cross section:

$$\left(\frac{dn}{dwdx}\right)_R = \frac{2\pi N Z_1^2 e^4}{mv^2 w^2} \quad . \qquad \text{III.44}$$

By assuming non-relativistic projectile motion, $w_{max} = 2mv^2$ for $M_1 >> m$. It is also assumed that $w_{max} >> w_{min}$,[24] in which case:

$$\sigma_B^2 = 4\pi N Z_1^2 e^4 x \qquad \text{III.45}$$

This is the result obtained by Bohr (1915) and it is the one against which theory and experiment is usually compared. Hvelplund (1978) emphasizes that the Bohr formula requires the following conditions for its validity: 1) the target must be randomly oriented; 2) the energy lost must be much less than the incident energy; 3) the projectile velocity must be much larger than the orbital electron velocities of the target; 4) there must be no correlation effects among scattering atoms; 5) there is no straggling due to variation in incident energy; 6) there is no straggling due to nuclear scattering. To this list should be added the requirement that the projectile charge does not fluctuate due to electron capture and loss processes. Much recent work has been involved with unraveling energy loss fluctuations in the non-relativistic regime. Bonderup and Hvelplund (1971) discuss a modification of the straggling theory of Lindhard and Scharff (1953).[25] Hoffman and Powers (1976) present evidence that the Bonderup and Hvelplund technique does not fit the data well at low energies (~100 keV/amu). Sigmund (1976) pointed out the importance of pair correlation effects in straggling and Chu (1976) has calculated σ^2

with the use of Hartree-Slater-Fock wave functions. Besenbacher et al. (1977) and Bednyukov et al. (1977) have observed effects due to charge state fluctuations. The latter group observes that σ_B^2 fits the data well for protons in aluminum at 1 MeV and is still accurate to within 10% (5% accuracy for σ_B) at 100 keV.

As it is well known by experimentalists, it is much more difficult to measure the width of a distribution with any degree of accuracy than it is to locate the peak. Hence the experimental data for the widths of energy straggling distributions are not as reliable as those for the mean value which, as we have previously noted, becomes less reproducible below 1 MeV/amu. In addition, a great multitude of practical and fundamental complicating factors come into play at these low energies. Much work needs to be invested in order to separate the various contributions to low energy straggling. For the purpose of this Review, we will assume that Bohr's formula is valid above 1 MeV/amu (with appropriate modifications for relativistic effects) for those cases where a Gaussian distribution is in order. For lower velocities the reader should consult the references named above for a more complete discussion.[26]

Bohr's formula is easily modified for relativistic velocities. One merely replaces the Rutherford cross section with the first Born approximation of the Mott cross section. In this Review, we will reserve the description "Mott cross section" for the differential cross section for the Coulomb scattering of Dirac particles by an infinitely heavy scattering center. See Mott (1929, 1932) for a

derivation of the exact cross section, without recourse to perturbation techniques, via an exact phase shift analysis. This term is often applied to the cross section obtained from the first Born approximation (which considers only single photon exchange processes). The first Born approximation to the Mott cross section yields the free electron production spectrum analogous to eq. III.44:

$$\left(\frac{dn}{dwdx}\right)_{FB} = \frac{2\pi N Z_1^{\,2} e^4}{mv^2 w^2}\left(1-\beta^2 w/w_m\right) \qquad \text{III.46}$$

where $w_m = 2mc^2\beta^2\gamma^2$ for $m\gamma << M_1$. In the above equation FB denotes first Born. With the use of eq. III.46, eq. III.45 becomes:

$$\sigma^2 = \sigma_B^{\,2}(1-\beta^2/2)/(1-\beta^2) \qquad \text{III.47}$$

Although eq. III.47 is actually a valid expression for the variance of the energy loss over a wide range of experimental conditions, it is a measure of the width in the sense that the FWHM (full width at half maximum) is equal to 2.355 σ for only a rather limited regime. This regime is that of the above mentioned Gaussian distribution. For any charge and velocity we can always imagine an absorber which is thin enough so that only a very small probability exists for ejecting a high energy electron (i.e. a delta ray). If we let w_o denote some energy well above an atomic electron energy, $P(w_o) = \int_{w_o}^{w_{max}} (dn/dwdx)dw$ is the probability per unit length of ejecting a delta ray with an energy at least as great as w_o. If $P(w_o)x$ is less than unity, the differential spectrum for total energy loss Δ, $f(x,\Delta)$, must approach $(dn/dwdx)x$ with the transcription $w = \Delta$ for $\Delta > w_o$ and $\Delta >> Sx$. This is manifestly different from a Gaussian distribution, and eq. III.47

cannot be used as a measure of the width of the distribution. Bohr (1915) recognized this problem and he realized that the resulting distribution would be asymmetric with a tail on the high energy loss side. The experimentally meaningful quantities in this case become the most probable energy loss and the FWHM.[27] It remained for Landau (1944) to solve the transport equation for $f(x,\Delta)$ in the limit that $w_{max} \to \infty$. Landau's treatment also relied on the assumption that the mean energy lost in the absorber is much greater than typical atomic energies. This enabled him to legitimately neglect the effects of distant collisions and to use the free electron production cross section.

The key parameter in Landau's theory is:

$$\xi = (2\pi N Z_1^2 e^4/mv^2)x \qquad \text{III.48}$$

If $\xi/w_m < 0.01$, (where $w_m = 2mc^2\beta^2\gamma^2$) there are a sufficiently small number of high energy delta rays so that Landau's approximations are valid. One obtains:

$$f(x,\Delta) = \phi(\lambda)/\xi \qquad \text{III.49}$$

where:

$$\phi(\lambda) = \frac{1}{2\pi i}\int_{\sigma-i\infty}^{\sigma+i\infty} \exp[u\ell nu+\lambda u]\, du \qquad \text{III.50}$$

and:

$$\lambda = [\Delta - \xi(\ell n\xi/\varepsilon'+1-C)]/\xi \qquad \text{III.51}$$

with:

$$\ell n\varepsilon' = \ell n[(1-\beta^2)\, I^2/2mv^2] + \beta^2 \qquad \text{III.52}$$

and C = 0.577... is Euler's constant. Results of the appropriate numerical integration enabled Landau to conclude that the most probable energy loss becomes:

$$\Delta_{mp}(\text{Landau}) = \xi[\ell n(\xi/\varepsilon') + 0.373] \qquad \text{III.53a}$$

Maccabee and Papworth (1969) have re-examined this problem. These authors also perform the indicated numerical integration and obtain:

$$\Delta_{mp} = \xi[\ell n(\xi/\varepsilon') + 0.198] \qquad \text{III.53b}$$

This differs from Landau's result by 3% for 10 MeV protons in 0.1 mg/cm^2 Al, by 2.2% for 50 MeV protons in 1.0 mg/cm^2 Al, by 1.7% for 100 MeV protons in 10 mg/cm^2 Al and by 1.2% for 1 GeV protons in 0.5 g/cm^2 Al. Maccabee and Papworth (1969) also find that the FWHM is:

$$\text{FWHM} = 4.02\ \xi \qquad \text{III.54}$$

These expressions neglect the polarization phenomena associated with the density effect. Since the density effect is essentially independent of the close collisions which govern the overall shape of the energy loss distribution, one merely subtracts the mean density effect correction from eq. III.53b to obtain the correct value for the most probable energy loss:

$$\Delta_{mp} = \xi[\ell n(\xi/\varepsilon') + 0.198 - \delta] \qquad \text{III.53c}$$

The expression for the FWHM remains unchanged. From eq. III.36c and Table III.1, we see that $\delta \to 2\ell n(\beta\gamma\hbar\omega_p/I) - 1$ as $\beta \to 1$. This implies that in this limit:

$$\Delta_{mp}(\beta=1) = \frac{\omega_p^2 Z_1^2 e^2 x}{2c^2} \ln \frac{1.219 Z_1^2 x}{a_o} \qquad \text{III.55}$$

where a_o is the Bohr radius. Equation III.55 is remarkable in that it is independent of the detailed atomic properties of the absorbing medium (I has been cancelled by the density effect correction) and of the projectile energy.

Crispin and Fowler (1970) have reviewed the experimental status of the density effect. Interpretation of measurements related to this effect rely on proper evaluation of the experimental mode (i.e. does one measure the mean or most probable energy loss). Hence any conclusions implicitly contain an assumption of the validity of the Landau theory (most density effect related experiments are such that $\xi/w_m < 0.01$). It is found (see Crispin and Fowler for references) that within experimental errors (typically ~±5% in stopping power) eq. III.53c is valid (any distinction between Landau's result and that of Maccabee and Papworth is lost in the noise) when one calculates δ by Sternheimer's procedure.

Symon (1948) and Vavilov (1957) have dealt with the regime between that of Bohr and that of Landau. As with their predecessers, Symon and Vavilov assumed negligible slowing and each assumed the free electron collision spectrum. Corrections from this latter assumption should be small (as are those for the Bohr formula for T > 1 MeV/amu). They are discussed by Bichsel and Yu (1972), Bichsel (1970), Shulek et al. (1967) and Blunck and Leisegang (1950). Vavilov's distribution function is the same as Landau's for $\xi/w_m < 0.01$. For $0.01 < \xi/w_m < 1$ the

distribution function is rather complicated and is given by eq. 16 of Vavilov (1957). For $\xi/w_m \gtrsim 1$ the distribution becomes nearly Gaussian and a relatively simple expression for the difference between the mean and most probable values of the energy loss can be obtained in terms of Airy functions. Sellers and Hanser[28] (1972) express this difference as:

$$\bar{\Delta} - \Delta_{mp} = (a^2 - t_p)\,\eta \qquad \text{III.56}$$

where $\bar{\Delta}(\Delta_{mp})$ is the mean (most probable) energy lost and where $\eta = \xi(2\kappa)^{-2/3}\,(1 - \frac{2}{3}\beta^2)^{1/3}$, $\kappa = \xi/w_m$, $a = (2\kappa)^{1/3}(1 - \frac{1}{2}\beta^2)(1 - \frac{2}{3}\beta^2)^{-2/3}$ and t_p is found from:

$$1/a = -Ai(t_p)/Ai'(t_p) \qquad \text{III.57}$$

The properties of the Airy function, Ai(t), can be found in Abramowitz and Stegun (1970). In Fig. III.7 we reproduce Fig. 1 of Sellers and Hanser (1972) which gives $(\bar{\Delta}-\Delta_{mp})/\eta$ as a function of 1/a. As an example we use Fig. III.7 to calculate $(\bar{\Delta}-\Delta_{mp})/\bar{\Delta}$ for a 600 MeV/amu Ne^{10} nucleus in a 1 cm thick plastic scintillator. It is found that $\kappa = 6$ and that $(\bar{\Delta}-\Delta_{mp})/\bar{\Delta} = 0.2\%$ which is indicative of how rapidly the distribution becomes symmetric for $\kappa > 1$.

For very thick absorbers, in which a substantial fraction of the incident energy is lost, the work of Tschalär (1967, 1968a, 1968b) should be consulted. Bichsel (1972) gives the following approximations to Tschalär's results for moderate energy losses:

$$\sigma^2 = Q\sigma_B^{\cdot 2}(1-\beta^2/2)/(1-\beta^2) \qquad \text{III.58}$$

where

$$Q = \left(\frac{T}{T_1}\right)^{1/3} \quad \text{for} \quad \frac{B}{Z_2} \sim 2.3 \quad \text{and} \quad \frac{T_1}{T} > 0.4$$

$$= 0.99 \left(\frac{T}{T_1}\right)^{1/2} \quad \text{for} \quad \frac{B}{Z_2} \sim 3.5 \quad \text{and} \quad \frac{T_1}{T} > 0.4$$

$$= 0.985 \left(\frac{T}{T_1}\right)^{2/3} \quad \text{for} \quad \frac{B}{Z_2} \sim 6.9 \quad \text{and} \quad \frac{T_1}{T} > 0.6$$

and where $T(T_1)$ is the initial (residual) kinetic energy per atomic mass unit and $B/Z_2 = \ell n\left(\frac{2mv^2}{I}\right) - \ell n(1-\beta^2) - \beta^2 - C/Z_2$, β being the incident velocity.

Finally we briefly consider how these fluctuations in energy loss affect the straggling in range of a projectile. It is straightforward to invert the standard problem and to inquire as to the range required to bring a particle of fixed energy to rest rather than the energy lost in a fixed thickness. In both cases, the quantity which is not fixed is subject to fluctuations. Bichsel (1972) presents results from a calculation of range straggling for which quantum mechanical effects involving distant collision fluctuations have been included. The distribution of ranges is well represented by a Gaussian function with a fractional standard deviation for protons, σ/R, given in Fig. III.8. For other particles of mass M_1 the fractional straggling is given by:

$$\frac{\sigma}{R}(T)_{M_1} = \sqrt{\frac{m_p}{M_1}} \; \frac{\sigma}{R}(T)_{m_p} \qquad \text{III.59}$$

where T is the same energy per amu for protons as for the heavier particle. To a very good approximation one can write $\sigma/R \sim \frac{1}{2}\sqrt{m/M_1}$

which is of the order of the fractional fluctuation in the number of electronic collisions needed to bring the heavy particle to rest.

We next turn to a rather critical review of the assumptions and approximations which have been utilized in this section. The results which have been summarized agree very well with experimental results obtained with singly charged, fully stripped particles for data in the regime 10-1000 MeV/amu (~1%). At smaller energies, use of shell corrections extends the regime of accuracy to ~1 MeV/amu and for very large energies ($\gamma \sim 1000$) Sternheimer's density effect correction and Landau's energy loss distribution provide agreement with data to within several percent. The question naturally arises as to what point in charge and energy significant deviations from this first order theory will arise.

IV. FAILURE AND EXTENSION OF THE BOHR, BETHE, BLOCH STOPPING POWER THEORIES

In the previous section we summarized the early theories of stopping power and indicated the required conditions for their validity. In this section we will discuss the modifications which must be made in order to extend the applicability of these theories. We will concentrate on the list of fifteen assumptions and approximations given in sub-section III.E. However, in sub-sections IV.F and G we will also discuss the effects of multiple Coulomb scattering and nuclear interactions which can be important in certain instances.

A. Ultra-Relativistic Effects

1. Radiative Correction

In this section we will discuss modifications of the relativistic Bethe formula at ultra-relativistic velocities. It is convenient to separately consider ultra-relativistic effects for distant and close collisions. These effects are not severe for the distant collisions, which involve interactions between atomic electrons and the projectile with impact parameters of the order 1 Å or larger. This distance is huge compared to any associated with particle size or wave packet dimensions so that interactions given by classical relativistic electromagnetic fields (or their quantized counter parts) should be adequate. There is, of course, the density effect correction which involves the macroscopic polarization of the medium, but this again should be adequately handled within the framework of classical electrodynamics.

The close collisions, on the other hand, are more subject to non-classical ultra-relativistic effects since this class of collisions

involves very small impact parameter events where a quantum-electro dynamical description is required. If we consider close collision energy loss to be represented by free electron scattering in the CM frame, then:

$$S_{>w_o} = \frac{4\pi N}{w_m}\left[\int_{w_o}^{w_m} \left(\frac{d\sigma}{d\Omega}\right)_{\text{elastic}} w\,dw + \int_{w_o}^{w_m} \left(\frac{d\sigma}{d\Omega}\right)_{\text{brem}} \eta\,dw\right] \qquad \text{IV.1}$$

where $S_{>w_o}$ is the energy loss of the projectile per unit pathlength due to collisions with the electrons of the absorbing material which involve losses greater than w_o. w_m is the maximum energy which can be lost by the projectile in the laboratory frame in such a collision and is given by:

$$w_m = \frac{2mM_1{}^2c^2\beta^2\gamma^2}{2mM_1\gamma+M_1{}^2+m^2} \qquad \text{IV.2}$$

and w is the projectile energy loss in the lab frame for elastic scattering with the CM scattering angle θ:

$$w = w_m \sin^2\frac{\theta}{2} \qquad \text{IV.3}$$

$\left(\frac{d\sigma}{d\Omega}\right)_{\text{elastic}}$ is the CM cross section for electrons to be scattered into $d\Omega$ with an energy (in the CM frame) of $mc^2\gamma$ within an energy resolution window ΔE. ΔE characterizes how accurately we can determine if the particle-electron collision resulted in the emission of a bremsstrahlung photon. $\left(\frac{d\sigma}{d\Omega}\right)_{\text{brem}}$ is the CM cross section for the scattering of an

electron into $d\Omega$ accompanied by a bremsstrahlung photon with an energy between ΔE and $mc^2\gamma$. η is the total energy lost by the heavy particle in the collision.[29] It should be noted that eq. IV.1 does not include energy lost by primary bremsstrahlung radiation by the projectile. The magnitude of this effect will be considered at the end of this sub-section.

By considering the nature of the bremsstrahlung spectrum (it is proportional to the inverse of the frequency of the emitted photon) it can be shown from conservation of energy in the CM frame that on the average:

$$\eta = \begin{cases} w[1-1/\ell n(\frac{mc^2\gamma}{\Delta E})], & \text{large } \gamma,\ w >> m^2 \\ mc^2/\ell n(\frac{mc^2\gamma}{\Delta E}), & \text{large } \gamma,\ w << m^2 \\ w(1 + \frac{\cos\theta}{4\sin^2\theta\,\ell n(\frac{m\beta^2c^2}{2\Delta E})}), & \text{small } \beta \end{cases} \qquad \text{IV.4}$$

By assuming the heavy particle is sufficiently massive we can express $(\frac{d\sigma}{d\Omega})_{brem}$ in terms of the elastic cross section (Bjorken and Drell, 1964):

$$(\frac{d\sigma}{d\Omega})_{brem} = \frac{2}{\pi}\alpha(\frac{d\sigma}{d\Omega})_{elastic}\ \ell n\ \frac{k_{max}}{k_{min}} \begin{cases} \frac{2}{3}\frac{w}{mc^2}, & w << mc^2 \\ \ell n\frac{2w}{mc^2}, & w >> mc^2 \end{cases} \qquad \text{IV.5}$$

The above expression is applicable to scattering off of a Coulomb potential for soft photon emission. With the same assumption of soft photon emission it can be shown that the ratio of bremsstrahlung to elastic cross section is independent of the exact form of the static

(where we assume the projectile to be sufficiently massive so that it is at rest in the CM frame) electromagnetic interaction (each of these cross sections is proportional to $|\bar{U}_f A_\mu(\vec{q})\gamma^\mu U_i|^2$ where $A_\mu(\vec{q})$ is the Fourier transform of the static interaction and $\vec{q}$ is the momentum transfer). The above expression is therefore applicable to very massive magnetic monopoles with the same accuracy as for nuclei and anti-nuclei. Furthermore, the radiative corrections to the elastic cross section derived from the Dirac equation arise from multiplicative vertex and propagator corrections which depend only on the momentum transfer and not on the nature of the scattering potential.[30] This means that our treatment of radiative corrections below is equally valid for magnetic monopoles as for nuclei and anti-nuclei.

We now estimate the size of the bremsstrahlung correction to $S_{>w_o}$. We use $(\frac{d\sigma}{d\Omega})_{\text{elastic}} = 1/w^2$ which is valid within a multiplicative constant to a first approximation for both magnetic and electric charges. We also make the very crude extrapolation of eq. IV.5 to include hard photon emission by setting $k_{max} = mc^2(\gamma-1)$ and $k_{min} = \Delta E$. We thus find:

$$S_{>w_o} = \frac{4\pi N}{w_m}\,[1+F(\beta)] \int_{w_o}^{w_m} (\frac{d\sigma}{d\Omega})_{\text{elastic}}\, w\,dw \qquad \text{IV.6}$$

where:

$$F(\beta) = \begin{cases} \lambda\alpha\beta^2 (\ell n\, \frac{m\beta^2c^2}{2\Delta E})/(\ell n\, \frac{2m\beta^2c^2}{w_o}) & \text{small } \beta \\ \frac{\alpha}{\pi}\,(\ell n 4\gamma^2)^2 (\ell n\, \frac{mc^2\gamma}{\Delta E})/(\ell n\, \frac{2m\gamma^2c^2}{w_o}) & \text{large } \gamma \end{cases} \qquad \text{IV.7}$$

with $\lambda \sim 1$.

Although ΔE has been described as characterizing the energy resolution width it has been used here to divide photon energies into those

for which it is legitimate to replace η with w and those for which it is not. $\Delta E \sim \gamma w_o$ certainly serves this purpose. However, since η deviates from w by the fraction $1/(\ell n \frac{mc^2\gamma}{\Delta E})$ the choice for ΔE is completely arbitrary provided this fraction is small and can be neglected to this order of approximation. Hence, ΔE is not experimentally relevant for the energy loss process. Even if we measure the energy loss with a detector insensitive to hard photons, ΔE is not important since on the average, hard photons remove much less energy from the massive particle than the electrons do. To eliminate ΔE we must consider the radiative corrections to the elastic cross section.

If we assume that $m\gamma << m_p$, it is possible to write the elastic cross section in terms of the Dirac cross section and the radiative corrections.[31] By using the radiative corrections given by Eriksson et al. (1963) it is found that:

$$S_{>w_o} = \frac{4\pi N}{w_m} [1+F(\beta)+G(\beta)] \int_{w_o}^{w_m} (\frac{d\sigma}{d\Omega})_{Dirac} \, wdw \qquad IV.8$$

where:

$$G(\beta) = \begin{cases} -\frac{4\alpha}{\pi} \beta^2/(\ell n \frac{2mc^2\beta^2}{w_o}) & \text{small } \beta \\ -\frac{\alpha}{\pi} (\ell n 4\gamma^2)^2 (\ell n \frac{mc^2\gamma}{\Delta E})/(\ell n \frac{2mc^2\gamma^2}{w_o}) + \frac{\frac{\alpha}{\pi}(\ell n 4\gamma^2)^2}{\ell n \frac{2mc^2\gamma^2}{w_o}} & \\ +\frac{2\alpha}{\pi} \ell n \frac{mc^2\gamma}{\Delta E} + O(\alpha) & \text{large } \gamma \end{cases} \qquad IV.9$$

and where $(\frac{d\sigma}{d\Omega})_{Dirac}$ is the cross section obtained by assuming the scattering center to be infinitely massive.

For $\beta \leq 0.9$ F + G can be safely neglected. For large γ the big ΔE term in G cancels that with F and ΔE can be made large enough so that:

$$F + G \rightarrow \frac{\alpha}{\pi} (\ell n 4\gamma^2)^2 / (\ell n \frac{2mc^2\gamma^2}{w_o}) \qquad \text{IV.10a}$$

In Table IV.1 we list the fractional correction to <u>total</u> energy loss as given by eq. IV.10 for heavy projectiles in argon gas. The density effect is not considered. We also list the radiative corrections given by Jankus (1953) for the same situation and for two values of his parameter Q:

$$(F+G)/2 = \frac{\alpha}{\pi}[0.333(\ell n 2\gamma)^3 + 2.42(\ell n 2\gamma)^2 \qquad \text{IV.10b}$$

$$-7.26\ell n 2\gamma - 1.54 \ell n \frac{Q}{m} + 6.18] / (\ell n \frac{2mc^2\gamma^2}{w_o})$$

Jankus' result is more reliable than that obtained here due to his more realistic treatment of hard bremsstrahlung radiation. However, it is encouraging to note that there is not a large disagreement between eq. IV.10a and b below $\gamma \sim 100$. Thus we expect our remarks regarding monopole radiative corrections to have approximate validity in this regime. It should be noted that the radiative corrections are positive, which correspond to the added channel of energy loss via secondary bremsstrahlung. Consideration of only the corrections to elastic scattering leads to a negative energy loss correction (Jauch, 1952).

Generally speaking, we see that it is legitimate to ignore the radiative corrections for $\gamma < 100$. The close collision energy loss is then given by:

$$S_{>w_o} = \frac{4\pi N}{w_m} \int_{w_o}^{w_m} \left(\frac{d\sigma}{d\Omega}\right)_{Dirac} w\,dw \qquad IV.11$$

In evaluating $\left(\frac{d\sigma}{d\Omega}\right)_{Dirac}$, the renormalized values for electric (or magnetic) charge are to be employed. If, as indicated by Schwinger (1966), magnetic and electric charges are renormalized by the same factor, then eq. IV.11 allows comparison between magnetic and electric stopping powers with no systematic discrepancies. In the event that renormalization is not universal, such a comparison may be subject to a systematic error of several percent.

2. Kinematic Correction

If one uses the first Born-Mott cross section for $\left(\frac{d\sigma}{d\Omega}\right)_{Dirac}$ and lets $I = w_o$, $M_1 = \infty$ then:

$$S_{>I} = \frac{2\pi N Z_1^{\,2} e^4}{mv^2} \left[\ell n \frac{2mc^2\beta^2\gamma^2}{I} - \beta^2\right] \qquad IV.12$$

which indicates that 1/2 of the total energy loss occurs for close collisions. Equation IV.12 is essentially that obtained by Bethe for close collisions. It is based upon the assumption that the projectile is an infinitely heavy point projectile with no internal structure with a value of $Z_1\alpha/\beta << 1$ so that the first Born approximation is valid for determining the projectile-electron differential scattering cross-section. Motz et al. (1964) discuss in great detail elastic electron scattering off of atoms and nuclei. They present numerous cross sections and their conditions of validity. Here we consider some of the simpler cases which indicate approximate degrees of validity for the assumptions mentioned above. In the next sub-section we will

discuss in some detail the effect of large values of Z_1/β on the close collision energy loss.

Motz et al. (1966) give the Mott-Born formula for electron-nuclear scattering, valid for large momentum transfer, finite nucleus with recoil and no atomic screening:

$$\frac{d\sigma}{d\Omega'} = \frac{4Z_o^2 r_e^2 E_1^2}{q_o^4} \frac{[1 - \frac{q_o^2}{4E_1^2}]}{[1 + \frac{m}{M_1}\frac{q_o^2}{2E_1}]} G_E^2(Q) \qquad \text{IV.13}$$

where $q_o = 2\beta_1\gamma_1\sin(\theta'/2)$ (θ' is the electron scattering angle in the frame where the nucleus is initially at rest), $r_e = e^2/mc^2$, $E_1 = \gamma_1$, $\beta_1 c$ is the initial projectile velocity in the lab frame and $\gamma_1^2 = 1/(1-\beta_1^2)$. $G_E(Q)$ is defined as the nuclear form factor and is given by:

$$G_E(Q) = \int_\tau \rho(\vec{r}) \exp(i\vec{Q}\cdot\vec{r})\, d^3r \qquad \text{IV.14}$$

where τ is the nuclear volume, $Z_o e\rho(\vec{r})$ is the nuclear charge density distribution and Q = four dimensional momentum-energy transfer. $G_E = 1$ for a point charge nucleus or for $Q = 0$. Equation IV.13 is valid only for nuclei with negligible spin effects, i.e. $(q_o/Z_o)^2(m/m_p)^2 << 1$. In order to utilize eq. IV.11 to evaluate the close collision energy loss we must first express eq. IV.13 in terms of CM coordinates. This is straightforward and to first order in $y = m\gamma/M_1$ one obtains for $G_E = 1$:

$$S_{>I} = \frac{2\pi N Z_o^2 e^4}{mv^2}\left[\ln\frac{2mc^2\beta^2\gamma^2}{I} - \beta^2 - \ln(1+2y) - y\frac{\beta^2}{\gamma^2}\right] \qquad \text{IV.15}$$

It is important to note that all corrections occur within the brackets so that rather than being of order y, the corrections are of

order $\gamma/\ell n(\frac{2mc^2\beta^2\gamma^2}{I})$.

In Table IV.2 we tabulate the kinematical corrections to the Bethe formula for protons in Argon gas. We have neglected the density effect for this tabulation. As for the radiative corrections we tabulate corrections to <u>total</u> energy loss, not just to the close collisions. It is seen that the correction is quite small. Even when $m\gamma/M_1$ is equal to 0.5 the correction is only ~2%. For the purposes of this Review, where, for the most part $\gamma < 100$ and $M_1 > m_p$, it is seen to be legitimate to neglect radiative and kinematical corrections. This is accurate at least at the 1% level.

3. Projectile Structure Correction

A more severe problem is encountered with respect to the internal structure of the projectile. This is represented by the nuclear form factor. One might suspect that problems relating to non-point like charge distributions would arise when the de Broglie wavelength of the electron in the CM frame becomes comparable to the nuclear radius. With $R_E = 1.07\ A_1^{1/3}\ F$ (Hahn et al., 1965) for the 50% peak charge density radius, internal charge structure effects should be important at $\gamma = 361/A_1^{1/3}$.

For extreme relativistic energies one can replace Q by $mcq_o/\hbar$. Nuclear form factors can be found in Herman and Hofstadter (1960). It is beyond the scope of this work to give accurate correction factors for nuclear charge distribution effects based on detailed electron scattering information for individual nuclides. However, it is valuable to have a ready estimate for the size of these correction factors. To this end we utilize a model of the nucleus in which there is uniform

charge density out to a radius R_A, beyond which the charge density vanishes. Motz et al. (1964) give:

$$R_A = 1.44\ A_1^{1/3}\ F. \qquad \text{IV.16}$$

The form factor is easily shown to be:

$$G_E = \frac{4\pi\rho}{Q^3}\left[\sin QR_A - QR_A\cos QR_A\right] \qquad \text{IV.17}$$

where

$$\rho = (0.080/A_1)\ F^{-3} \qquad \text{IV.18}$$

By inserting eq. IV.17 into eq. IV.13 and setting $M_1 = \infty$ (i.e. neglecting recoil effects) we can numerically evaluate the correction factor to the close collision energy loss due to internal charge structure. In Table IV.3 we list the correction factor to total energy loss (which is 1/2 of that for close collision energy loss) for w_o = 200 eV (the correction factor changes by only 10% in going from w_o = 100 eV to w_o = 1000 eV) and for several values of A_1. This has been done in the first Born approximation of the Mott cross section. This corresponds essentially to the case of an Argon gas absorbing medium and hence can be directly compared to the radiative and recoil corrections in Tables IV.1 and IV.2 respectively. It should be noted that the radiative corrections are independent of projectile mass and that the recoil corrections scale approximately as $1/A_1$. It should also be noted that the signs of all three of these corrections are independent of the sign of the projectile charge and hence apply equally to antinuclei as to ordinary nuclei.

The form factor given by eq. IV.17 is most suitable for describing very heavy nuclei. In addition, it is to be emphasized that it contains only information regarding charge structure. Nuclear spin effects are taken into consideration by inclusion of the magnetic moment and magnetic form factor in the scattering cross section such as in the Rosenbluth and Walecka-Pratt formulas (see Motz et al., 1964). Turner et al. (1969) calculate corrections to the Bethe formula for protons in several solid absorbers by including the complete set of form factors and by treating the kinematics exactly. Vera and Turner (1970) do the same for deuterons. In Table IV.4 we list their correction factors to the Bethe formula for an aluminum absorber, neglecting the density effect. In the proton column, we list in parentheses the correction obtained by adding the appropriate numbers in Table IV.2 and Table IV.3. The discrepancy is due to the naive structure for the proton imposed by eq. IV.17

It is quite easy to estimate the size of the correction to the total stopping power due to the magnetic moment of the projectile by using the Walecka-Pratt formula (this formula as given by Motz et al., 1964, p. 905, is in error; their M_o should be replaced by the proton mass; see for example Ginsberg and Pratt, 1964). Again, in the first Born approximation (as $\beta \to 1$):

$$S = S(\text{Bethe})\left[1 + \left(\frac{\mu c \gamma m}{Z_1 e\hbar}\right)^2 \left(\frac{J+1}{J}\right) \Big/ \left(\ell n \frac{2mv^2\gamma^2}{I} - 1\right)\right] \qquad \text{IV.19}$$

where $\mu = \lambda \frac{e\hbar}{2m_p c}$ is the nuclear magnetic moment of the projectile and J is the nuclear spin. For most nuclei J is of the order 1 (within a factor of 2) and λ is of the order 3 (within a factor of 2). For

extreme relativistic energies the above fractional correction is, for these typical values of λ and J, $(m\gamma)^2/(2Z_1 m_p)^2$ which is less than 0.1% for all nuclei if $\gamma < 100$. It should be emphasized that the magnetic moment affects the close collisions much more strongly than the distant collisions (due to the r^{-3} behavior of dipole fields) and so is completely negligible in considering the latter class of collisions. This is reflected by the Walecka-Pratt formula insofar as it approaches the purely electric moment cross section as $Q \to 0$).

4. Particle Bremsstrahlung and Pair Production Correction

To conclude this sub-section we should briefly consider means by which heavy charged particles can lose energy via electromagnetic interactions other than by elastic and inelastic atomic collisions. Such interactions include primary particle bremsstrahlung as well as higher order quantum electrodynamical processes such as pair production (electron-positron pairs predominantly).

A rough comparison of radiative loss to collision loss is given by Jackson (1975):

$$\frac{dE_{rad}}{dE_{coll}} = \begin{cases} \frac{4}{3\pi}\left(\frac{Z_1^2 Z_2}{137}\right)\frac{m}{M_1}\beta^2\frac{1}{L} & \beta << 1 \\ \frac{4}{3\pi}\left(\frac{Z_1^2 Z_2}{137}\right)\frac{m}{M_1}\gamma\frac{\ell n\left(\frac{\lambda 192 M_1}{m Z_2^{1/3}}\right)}{L} & \gamma >> 1 \end{cases} \qquad \text{IV.20}$$

where $L = \ell n\left(\frac{2mc^2\beta^2\gamma^2}{I}\right) - \beta^2$ and $\lambda \sim 1$. Using the electron-positron pair production cross section given by Bhabha (1935) it is straightforward to show that the ratio of pair production to radiative (i.e. primary bremsstrahlung) energy loss is roughly:

$$\frac{dE_{pair}}{dE_{rad}} \sim M_1/(1000mZ_1^2) \quad \gamma >> 1 \qquad \text{IV.21}$$

For ordinary nuclei this ratio is $\sim 4/Z_1$ which indicates that relativistic cosmic ray nuclei lose roughly the same fraction of their energy to pair production as they do to primary bremsstrahlung. Muon pair production is down by a factor 200.

In Table IV.5 we list the ratio given by eq. IV.20 for various values of A_1 and γ for the case of an argon gas absorbing medium.

We see from Tables IV.1 to IV.5 that for $\gamma < 100$, the ultra-relativistic corrections are less than 1% (when summed) for protons. For $\gamma \sim 100$ the corrections are significant for heavy nuclei due to form factor contributions and to the large amount of bremsstrahlung radiation (and pair production). We should emphasize that our treatment in this sub-section has involved average energy loss. If one is interested only in setting limits on the size of corrections to the stopping power, then he need not be too concerned with the distinction between mean and most probable energy loss. On the other hand, if quantitative comparisons with experiment are to be made, a careful treatment of energy loss statistics will be required, particularly since the ultra-relativistic effects involve the relatively infrequent close collisions. However, for $\xi/w_m \geq 1$, it should be a good approximation to set the mean and most probable energy loss equal to one another. For this case, there is a sufficient number of high energy delta rays produced up to the kinematic limit so that Gaussian statistics should prevail. The small effects discussed in this sub-section should not alter this conclusion.

B. Failure of the First Born Approximation

In the non-relativistic limit, a well known property of the Coulomb force is that its differential scattering cross section is identical as obtained by classical theory, first Born quantal theory or exact quantal theory. Unfortunately, this does not remain the case as relative particle velocities approach the speed of light. If projectile recoil and internal structure effects are ignored (corrections for which are indicated in the previous sub-section) one requires the elastic scattering cross section for an electron off of a point source located at the origin. Radiative corrections have been shown to be quite small in the previous sub-section and it is sufficient to evaluate the cross section for scattering in a static field with complete neglect of the electromagnetic field. Mott (1929, 1932) performed this calculation within the framework of the Dirac theory of the relativistic electron. The cross section thus obtained is known as the Mott-exact "phase shift" formula and it is given along with other theoretical cross sections in Motz et al. (1964). As related by Jackson and McCarthy (1972), it was Fermi who first considered the effect of the actual Mott cross section on the stopping power of oppositely charged particles. He attempted to explain the range discrepancy between positive and negative pions measured by Barkas et al (1956) with an incorrect form of the second Born approximation to the Mott cross section. Jackson and McCarthy (1972) repeated Fermi's calculation with the correct form of this approximate cross section as given by McKinley and Feshbach (1948). Due to the slowly converging Legendre expansions which are necessary for an evaluation of the exact Mott

cross section, it is difficult to evaluate the accuracy of these corrections. These expansions have been summed numerically by Doggett and Spencer (1956), among others (see Doggett and Spencer for additional references). However the tabulated cross sections are not easily incorporated into the close-collision energy-loss formula since an integration over CM scattering angles is required. Eby and Morgan (1972) and Morgan and Eby (1973) have performed such calculations for several values of Z_1 and β which agree with Jackson and McCarthy's results for $Z_1 < 20$. Ahlen (1978a) has taken advantage of the Z_1^7 expansion derived by Curr (1955) for the Mott cross section to obtain an analytical expression for the stopping power which is valid to within 1% for $|Z_1|/\beta < 100$. According to Ahlen (1978a):

$$S = \frac{4\pi N Z_1^2 e^4}{mv^2}\left[\ell n\,\frac{2mv^2\gamma^2}{I} - \beta^2 - 1 - 0.202\left(\frac{Z_1\alpha}{\beta}\right)^2\right.$$

$$\left. + \frac{1}{1+(Z_1\alpha/\beta)^2} + \frac{1}{2}\,G(Z_1,\beta) - \frac{1}{2}\,\delta(\beta)\right]$$

$$\times\left[1 + 2Z_1 F(V)/Z_2^{\frac{1}{2}}\right] \qquad \text{IV.22}$$

$G(Z_1,\beta)$ is the close collision Mott correction which is given by:

$$G(Z_1,\beta) = (Z_1\alpha\beta)[1.725 + 0.52\pi\cos\chi - 2(w_o/w_m)^{\frac{1}{2}}\pi\cos\chi]$$

$$+ (Z_1\alpha)^2(3.246 - 0.451\beta^2)$$

$$+ (Z_1\alpha)^3(1.522\beta + 0.987/\beta)$$

$$+ (Z_1\alpha)^4(4.569 - 0.494\beta^2 - 2.696/\beta^2)$$

$$+ (Z_1\alpha)^5(1.254\beta + 0.222/\beta - 1.170/\beta^3) \qquad \text{IV.23}$$

where $w_m = 2mv^2\gamma^2$, $\sqrt{w_o} = \sum_i f_i\sqrt{\hbar\omega_i}$ is the mean square-root ionization potential. Values for the oscillator strengths f_i and the ionization

potentials $\hbar\omega$ can be obtained from the early work by Sternheimer. Accurate values for w_o are not critical. It can be set to zero with negligible error in stopping power for all but the heaviest absorbers. The function $\cos\chi$ is defined by Doggett and Spencer (1956) and various values of this term as a function of $|Z_1|\alpha/\beta$ are given in Table IV.6 (note that there is a typographical error in the Z_1^5 term in Ahlen (1978a). The remaining expressions within the first set of brackets in eq. IV.22 correspond to: a) an approximate form of Bloch's correction which yields the correct stopping power to better than 1% for $|Z_1|/\beta < 137$ and b) the density effect correction discussed earlier. The remaining term in brackets corresponds to a distant collision correction which will be discussed next.

It is to be emphasized that Z_1 can be positive or negative, corresponding to ordinary nuclei or to anti-nuclei. Since $G(Z_1,\beta) \neq G(-Z_1,\beta)$, and since the same holds true for the distant collision correction, it is apparent that the stopping power is different for particles of opposite charge at the same velocity. The physical reason for this is that positively charged projectiles draw atomic electrons closer to them while negative charges repel the electrons. For both the distant and close collisions the dynamics is sufficiently different for those two cases to alter the energy transfer. It is <u>not</u> legitimate to explain the enhanced stopping power for positive charges as being due simply to the greater "kick" given to the electrons. This argument should apply equally to close collision classical stopping power. It does not in fact apply due to the rather remarkable fact that the CM scattering angle is the same for positive and negative

scattering centers with the same impact parameter, in spite of the fact that the positive charge draws the electron much closer to it than the negative charge does. Relativistic quantum effects or external interactions (atomic binding) are required to break this rather peculiar symmetry of the non-relativistic Coulomb force.

As mentioned above, deviations from the first Born approximation are more difficult to evaluate for the distant collisions than for the close collisions due to the interference of the dipole approximation. In a quantal approach the dipole and first Born approximations are imposed separately. The classical impulse approximation used by Bohr includes both approximations in a natural way. Barring a completely second order solution via quantum mechanics, it seems that the most promising strategy for examining distant collision corrections lies in the classical approach of Bohr. It is to be recalled that the fundamental assumption of the impulse approximation is that the electron sees at all times a spatially uniform electric field. For very small projectile velocities this will be valid if the separation between projectile and traget electron is very large (dipole approximation). For very large projectile velocities, it seems physically plausible that small spatial separations will permit the validity of the impulse approximation if the electron does not move appreciably until the projectile has completely passed out of sight. This will be the case for very weak interactions (i.e. the analog to the quantal first Born approximation).

By allowing for the first order motion of the harmonically bound electron, Ashley, Ritchie and Brandt (1972, 1973) have calculated the

first order correction to the classical impulse approximation. The expansion is carried out with the ratio of electron displacement to electron-projectile separation as the expansion parameter. Ashley et al. separate the distant collisions from the close ones by an impact parameter given roughly by the atomic radius. Close collisions are treated in the free electron approximation and hence energy loss scales as Z_1^2 for these collisions in the non-relativistic limit. Jackson and McCarthy (1972) have extended the non-relativistic calculations of Ashley et al. to the relativistic case, using a slightly different dividing impact parameter (which is also given essentially by the atomic radius). The relativistic corrections are shown to be small (in the sense that the value of the correction to which the relativistic correction is applied becomes very small at large velocities) and the correction can be expressed as:

$$C_1 = Z_1 F(V)/Z_2^{\frac{1}{2}} \qquad \text{IV.24}$$

where C_1 is the fractional correction to total energy loss and $V = 137\beta/Z_2^{\frac{1}{2}}$. C_1/Z_1 is plotted as a function of β for various values of Z_2 in Fig. IV.1.

Hill and Merzbacher (1974) performed a non-relativistic quantum mechanical calculation of the energy loss to a harmonic oscillator by treating the quadrupole term as a perturbation. The dipole interaction was treated exactly, without recourse to perturbation theory. They obtained the same result as obtained by Ashley et al. (1972, 1973) as one might expect for a harmonic oscillator. The question of whether or not this equivalence will obtain for realistic atomic systems remains to be shown.

Lindhard (1976) and Esbensen (1977) have used an alternative approach to that of the above authors in that they consider the atoms to be well represented by a plasma absorbing medium. In their calculation, both close and distant collisions are subject to the polarization effect considered by Ashley et al. (1972, 1973). This is reflected by their result which is about a factor of two greater than eq. IV.24.

C. Complete, Corrected Stopping Power Formula and Comparison with Experiment

Andersen et al. (1977) have utilized an elegant method for measuring the stopping power of thin metal foils by means of a calorimetric technique (see Andersen et al., 1966 for details) to determine the absolute stopping power of 0.8 - 7.2 MeV/amu H, He and Li ions in Al, Cu, Ag and Au. Their quoted accuracy is 0.5% which is good enough to isolate higher order contributions to the stopping power. In Fig. IV.2 we reproduce their figure which displays the terms L_o, L_1 and L_2 where:

$$S = \frac{4\pi N Z_1^2 e^4}{mv^2} [L_o + L_1 Z_1 + L_2 Z_1^2] \qquad \text{IV.25}$$

$v_o = \alpha c$ is the Bohr velocity. The quoted uncertainty in L_o is 0.5%, and is 25% for L_1 and L_2. Hence the detailed shapes of the L_1 and L_2 curves are of no significance. For comparison the theoretical calculations of Jackson and McCarthy (1972) are displayed for L_1 and those of Bloch (1933a) for L_2. It is seen that the measured L_1 is a factor of ~2 larger than the Jackson, McCarthy result which supports the theory of Lindhard and that the L_2 correction is, within experimental errors, consistent with the Bloch correction. Andersen et al. (1977) also found that the scaling predicted by Jackson and McCarthy (1972), namely

$L_1 \propto F(137\beta/Z_2^{\frac{1}{2}})/Z_2^{\frac{1}{2}}$ is approximately valid but is more accurately given by $F(137\beta/Z_2^{1/3})/Z_2^{\frac{1}{2}}$. Andersen et al. (1977) compared their scaled stopping power Z_1 correction with that measured by Heckman and Lindstrom (1969) for positive and negative pions in emulsion. This comparison is shown in Fig. IV.3 where it is seen that the results essentially agree.

Inclusion of the distant collision correction of Lindhard and the Bloch correction in eq. IV.22 reflects the experimental justification provided by Andersen et al. (1977). Such verification is absent in the channeled stopping power data of Datz et al. (1977). However, various channeling effects and distribution asymmetry effects (Ahlen, 1977 and Datz, 1977) are quite possibly sufficient to explain the differences.

It is interesting to note that for a classical harmonic oscillator with frequency ω, the Jackson and McCarthy (1972) correction can be written:

$$L_1 \sim \frac{3}{2} \frac{\alpha}{\beta^3} \frac{\hbar\omega}{mc^2} \ln \frac{1.60v}{a\omega} \qquad \text{IV.26}$$

in the non-relativistic limit; a corresponds to the minimum impact parameter for which the correction is required. If one chooses $a \sim \sqrt{\hbar/(2m\omega)}$, which corresponds to the atomic radius, the logarithmic term is given by $\frac{1}{2} \ln(5.12mv^2/(\hbar\omega))$. As Lindhard (1976) points out, there is no obvious reason why this choice for a should be sufficient. In the usual semi-classical derivation of the stopping power formula, one typically evaluates the distant collision result via the classical Bohr approach and incorporates quantum physics by letting the minimum impact parameter be given by the de Broglie wavelength of the electron

in the CM frame.[32] That this technique works so well is convincing evidence that there may be more validity to the Bohr approach than one might suspect. This is further evidenced when one inserts $\hbar/(mv)$ for a in eq. IV.26, thus obtaining $\ell n(1.60mv^2/(\hbar\omega))$ which is of the order of 2 times the result obtained when a is given by the atomic radius. This is the experimental result. It seems then that the close collisions are not really those involving free electrons: polarization effects are as significant for close collisions as for distant collisions.[33]

Andersen et al. (1977) used their measured higher order corrections to separate the charge-independent (to first approximation) shell corrections from higher order Born terms. In Fig. III.2c-III.2f these corrections, (C/Z_2), are compared with those which include higher order corrections $(C/Z_2)'$ and those calculated by Bonderup (1967) $(C/Z_2)_{Th}$. Good agreement is obtained between (C/Z_2) and $(C/Z_2)_{Th}$.

Finally, the Mott and Bloch corrections from Ahlen (1978a) are shown in Fig. IV.4 for an aluminum absorber for nuclei with atomic numbers 26, 52, 80 and 92. Electron capture has been accounted for in a manner to be subsequently discussed. The quantity L in Fig. IV.4 is given by $\ell n(2mv^2\gamma^2/\beta^2) - \beta^2$ and the distant collision correction is shown for $Z_o = 26$. The solid black circles are taken from the exact calculations of Eby and Morgan (1972) for the Mott corrections. The open circles are taken from Morgan and Eby (1973). They agree within 1% for total stopping power with those values obtained from the formulae of Ahlen (1978a) for the Mott corrections. Morgan and Eby (1973) show that similar accuracy is obtained for $|Z_1|/\beta < 20$ with the second Born

approximation to the Mott cross section and for $|Z_1|/\beta < 55$ with the third Born approximation.

The first measurement of higher order deviations from the Bethe theory for relativistic heavy ions has been recently achieved by Tarlé and Solarz (1978). They very accurately measured the range of 600 MeV/amu ^{56}Fe ions in a variety of samples. The particles stopped short of the range predicted by Bethe theory by ~3%, compared with a predicted range discrepancy of ~2% (Ahlen, 1978a).

D. Electron Capture and Loss

The results of the previous sections and sub-sections can be unambiguously applied to projectiles such as fully stripped nuclei or anti-nuclei. However, it is well known that as ordinary nuclei slow in matter, atomic electrons become attached to the nuclei until they become fully neutralized, at which point nuclear scattering becomes the dominant energy loss process. The question naturally arises as to what one should use for Z_1: should one use the root mean square charge as measured with static electromagnetic fields or is it more appropriate to use the nuclear charge Z_o, or something in between Z_{rms} and Z_o? Betz (1972) reviews theoretical aspects of charge states and charge-changing cross sections of fast heavy ions in gaseous and solid media. He gives numerous references to earlier work to which the interested reader is directed. Most of this work involves energies outside of the scope of this Review (in particular, energies less than ~1 MeV/amu). At these low energies there are a multitude of effects which serve to cloud interpretation of stopping power data. However, it is relatively straightforward to measure initial and final charge

states with any of a number of possible electro-magnetic field configurations. Betz presents a number of semi-empirical formulae for the ion charge state as a function of Z_1, β, Z_2 and density. The long known density effect, whereby charge states as measured with solids are larger than those in equivalent gases (i.e. fewer electrons are attached when ions penetrate solid absorbers) has been explained as one involving capture and loss into excited states. Whether or not the discrepancy exists in the material itself or is a transition effect has been the subject of much discussion. Betz and Grodzins (1970) have argued that the charge state of the ion is approximately the same in solids as it is in equivalent gases (within 1 or 2 charges). The apparent difference between gaseous and solid charge state arises due to the prompt emission of Auger electrons upon departure of the ion from the solid. This serves as a de-excitation mechanism of the ion which does not occur in the solid due to the fact that Auger processes are not fast enough to allow the ion to return to its ground state within the short time between collisions in a solid.

A very desirable consequence of the Betz and Grodzins theory is that it explains the difference between the "effective charge" and the rms charge of ions determined with solid absorbers. The effective charge is defined by:

$$Z^2_{eff} = S(Z_o,\beta)/S(1,\beta) \qquad \text{IV.27}$$

For a summary of experimental work relating to Z_{eff} the reader should consult Northcliffe (1963). Although Z_{eff} clearly contains in it higher order Born terms, there is a large range of velocities for which

these effects should be small compared to the effects of electron capture and loss. Hence Z_{eff} is a reasonable measure of the effective charge of the ion for ionization and excitation processes. The most naive initial guess would be that $Z_{eff} = Z_{rms}$. This would be the case provided the bulk of the collisions occurred for impact parameters larger than the radius of the electron cloud of the projectile. Bohr (1941, 1948a) argues that this is indeed the case. This conclusion is supported by the following two observations (see Betz, 1972):

i) Z_{eff} does not depend significantly on whether the stopping material is a gas or solid.

ii) Z_{eff} is very close to Z_{rms} as measured with gas strippers.

Any discrepancies regarding the density effect are eliminated if one accepts the Betz, Grodzins theory.

The semi-empirical expression originally used by Barkus (1963) and later modified by Pierce and Blann (1968) has been widely used for evaluation of Z_{eff}. This is given by:

$$Z_{eff} = Z_o[1 - \exp(-130\beta/Z_o^{2/3})] \qquad \text{IV.28}$$

It should be noted that this expression is independent of the atomic number of the absorbing material. This is certainly not the case in principle but is a remarkably good approximation in practice. It should also be noted that the fractional stripping of an ion is a function only of the parameter $\beta/(\alpha Z_o^{2/3})$. This corresponds to the ratio of the ion velocity to the typical velocity of an electron carried along by the ion. The scaling power of 2/3 reflects the fact that the measurements upon which eq. IV.28 were based were done at

low energies where a large number of captured electrons are present so that a Thomas-Fermi description is valid. It is a remarkable coincidence that eq. IV.28 appears to work in the relativistic regime for which there is no independent experimental justification (Shirk and Price, 1978 and Fowler et al., 1977). That this is the case is not so surprising when one uses eq. IV.28 to evaluate Z_{eff} at the velocity for which the Bohr criterion[34] predicts the ion will pick up its first electron, namely at $\beta = Z_o/137$. These values for Z_{eff} are given in Table IV.7. Equation IV.28 predicts the "correct" value, to within 1/2 of a charge, for most values of Z_o. Further justification for the use of eq. IV.28 at high energies is obtained when one compares values given by it with those calculated from reasonably well known attachment and loss cross sections for single electrons. Hence, we will assume, with some justification, that:

$$Z_1 = Z_{eff} \text{ (Pierce and Blann)} \qquad \text{IV.29}$$

There exist many other semi-empirical formulae (see Betz, 1972) for Z_{eff} but the differences between them and that of Pierce and Blann are essentially a measure of experimental accuracy, which is of the order of a few charge units. For relativistic heavy ions, where only a small fraction of the ion nuclear charge is neutralized, these errors are quite small compared to higher order Born and Bloch corrections.

In order to evaluate fluctuations in energy loss due to fluctuations in ion charge state it is important to use correct stripping and loss cross sections, such as those given by Betz (1972), for thin absorbers. By thin, we mean small in comparison to the charge equilibration distance, which is of the order of several $\mu g/cm^2$ for low

energy ions. For thick absorbers an ion has ample time to sample its available charge state space and $2\Delta Z_{eff}/Z_{eff}$ is a measure of the energy loss fluctuation where ΔZ_{eff} is the standard deviation of an ensemble of charge states as measured with an ion beam. Nikolaev and Dmitriev (1968) have presented an expression for ΔZ_{eff} for solid strippers:

$$\Delta Z_{eff} = 0.5[Z_{eff}(1-(Z_{eff}/Z_o))^{1.67}]^{\frac{1}{2}} \quad . \qquad \text{IV.30}$$

Betz (1972) gives other semi-empirical expressions but eq. IV.30 has the advantage that it goes to zero as $Z_{eff} \rightarrow Z_o$.

For a discussion of electron capture and loss cross sections in the high energy regime where the probability for loss exceeds by a large amount that for capture, see Wilson (1978), Raisbeck et al. (1977), Reames (1974) and Fowler et al. (1970). This problem is quite important with regard to abundance measurements of cosmic ray nuclei which have a very large branching ratio for nuclear decay via electron capture.

E. Range-Energy Tabulations

There exist a number of theoretical and semi-empirical tabulations of range-energy relations for heavy ions. Barkas and Berger (1967) use empirical proton range data between 1 MeV and 8 MeV and calculate, with the use of the Bethe formula, Walske shell corrections, and Sternheimer density effect corrections, the range from energies up to 5000 MeV down to the 8 MeV empirical cut. Heavy ion ranges are calculated with the expression:

$$R(\beta) = \frac{M_1}{Z_o^2}\,[\lambda(\beta) + B_{Z_o}(\beta)] \qquad \text{IV.31}$$

where $\lambda(\beta)$ is the range of an ideal proton and $B_{Z_o}(\beta)$ is the ion range extension due to electron capture. Low energy heavy ion data are used to estimate B_{Z_o} which necessarily includes higher order corrections. For $\beta > 2Z_o/137$ the range extension is assumed to be constant, and hence, the stopping power above this velocity is assumed to scale as Z_o^2 which, as we know, breaks down for large enough values of Z_o/β. Northcliffe and Schilling (1970) concentrate on low energy heavy ions (<10 MeV/amu) where extensive use is made of experimental data. Benton and Henke (1969) extend the approach of Barkas and Berger to energies below 1 MeV/amu. A minor modification of the range extension is utilized by these authors. Steward and Wallace (1970) divide the Z_1, Z_2, β space into a number of regions with the use of appropriate theoretical and experimental results. The range of kinetic energies extends from 10 to 1000 MeV/amu. Bichsel (1972) calculated ranges for protons based on the Bethe theory with Walske shell corrections. All of the above calculations apply to CSDA (continuous slowing down approximation) ranges, where rectilinear motion is assumed. Multiple scattering corrections and inelastic nuclear collisions modify these results to a small extent for realistic situations.

Fleischer et al. (1975) and Benton and Henke (1969) have used dielectric track detectors to accurately measure ion ranges for $Z_o \leq 26$ and $T < 10$ MeV/amu. In this regime it is found that good agreement with the Benton and Henke (1969) calculations (to within ~2%) is obtained for $T > 0.1$ MeV/amu and that for $T < 0.1$ MeV/amu the Northcliffe and Schilling (1970) tabulations are most accurate. The calculations of Steward and Wallace (1970) are systematically greater than those

of Benton and Henke and of Northcliffe and Schilling as well as those measured values for the low energy region.[35]

At large energies, all calculated ranges agree, being based as they are on the Bethe theory. Small differences in range extensions lead to negligible differences in ranges for large incident energies. Consequently, since the Benton and Henke (1969) algorithm is based on that originally presented by Barkas and Berger (1967), we adopt the latter calculation as that against which measurement should be compared. The reader is cautioned to distinguish between data, calculated ranges and polynomial fits to calculated ranges. There are scant data above 10 MeV/amu. Hence most ranges quoted in this regime are theoretical. Barkas and Berger calculate these theoretical ranges by integrating the Bethe formula exactly down to 8 MeV. They also fit a polynomial in $\log(\lambda)$ vs $\log(E)$ which agrees with the exact integrations to within an rms error of 0.6% with a maximum error of 2.8%. Since there is good reason to believe that above 10 MeV the Bethe theory (with shell corrections and density effect corrections) yields stopping power results which are accurate to much better than 1%, any comparison with experiment should be made with Barkas and Berger's tabulated ranges, rather than with their fitted formulae. It should be emphasized once more that low energy results obtained by Barkas and Berger (below 10 MeV/amu) are based on empirical values which contain electron capture effects, shell corrections, and higher order effects such as second order Born terms and Bloch corrections. The ranges given at these energies can be assumed to be accurate to within a few percent for $Z_1\alpha/\beta \lesssim 1$.

Schimmerling et al. (1973) have measured the ranges of ^{14}N, ^{20}Ne

and ^{40}Ar nuclei at energies up to 284 MeV/amu and have found that within experimental error (~2% in range) the ranges agree with the Barkas and Berger values. Tarlé and Solarz (1978) have performed more accurate range measurements of ^{56}Fe nuclei at 600 MeV/amu in a variety of substances and have found range discrepancies of ~3% with Barkas and Berger results. This is a three standard deviation effect and is approximately consistent with what one would expect if the Bethe formula were modified as in Ahlen (1978a). There is still some doubt as to the validity of the Bloch correction. The results of Tarlé and Solarz indicate that it may be smaller than as given by the non-relativistic form of this correction. In any case, it seems clear that the use of high energy heavy ion beams is a very fruitful means of investigating stopping power phenomena.

F. Multiple Coulomb Scattering

In the preceding we have invariably assumed that the projectile trajectory is well approximated by a straight line. Strictly speaking, this is not the case due to multiple Coulomb scattering. We have also assumed that the particle maintains its identity as it slows down. This is indeed the case in the absence of nuclear interactions. For high incident energies, however, it becomes increasingly probable for the projectile to undergo an identity changing interaction before it comes to rest. In this sub-section we will discuss these effects.

The theory of multiple Coulomb scattering is quite complex and the interested reader is referred to Scott (1963), Hemmer and Farquhar (1968) and Gnedin et al. (1968). For our purposes, it is sufficient to note that the Moliere theory, which is a small angle approximation

to the general problem (Moliere, 1948, 1955), is in agreement with experimental results with the exception of electrons in heavy elements and at small energies ($\beta < 0.05$). Bichsel (1972) gives the square of the characteristic angle for transmission of a charged particle through an absorber of thickness x:

$$\theta_o^2 = 0.157 \frac{Z_1^2 Z_2 (Z_2+1)}{A_2} \frac{\rho x}{(M_1 v^2 \gamma)^2} B \ \text{MeV}^2\text{cm}^2/\text{g} \qquad \text{IV.32}$$

As summarized by Bichsel (1972), B is defined in Moliere (1948). For practical purposes, representative values can be found in Table IV.8 (Marion and Zimmerman, 1967). For $Z_1 = 1$ the values given there are accurate to within 5%. For $Z_o > 1$ Bichsel (1972) recommends use of the effective charge Z_1 instead of the nuclear charge. For $Z_1 \gtrsim 6$ and $Z_2 \gtrsim 50$ all values $B(\beta, Z_1)$ are larger than 0.98 $B(0,1)$ but smaller than $B(0,1)$; for $Z_1 \gtrsim 6$ and $Z_2 \gtrsim 20$ all $B(\beta, Z_1)$ are larger than 0.95 $B(0,1)$ but smaller than $B(0,1)$. The distribution function $xF(x)dx$ for the relative number of particles entering a cone of reduced half angle x ($x = \theta/\theta_o$) and width dx is tabulated by Bichsel (1972). Of more immediate experimental interest is the integral of this function. In Table IV.9 we reproduce this multiple-scattering integral distribution function given by Bichsel (1972) for the fraction of incident particles found inside a cone of reduced half angle x. Note that ~90% of the projectiles are in the cone with half angle $2\theta_o$. For $\beta \sim 0.5$, $\rho x \sim 1$ g/cm^2 and $Z_1/A_1 \sim 0.5$, θ_o is approximately 9.0 mrad for $A_2 = 40$, $Z_2 = 20$. The increased path length due to this multiple scattering should be considered in evaluation of accurate stopping power experiments.

Small angle Coulomb scattering is also a consideration in experiments for which the total range for a particle with a given initial energy is measured. In such cases the actual range or pathlength is somewhat larger than the penetration depth because of the multiple scattering. An estimate of the size of this effect can be found in the review article by Fano (1963). If the actual pathlength is denoted by s and the penetration depth by t then one has approximately:

$$\frac{\langle s-t\rangle}{s} = Z_2 \frac{m}{M_1} \langle \ell \rangle \qquad \text{IV.33}$$

where $\langle \ell \rangle$ is a suitably averaged quantity which lies between 0.3 and 0.6. For the worst case (say protons on lead), the pathlength is roughly 2% larger than the penetration depth. For heavier particles, such as we consider in this review, the effect is usually negligible. It should be emphasized that the fractional range correction eq. IV.33 is independent of the charge of the projectile. This is so because ρx scales as A_1/Z_1^2 for a given velocity. This factor cancels Z_1^2 in eq. IV.32.

The above remarks are concerned with average scattering parameters. There is always the possibility that a very massive projectile will undergo a large angle scattering collision with an absorber nucleus. Note the famous Rutherford experiments in which the nuclear atom was discovered by the observation of these very collisions. However, the Rutherford cross section is strongly peaked in the forward direction and such collisions are quite rare. If one assumes unscreened Coulomb scattering from the nuclei, the Rutherford cross section yields the following approximate mean free path for scattering through an angle

larger than θ_o (measured in degrees):

$$\bar{\ell}(\theta_o) = (0.032\text{cm}) \frac{\beta^4 (\theta_o/\text{deg})^4}{\rho Z_2} \frac{g}{cm^3} \qquad \text{IV.34}$$

It has been assumed that the incident particle and the nucleus both have A/Z = 2 and it has also been assumed that $A_2 >> A_1$ so that θ_o is the lab scattering angle. For θ_o = 10 deg, β = 0.5, Z_2 = 10 and ρ = 3 g/cm^3, $\bar{\ell}$ = 0.7 cm. For θ_o = 20 deg, $\bar{\ell}$ = 11 cm. The large angle scattering events occur about as frequently as do nuclear interactions to which we now briefly turn our attention.

G. Nuclear Interactions

If the projectile is hadronic (i.e. a nucleon, nucleus, pion, etc.) it can interact with the matter it is traversing via the strong nuclear force. Electrons and muons, being leptons, do not interact via this mechanism. At low energies (<20 MeV/amu) nuclear interaction cross sections are characterized by a strong energy dependence caused by compound nucleus effects. At these energies, neutron stripping reactions are preferred (due to the absence of a Coulomb penetration factor for the neutron). At large energies ($\gtrsim$1 GeV/amu) the cross sections approach asymptotic values which are determined by geometrical factors. The Bradt Peters (1948) relation is a useful expression for evaluating the total inelastic nuclear cross section for two colliding nuclei. More accurate expressions are available (see Karol, 1975) but are not necessary for our purposes here. The Bradt Peters expression is the geometrical cross section with a provision requiring an overlap of the nuclei in order for them to interact:

$$\sigma = \pi(R_1 + R_2 - 2\Delta R)^2 \qquad \text{IV.35}$$

where,

$$R_i = 1.45\ A_i^{1/3}\ F \qquad \text{IV.36}$$

and $\Delta R = 0.85$ F. In Table IV.10 we list the mean free path for interactions given by eq. IV.35 in units of the range of a 1 GeV/amu projectile of the appropriate type in the given material. It is seen that fewer interactions occur in bringing a nucleus to rest as Z_1 and Z_2 increase.

Fragments produced in high energy collisions are most likely to be stripped of only a few nucleons. See Silberberg and Tsao, 1973 for a summary of theoretical and experimental partial cross sections. The distributions in fragment transverse and longitudinal momenta have been measured by Greiner et al. (1975) for ^{12}C and ^{16}O projectiles up to 2 GeV/amu. They found that for peripheral reactions fragments of the projectile have the same momentum per nucleon as the incident particle to within 0.1%. The distributions for transverse and longitudinal momenta of the fragments in the projectile rest frame are Gaussian with a standard deviation from 90 to 160 MeV/c (this is <u>not</u> momentum per nucleon). The distributions are consistent with isotropy in the projectile frame.

V. MAGNETIC MONOPOLE STOPPING POWER

Ever since the prediction of its existence by Dirac (1931) the magnetic monopole has been the subject of numerous papers. Stevens (1973) has compiled a bibliography of 181 references up to 1973 and Carrigan (1977) has supplemented this with a bibliography of 323 references for the period 1973 to 1976. The recent surge of publications can be attributed to excitement generated by the monopole candidate detected by Price et al. (1975) and to theoretical breakthroughs by 't Hooft (1974) and Polyakov (1974). Although it is now generally accepted that the Price event was probably not caused by a magnetic monopole (Price et al., 1978) it seems that there is sufficient interest in magnetic monopoles as hypothetical particles to warrent inclusion of their effects on matter in this Review. It is beyond the scope of this work to delve too deeply into the particle theory of monopoles or into searches for these particles.[36] We merely summarize some of the more salient features. Most monopole theories quantize magnetic and electric charge:

$$2g = ne/\alpha \qquad V.1$$

where $n = \pm 1, \pm 2, \ldots$ in the Dirac (1931) theory and $n = \pm 2, \pm 4, \ldots$ in the Schwinger (1975) theory. Ever since the introduction of the monopole conjecture it has been assumed that the monopole mass must be very large due to its large self energy. The 't Hooft theory confirmed this with the result that M(monopole) $\approx$ 137 M(intermediate vector boson) which has a plausible range of 5-10 TeV/c^2 (Carrigan, 1977). Dirac (1931) recognized that the rate of energy loss by monopoles

should be very large due to its large value of $g(\pm(137/2)e, \pm 137e, \ldots)$. He also pointed out that the rate of ionization would not increase near the end of range as it does for ordinary nuclei. This is easily seen to be the case when one recognizes that the electric field of a moving monopole as seen by an atomic electron is proportional to β. Stopping power is proportional to the square of the field and this β^2 term cancels the β^2 denominator term which causes the increase of electric particle ionization.

Accurate theories of monopole stopping power have lagged behind their electric particle counterparts for several reasons. It has been assumed that experimental searches relying on identification based on ionization rates would not be subject to a background due to the large value of g. Hence, very accurate knowledge of stopping power should not be required. There have also been problems of a fundamental nature regarding the proper means by which monopoles should be handled within a quantum mechanical framework. Recent developments have alleviated these theoretical problems to a considerable degree and it is now well known that the very heavy component of the cosmic radiation can, under suitable conditions, mimic the behavior of a monopole with a charge as large as 137e. Therefore, it is fitting to carefully consider the manner in which monopoles lose energy in matter.

Bauer (1951) and Cole (1951) were the first to extend electric particle stopping power theories to magnetic charges. Bauer (1951) calculated non-relativistic stopping power for monopoles both via a semi-classical technique (as in Jackson, 1975 for electric charges)

and via the Bethe (1930) technique wherein the monopole-electron interaction was taken to be given by the non-relativistic classical dipole interaction. In both cases he obtained, approximately:

$$S_m = \frac{4\pi N e^2 g^2}{mc^2} \ln \frac{2mv^2}{I} \qquad V.2$$

Cole (1951) followed Bohr (1913) to obtain:

$$S_m = \frac{4\pi N e^2 g^2}{mc^2} \ln \frac{1.61 mv^2 \hbar c}{geI} \qquad V.3$$

for the non-relativistic result. Note that with g = 137e, ($g = \hbar c/e$), Cole's value is essentially the same as Bauer's.

Tompkins (1965) adopted Fermi's (1940) classical electrodynamical single oscillator approach to calculate the distant collision energy loss for magnetic monopoles. He made no attempt to calculate the close collision energy loss.

Martem'yanov and Khakimov (1972) used the technique of Landau and Lifshitz (1960) to calculate monopole energy loss in conductors and ferro-magnetic materials. They assumed three separate projectile velocity intervals and obtained:

$$S_m = \begin{cases} \dfrac{4\pi^2 N v e^2 g^2}{mc^2 v_e Z_2}, & v \lesssim v_o \\ \dfrac{4\pi N^* e^2 g^2}{mc^2} \left[\ln \dfrac{2m^2 v^2 \sigma_o}{N^* e^2 \hbar} - \dfrac{1}{2}\right], & v_o < v < c \\ \dfrac{4\pi N e^2 g^2}{mc^2} \ln \dfrac{1.213 mc^2 \gamma}{\hbar \omega_p} & v \to c \end{cases} \qquad V.4$$

where v_o is a characteristic orbital electron velocity, v_e is the conduction electron Fermi velocity, σ_o is the zero frequency conductivity

and N^* is an effective electron number density which approaches N as $v \to c$.

Ahlen (1976) has used the relativistic classical cross section of Lapidus and Pietenpol (1960) to show that the monopole delta ray production cross section is given by:

$$\frac{dn}{dwdx} = \frac{2\pi Ne^2g^2}{mc^2w^2}(1+\lambda) \qquad V.5$$

where $\lambda \approx 0.08$ for the impact parameter $b = \hbar/(mv\gamma)$ and falls rapidly to zero as w becomes smaller. For $g = 137e$ the value of w for the de Broglie impact parameter is smaller than the kinematically limited energy transfer. This prompted Ahlen (1976) to insert $\hbar/(mv\gamma)$ into Tompkin's formula for the minimum impact parameter to obtain the following expression for total energy loss in non-conductors:

$$S_m = \begin{cases} \frac{4\pi Ne^2g^2}{mc^2}\left[\ell n\left(\frac{1.123mc^2\beta^2\gamma^2(\varepsilon-1)^{\frac{1}{2}}}{\hbar\omega_p}\right) - \frac{1}{2}\right], & \beta < \frac{1}{\sqrt{\varepsilon}} \\ \frac{4\pi Ne^2g^2}{mc^2}\left[\ell n\left(\frac{1.123mc^2\beta\gamma}{\hbar\omega_p}\right) + \frac{1-1/\beta^2}{2(\varepsilon-1)}\right], & \beta > \frac{1}{\sqrt{\varepsilon}} \end{cases} \qquad V.6$$

where ε is the low frequency dielectric constant. Note that as $\beta \to 1$, eq. V.6 is equal to eq. V.4 to within less than one percent.

It is difficult to compare any of the above stopping powers with those of electrically charged particles beyond saying that for a given velocity the monopole stopping power is $\sim(g\beta/Z_1)^2$ times bigger than that of an electric particle with charge Z_1e. More accurate conclusions can be reached only if as careful a treatment is applied to monopole-atom interactions as is done for the heavy ionizing electrical

counterpart. This is certainly not the case in any of the above treatments. The most severe problem has been the lack of knowledge of how to treat the close collisions. We have seen in the previous section how the correct Mott cross section predicts a close collision stopping power which is 40% larger than that given by the Rutherford cross section for $Z_o = 92$, $\beta \sim 1$. Since a monopole with $g = 137e$ is even more heavily ionizing than a relativistic uranium nucleus it might be expected that higher-order quantum electrodynamics would have an even more profound effect on monopole stopping power. The absence of a good theory for electron-monopole interactions in the relativistic regime prevented analysis of this problem until Kazama, Yang and Goldhaber (1977) managed to obtain a solution to the Dirac equation for an electron moving in the magnetic field of a fixed monopole. Ahlen (1978b) has used this cross section to obtain the close collision monopole energy loss for $|g| = 137e/2$ and for $|g| = 137e$. By using the semi-classical approach of Landau and Lifshitz (1960) for the distant collisions, assuming the validity of the magnetic analog to Bethe's generalized sum rule, and considering the Bloch correction to be valid for monopoles with the proviso $Z_1 e \to g\beta$, Ahlen has obtained the following expression for monopole stopping power in non-conductors:

$$S_m = \frac{4\pi N e^2 g^2}{mc^2} \left[\ell n \frac{2mc^2\beta^2\gamma^2}{I_m} + K(|g|)/2 - \frac{1}{2} - \delta_m/2 - B(|g|) \right] \qquad V.7$$

where $K(|g|)$ is the Kazama et al. cross section correction:

$$K(|g|) = \begin{cases} 0.406, & |g| = 137e/2 \\ 0.346, & |g| = 137e \end{cases} \qquad V.8$$

$B(|g|)$ is the Bloch correction:

$$B(|g|) = \begin{cases} 0.248, & |g| = 137e/2 \\ 0.672, & |g| = 137e \end{cases} \qquad V.9$$

and I_m, δ_m are the mean ionization potential and density effect corrections which apply for magnetic monopoles. Ahlen (1978b) has shown that $I_m \to I$ and $\delta_m \to \delta$ for gases. For non-conductors he has shown that I_m is independent of density. This is due to the absence of longitudinal dielectric screening for the monopole-electron interaction.[37] For comparison with their electric counterparts we give I_m and δ_m in terms of the parameter ρ defined earlier:

$$\ell n I_m = \frac{2}{\pi \omega_p^2} \int_0^\infty \omega \, \mathrm{Im}[\varepsilon(\omega)] \, \ell n \hbar\omega \, d\omega \qquad V.10$$

$$\delta_m = \frac{2}{\pi \omega_p^2} \left\{ \int_0^\infty \omega \, \mathrm{Im}[\varepsilon(\omega)] \, \ell n\left(1 + \frac{\rho^2}{\omega^2}\right) d\omega - \frac{\pi}{2} \rho^2 (1-\beta^2)/\beta^2 \right\} \qquad V.11$$

Ahlen (1978b) gives arguments that eq. V.7 is accurate to ±3% for $\beta \gtrsim 0.2$ (for which shell corrections are small) and for $\gamma \lesssim 100$ if the electrical values of I and δ are used. He emphasizes that higher order Born corrections to the distant collisions are independent of the sign of the monopole charge due to symmetry. By comparing the analogous corrections for electrically charged particles he shows that this correction should be less than 1% to stopping power for $|g| = 137e$. Similar arguments apply to Lindhard's close collision polarization corrections. Finally, Ahlen shows that it is completely legitimate to neglect the electron spin in the distant collisions (at the $\lesssim$1%

level in total stopping power) for $Z_2 < 82$, $\beta > 0.04$ and $\gamma < 25$. As we have previously mentioned, the radiative corrections for electric charges apply equally to massive monopoles.

To this list we should add that: 1) for $\gamma = 100$ bremsstrahlung contributes ~5% of the total energy loss for $Z_2 = 82$, $M_1c^2 = 5$ TeV and $|g| = 137e$; this fraction scales linearly with $Z_2\gamma$ so that for most cases bremsstrahlung can be completely neglected; 2) the effect of any monopole spin should be much less than for the corresponding electric charge case due to the incredibly small monopole charge to mass ratio for 't Hooft type monopoles; 3) unless the monopole has complex structure analogous to that of nuclei, any internal structure effects must be completely negligible for $\gamma < 100$.

In Fig. V.1 we plot S_m for $|g| = 137e$ monopoles in water. Shell corrections will probably become important for $\beta < 0.1$ but interpolation between $\beta = 0$ and $\beta = 0.1$ should give reliable results since the monopole ionization rate is a monotonically increasing function of velocity. The parameters used for eq. V.7 were taken from Sternheimer (1956) where we assume $I_m = I$ and $\delta_m = \delta$. For comparison the technique from Ahlen (1976) has been used to calculate S_m. The separation of the two curves at low velocities is due primarily to the Bloch correction. The two curves join at large γ due to the different manner in which the density effect correction was calculated.

Ahlen (1978b) points out that theoretical knowledge of monopole stopping power will not be on as firm a footing as its electric particle analog until the following tasks are accomplished: 1) derivation of the magnetic analog to Bethe's generalized sum rule and 2) calculation of the Bloch correction for monopoles.

VI. RESPONSE OF THE ABSORBING MEDIUM TO HEAVILY IONIZING PARTICLES

A. Nature of the Excitation of the Absorbing Medium

In the previous sections the behavior of the projectile was the principal object of our attention. In this section we briefly consider the effect which the penetrating projectile has on the material through which it passes in terms of ionization and excitation phenomena. It is beyond our means to do full justice to this subject which encompasses the diverse fields of radiation physics, chemistry and biology. We will restrict our treatment to those aspects which are relevant to the relativistic heavily ionizing particles which are of primary concern in this Review. Related topics are covered by Box (1972) ("Radiation Damage Mechanisms as Revealed Through Electron Spin Resonance Spectroscopy"), Upton (1968) ("Effects of Radiation on Man"), Ginoza (1976) ("The Effects of Ionizing Radiation on Nucleic Acids of Bacteriophages and Bacterial Cells"), and Mole (1965) ("Dose Response Relationships, Particularly in Mammalian Radiobiology"). Extensive references can be found in these review articles.

A proper understanding of the response of any system to radiation requires knowledge of the spatial distribution of the deposited energy. To a first approximation, the stopping power is a convenient parameter which characterizes the behavior of biological systems and particle detectors in response to excitation by charged particles. It has generally been observed that these objects are affected to an extent which increases with increasing values of S, for a given system linear dimension. However, it is usually not the case that the effect increases linearly with S nor is it generally true that the effect is the same

for two different types of particles with the same value of S. Some specific examples include the saturation of scintillators (Birks, 1964) and the notion of a critical dose for the degradation of certain polymeric substances (Golden and Hazel, 1963). Scintillator saturation has been satisfactorily explained in terms of a spatial dependence of scintillation conversion efficiency (Ahlen et al., 1977 and Becchetti et al., 1976) and the concept of a critical dose can be explained qualitatively in terms of a multi-hit Poisson process (Katz and Kobetich, 1968). It is apparent that any successful theoretical approach to an understanding of these phenomena must include a description of the volume distribution of energy deposition, rather than simply appeal to the projectile parameter S.

An ideal theoretical description of the effects of charged particle penetration in matter would include the volume densities as a function of position and time for all species: these would include excited and ionized atoms and molecules, free electrons, free radicals and other radiation induced chemical reaction by products. Needless to say this is a formidable task which is nowhere near being solved. The extreme complexity of the problem has rendered it susceptible to only the crudest theoretical and experimental analysis. In this section we will be content to discuss only the prompt dose. This is defined to be the energy deposition per unit volume (or mass) due to excitation and ionization caused by the primary particle and secondary, knock-on electrons (i.e. primary and secondary excitation and ionization). The time required for this phase is very short, namely $\sim 10^{-15}$ s. There are a host of delayed energy transport processes

which serve to dilute the prompt dose at any given point. Among these processes are Auger electron emission, x-ray fluorescence, optical fluorescence, exciton migration, long range resonance interactions, radiative emission and reabsorption and chemical and thermodynamic equilibration processes. These effects serve to smear the prompt dose isotropically. Their relative effectiveness depends strongly on the absorbing medium and in certain instances the observed response to deposited energy is the direct manifestation of one or more of these processes.

There has been a great deal of work done on the calculation and measurement of dose in connection with the radiation effects of heavy nuclei on biological systems and nuclear emulsions. Much of the early theoretical work (Bizzeti and Della Corte, 1959, Katz and Butts, 1965, Kobetich and Katz, 1968, Katz and Kobetich, 1969 and Katz et al., 1972) has been based on a model in which energy is transferred away from the particle trajectory by a line source of knock-on electrons. Various assumptions regarding binding effects, electron range and transmission formulae and electron emission angle have been employed. Katz et al. (1972) summarize these assumptions and indicate that the result:

$$D = \frac{NZ_1^2 e^4}{mv^2} \left[\frac{1}{r^2} - \frac{1}{r\tau}\right] \qquad \text{VI.1}$$

is relatively insensitive to the above assumptions. D is the secondary dose in units of energy per unit volume, r is the perpendicular distance from the particle trajectory and τ is the maximum range of the maximum energy delta ray. The above expression has been evaluated to lowest order in the ion-electron interaction strength. Effects of

higher order Born terms are discussed by Jensen et al. (1976). Various groups have tested eq. VI.1 with nuclear emulsions (Jensen et al., 1976, Jacobsson and Rosander, 1974 and McNulty and Filz, 1977) and have found that it is in good agreement with experiment for $Z_1 \lesssim 26$ and $\beta \lesssim 0.8$.

Fowler (1977) uses a slightly modified version of eq. VI.1 for analysis of ultraheavy cosmic ray data. He shows that x-ray fluorescence and Auger emission contribute ~10% of the dose in emulsions for $5\mu < r < 100\mu$ and obtains the empirical result:

$$D = A \frac{Z_1^2}{\beta^2 r^2} \exp(-10.3r^2/\tau^2) \qquad \text{VI.2}$$

where A is a constant. This result relies on the assumption that dose is proportional to the number of developed grains per unit volume, which is the quantity measured with emulsions. In view of the large fluctuations in dose which are to be expected at large distances from the particle trajectory it is not surprising that eq. VI.1 and 2 differ nor that omission of Auger emission and x-ray fluorescence does not seriously affect the validity of eq. VI.1. The use of free parameters to describe grain sensitivity also serves to shroud the accuracy of the above expressions. Hagstrom (1977) describes a Monte Carlo program which should be quite helpful in evaluating these secondary dose effects.

The above expressions should not be trusted for those values of r which are excluded from experimental verification by emulsion measurements. Since grain diameters are of the order of 1 micron, this should be chosen as the minimum value of r. Chatterjee et al. (1973)

and Paretzke (1977) have emphasized the importance of the distant collisions in determining track structure for biological and non-living organic systems respectively. These collisions were not included in the above mentioned emulsion dose models since they are important only for doses well within 1 micron. Chatterjee et al. (1973) and Chatterjee and Schaefer (1976) describe a technique for calculating the prompt dose which includes 3 classes of collisions: 1) distant collisions ($b \gtrsim 1\text{Å}$); 2) intermediate collisions with electron kinetic energies between 100 eV and 1600 eV which subsequently undergo a random walk in becoming thermalized and 3) close collisions which result in electron energies greater than 1600 eV; these electrons undergo linear motion with an ejection angle given by classical non-relativistic kinematics. The resultant particle track is considered as two regions, the core and penumbra. The core is the small cylinder containing the atoms which suffer distant collisions while the penumbra is the region familiar to emulsion workers wherein secondary processes determine the radiation effects. Chatterjee and Schaefer (1976) give the following expressions for water:

$$D_c = \frac{LET_\infty}{2\pi r_c^2} + \frac{LET_\infty}{4\pi r_c^2 \ell n(\sqrt{e}\,\frac{r_p}{r_c})}, \quad r < r_c$$

$$D_p = \frac{LET_\infty}{4\pi r^2 \ell n(\sqrt{e}\,\frac{r_p}{r_c})}, \quad r > r_c \qquad \text{VI.3}$$

where r_c and r_p are the core and penumbra radii respectively:

$$r_p = (0.768T - 1.925\sqrt{T} + 1.257) \text{ microns}$$

$$r_c = 0.0116\beta \text{ microns} \qquad \text{VI.4}$$

where T is the ion energy in MeV/amu. LET_∞ is simply the stopping power of the ion. It is seen that the penumbra dose is quite similar to those given by eq. VI.1 and 2. Furthermore, it is seen that the core dose has been averaged over a cross section of radius r_c, the first term being due to distant collisions and the second being due to scattered high energy secondary electrons.

The core contribution to the dose has been generally neglected. Katz et al. (1972) go so far as to discount it due to detector saturability and Chatterjee and Schaefer (1976) have, as we saw above, simply averaged it over the core radius. In view of the fact that completely satisfactory descriptions of the response mechanisms for most systems remain to be given, it seems somewhat premature to disregard a significant source of energy deposition a priori. As has been mentioned above, there exist a multitude of energy migration processes which are capable of removing the energy from the region of high detector saturability, should such a region exist. The high degree of linear response commonly encountered with gaseous and solid state ionization detectors is perhaps the best indication that full account must in general be taken of all types of energy deposition.

It is quite straightforward to calculate the primary dose. As Fano (1970) has indicated, the classical Bohr expression for energy transfer to an atom (eq. III.1) is equivalent to that given by a quantal calculation. The quantal approach is necessary, however, in

order to determine the spectrum of excited and ionized states. When this is done it is found that the most likely prognosis for a hydrogenic atom at impact parameter $b >> r_o$ is that nothing at all will happen to it. This is in fact the criterion for the validity of a perturbation treatment. If something does happen to the atom, it is most likely for it to be excited but not ionized. There is a reasonably probability for it to be ionized, however, in which case the most probable final state kinetic energy is 1/12th the binding energy. Beyond this the kinetic energy distribution of ejected electrons drops off more rapidly than $1/w^4$ and the relative probability that the kinetic energy exceeds the binding energy is less than 10^{-3}. In view of the fact that the close collision ionization cross section is smaller by no more than an order of magnitude than that for distant collisions and that the close collision delta ray spectrum falls off only as $1/w^2$, it is safe to conclude that of all high energy knock-on electrons with kinetic energy greater than the binding energy which are produced by the passage of the charged particle, no more than one in a hundred are created in a distant collision event. To quote Merzbacher (1972): "In these collisions the electron likes best to take on as little energy as possible. It prefers just barely to get out of the atom - that's overwhelmingly the most probable situation." Thus, it is quite reasonable to extend the division of the distant and close collisions to apply to dose deposition. The close collisions are almost exclusively responsible for secondary excitation and ionization while the distant collisions principally produce only primary excitation and ionization. As Fowler (1977) points out, Auger emission and x-ray fluorescence contribute a significant penumbra, or halo dose in

emulsion, of the order of 10%. This contribution should not be so great in water or organic compounds.[38] By extending eq. III.1 to a multi-electron atom, the prompt primary dose is seen to be:

$$D_p(r) = \frac{2NZ_1^2e^4}{mv^2r^2} \sum_{E_k} f_k[\xi_k^2K_1^2(\xi_k) + \frac{1}{\gamma^2}\xi_k^2K_o^2(\xi_k)] \qquad VI.5$$

where $\xi_k = (\omega_k r)/(\gamma v)$, $E_k = \hbar\omega_k$ is the kth excited energy level (the ground state has zero energy), K_o and K_1 are the modified Bessel functions of order 0 and 1 respectively and $f_k = 2m\hbar\omega_k|X_k|^2/(\hbar^2 Z_2)$ where $|X_k|^2$ is the sum of $|\sum_{i=1}^{Z_2} \langle k|x_i|0\rangle|^2$ over the degenerate substates which have energy E_k. The sum in eq. VI.5 is over energy levels, not states. The Bessel functions drop off exponentially for large arguments which means that excitation of the kth energy level extends to a radius:

$$r_k = \frac{\gamma v}{\omega_k} \qquad VI.6$$

beyond which excitation becomes quite inefficient due to the Adiabatic Theorem.

It is quite easy to extend the treatment above to magnetic monopoles. The primary prompt dose is given by:

$$D_p^m(r) = \frac{2Ne^2g^2}{mc^2r^2} \sum_k f_k \xi_k^2 K_1^2(\xi_k) \qquad VI.7$$

In Fig. VI.1 we plot the functions $F(\xi) = \xi^2K_1^2(\xi)$ and $G(\xi) = \xi^2K_o^2(\xi)$. It is seen that for small values of $\xi(\lesssim 0.5)$, $F(\xi) + G(\xi) \approx 1$ and for large arguments, $F + G \approx 0$. Since $G(\xi) \to 0$ as $\xi \to 0$ we see that the

primary monopole dose is $(g\beta/Z_1 e)^2$ times that of its electric particle counterpart. Since this is the same ratio of the classical free electron scattering cross sections we would expect a similar correspondence of doses in the penumbra, to a first approximation. In Fig. VI.2 we plot prompt dose profiles for a water absorber divided by Z_1^2 (we neglect higher order corrections). Curves A and B are primary doses for $\beta = 0.1$ and 0.9 respectively from eq. VI.5 with the relevant values of f_k and ω_k from Sternheimer (1952). Curves C and D are secondary doses for $\beta = 0.1$ and 0.9 respectively as calculated by Kobetich and Katz (1968). The dose is in units of Mrad where 1 rad = 100 ergs/g. For comparison we also show the small radius limit $2NZ_1^2 e^4/(mv^2 r^2)$ and the large radius limit which is 1/2 of this.

It should be emphasized that for the prompt doses of Fig. VI.2 energy transfer mechanisms have been neglected. Furthermore, polarization effects have been neglected so that no consideration of the density effect nor Cerenkov emission has been included.[39] This should limit the validity to velocities less than ~0.9 for solids. The velocity should be limited from below by $\beta \sim 0.1$ at which point the separation of distant and close collisions starts being invalid.

The above discussion has been limited to the micro-and sub-microscopic spatial distribution of energy deposition. It is sometimes of interest to have some idea of macroscopic features of energy deposition insofar as it affects the fraction of the energy lost by a particle in a thin absorber which is actually deposited in the absorber. Some energy is carried out by optical and x-ray fluorescence radiation, Cerenkov radiation, Auger electrons and delta-rays. Scintillation and

Cerenkov counters utilize the escaping optical radiation in order to ascertain various particle properties such as charge and velocity.[40] At all velocities (even as $\beta \to 1$) the fraction of total loss which escapes a solid absorber as Cerenkov radiation is quite small. By using a realistic atomic model, Sternheimer (1953a) has shown that the fraction of total energy loss which escapes a silver bromide grain (diameter ~0.2μ) as Cerenkov radiation is 0.1% (this includes radiation at all frequencies). The most efficient inorganic and organic scintillators have energy conversion efficiencies of 25% (ZnS(Ag)) and 5% (anthracene) respectively (Williams, 1972). Specially prepared plastic scintillators have an efficiency of 3% for minimum ionizing radiation. However, the large majority of solids have much smaller efficiencies than for these special materials due to the predominance of non-radiative de-excitation mechanisms (Birks, 1964). Thus, in general, optical fluorescence can be ignored as a source of escaping energy. Similarly x-ray fluorescence and Auger electron emission are inefficient means of energy removal for all but the thinnest absorbers. The mean free path of a carbon (or oxygen) KL x-ray is of the order of 100 Å in plastic (or water) (Morgan and Turner, 1972). The practical range of an inner shell carbon (or oxygen) Auger electron is of the order of 300 Å in plastic (or water) (Bichsel, 1972). Hence, an absorber with thickness greater than ~10 μ will have less than 1% of the deposited energy removed by fluorescence x-rays and Auger electrons. The only efficient means by which energy can be removed from absorbers of non-negligible thickness is via emission of delta rays. Laulainen and Bichsel (1972) have analyzed this problem in detail. They present results of numerical

analysis in which the amount of energy removed by delta rays is given for various absorbers as a function of absorber thickness. It is possible, with the aid of several mathematical approximations, to obtain an analytical expression which agrees with the numerical results to within 5% for removed energy. We present here for the first time the details of this calculation.

We first note that since the delta ray effect to be discussed amounts to less than 10% of the energy lost by the particle in the detector, a crude theory of the electron escape energy will suffice. If this theory is accurate at the 10% level, the error in the energy lost to the detector will be good to ~1%. Thus, it is sufficient to use the Rutherford cross section to describe delta ray production. Consider a particle normally incident on an absorber of thickness t. Let R(w) be the average penetration of an electron with energy w into the absorbing material. If we define R(w) to be the depth for which the transmission probability is equal to 0.5 then:

$$R(w) = hAw[1 - \frac{B}{1+Cw}] \qquad \text{VI.8}$$

where h, A, B and C are empirical constants determined by Kobetich and Katz (1968) and which describe R(w) adequately (i.e. better than 10%) for 300 eV < w < 10 MeV. A, B and C are relatively insensitive to material type and are given by A = 0.537 g/cm^2/MeV, B = 0.9815 and C = 3.123/MeV for aluminum. h is given by:

$$h = 0.63Z_2/A_2 + 0.27 \qquad \text{VI.9}$$

To facilitate calculation we make the approximation:

$$R(w) = aw^{\lambda} \qquad \text{VI.10}$$

It is well known that this is a good approximation for a limited range of energies in any given energy region. λ and a must be chosen to correspond to the appropriate region. Finally, we assume that the angular distribution of ejected electrons is given by the non-relativistic expression:

$$\cos\theta(w) = \sqrt{w/w_m} \qquad \text{VI.11}$$

where $w_m = 2mc^2\beta^2\gamma^2$. For the projectile at position X within the absorber we define $w_1(X)$ by:

$$(t-X)\ \sec\theta(w_1) = R(w_1) \qquad \text{VI.12}$$

If $w > w_1(X)$ the delta ray will escape and remove some energy from the absorber. If $w < w_1(X)$ all of the energy is deposited in the absorber. It should be noted that these statements pertain to the <u>average</u> behavior. Let w_r be the amount of energy removed.

$$w_r = w[1 - (\frac{w_1}{w})^{\lambda+\frac{1}{2}}]^{1/\lambda} \qquad \text{VI.13}$$

The total amount of energy removed is:

$$\delta = \int_0^t dX \int_{w_1}^{w_m} dw\ \frac{K}{w^2}\ w_r \qquad \text{VI.14}$$

where $K = \dfrac{2\pi N Z_1^{\,2} e^4}{mv^2}$.

A fair amount of manipulation leads to:

$$\delta = K(\lambda+\tfrac{1}{2})\ R(w_m) \int_0^{s_o} s^{\lambda-\frac{1}{2}}\, ds \int_s^1 \frac{dy}{y}[1-y^{\lambda+\frac{1}{2}}]^{1/\lambda} \qquad \text{VI.15}$$

where $s_o = 1$ if $t > R(w_m)$ and $s_o = [t/R(w_m)]^{\frac{2}{2\lambda+1}}$ if $t < R(w_m)$. We approximate $[1 - y^{\lambda+\frac{1}{2}}]^{1/\lambda}$ by $1 - \frac{1}{\lambda} y^{\lambda+\frac{1}{2}}$. For large s, $\int_s^1 \frac{dy}{y}[1 - y^{\lambda+\frac{1}{2}}]^{1/\lambda} = J$ is small and for small s, J is dominated by the 1/y factor. In each case, negligible error is introduced by the above approximation. Some more algebra yields:

$$\delta = R(w_m)\ K[\frac{t}{R(w_m)}]\ \frac{1}{\lambda(\lambda+\frac{1}{2})}\ [\lambda-1+\tfrac{1}{2}[\frac{t}{R(w_m)}] - \lambda \ell n[\frac{t}{R(w_m)}]] \qquad \text{VI.16}$$

where

$$[\frac{t}{R(w_m)}] = \begin{cases} t/R(w_m) & t < R(w_m) \\ 1 & t > R(w_m) \end{cases} \qquad \text{VI.17}$$

and the best choice for λ corresponds to w_m since this is the most efficient energy for escape:

$$\lambda = 1 + \frac{w_m BC}{(1+Cw_m)^2 - B(1+Cw_m)} \qquad \text{VI.18}$$

$R(w_m)$ should be taken from eq. VI.8. Results obtained from eq. VI.16 are compared with those from Laulainen and Bichsel (1972) for the case of protons on "thick" aluminum ($[t/R(w_m)] = 1$) in Table VI.1. The agreement is seen to be quite good.

We should emphasize that all of the dose effects discussed in this section pertain to average behavior. Consideration of the distribution of these effects requires a greater expenditure of effort.

Monte Carlo programs such as described by Hagstrom (1977) should be quite useful in determining the statistics involved with dose distributions. Further refinement would include the exact Mott or Kazama, Yang, Goldhaber scattering cross sections rather than the usual approximate relations. Ultimately, any theory must be tested fully before it should be trusted. One potential problem which does not seem to have been considered is that, for very heavily ionizing collisions, Bloch type corrections in differential form will be required to evaluate the CM electron scattering cross sections. It must be realized that even close collisions between bound electrons and heavy nuclei (or anti-nuclei or monopoles) are likely to exhibit features not present in free plane wave electron scattering off of these same objects.

Having concluded our discussion of energy deposition, we next consider how this relates to response mechanisms for various charged particle detectors.

B. Charged Particle Detectors

In this sub-section we will describe various charged particle detectors which are currently in use. We will be emphasizing the underlying physical mechanisms which determine the response of a system to radiation. Such an understanding is required for accurate extrapolation of response curves to untested domains.

1. Cerenkov Counters

Cerenkov radiation was discovered by Vavilov (1934) and Cerenkov (1934). Tamm and Frank (1937) developed a classical theory for this radiation which has since been explained by Ginsburg (1940) in terms

of quantum mechanics. Fermi (1940) demonstrated that Cerenkov radiation is just that component of the distant collision energy loss which escapes to infinity. In most simple terms, Cerenkov radiation is an electromagnetic shock wave which is emitted by a charged particle which moves through a medium at a velocity greater than the velocity of light in the medium. As such it propagates at an angle θ relative to the particle direction which is given by the Mach relation:

$$\cos\theta(\omega) = v_{light}(\omega)/v_{particle} = \frac{1}{\beta n(\omega)} \qquad \text{VI.19}$$

where ω is the circular light frequency. The number of photons per unit wavelength (where wavelength is defined by $\lambda = 2\pi c/\omega$) per unit distance traveled by the projectile was obtained by Tamm and Frank (1937):

$$\frac{dN}{d\lambda dx} = 2\pi\alpha Z_1^2[1 - \frac{1}{n^2\beta^2}]/\lambda^2 \qquad \text{VI.20}$$

A classical derivation of the above expression is given by Jackson (1975). A quantum electrodynamical derivation of eq. VI.20 is quite simple as well as being very instructive. We will briefly sketch such a derivation.

It is straightforward to show that non-absorbing dielectrics are characterized by a quantized vector potential which is given by eq. III.10 with c replaced by $c/\sqrt{\varepsilon}$. This results in a modified dispersion relation: $k^2 - \varepsilon\omega^2/c^2 = 0$. It is well known that energy momentum conservation forbids the emission of photons by particles moving in vacuum with uniform velocity. However, as will be seen below, this is not the case for particles moving in matter.

We consider the rate for production of photons with energy $\hbar\omega$ and momentum $c\vec{k}$ with the dispersion relation above. It is easy to show that momentum and energy are thus conserved if the emission angle is given by eq. VI.19 with $n = \sqrt{\varepsilon}$. By using the techniques outlined in section III it can be shown that the probability per unit time of producing a photon of momentum $\hbar\vec{k}$ and polarization $\hat{\varepsilon}^{\alpha}$ is given by:

$$\frac{dP}{dt} = \frac{4\pi^2 Z_1{}^2 e^2 c^2}{\varepsilon\omega V} (\vec{\beta}\cdot\hat{\varepsilon}^{\alpha})^2 \delta_{\hbar\vec{k}+\vec{p}',\vec{p}} \, \delta(E_k + E_{p'} - E_p) \qquad \text{VI.21}$$

where $\vec{p}(\vec{p}')$ is the initial (final) momentum of the charged particle. The Kronecker delta function expresses momentum conservation and the Dirac delta function expresses energy conservation. The expression $(\vec{\beta}\cdot\hat{\varepsilon}^{\alpha})^2$ demonstrates that the emitted photons are linearly polarized in the plane of emission. By summing over $\vec{p}'$ and photon emission solid angle, and by imposing the requirement $\hbar k \ll p$, one obtains the result of eq. VI.20.

In addition to emphasizing the role of energy momentum conservation in Cerenkov emission, the QED derivation has the advantage of indicating the existence of higher order corrections which is often not apparent in classical calculations. In Fig. VI.3 we depict the first order Feynman diagram responsible for the result of eq. VI.20. Two higher order diagrams are shown for comparison. Since the number of photon-projectile vertices is always an odd number, it is seen that Cerenkov radiation is a function only of $|Z_1|$, being the same for both positive and negative charges. It is difficult to calculate higher order contributions due to the need for an accurate knowledge of the detailed properties of the absorbing medium. Such a knowledge

is not required for the first order result beyond imposing the limitation that light is emitted only for those frequencies for which $\varepsilon(\omega)$ is real. In this connection we might note that Bohr (1948b) first pointed out that for a medium with no absorption and described by a single type of dispersion oscillator , the relativistic rise of energy loss as obtained from Fermi's (1940) theory should escape entirely as Cerenkov radiation. Sternheimer (1953a) has shown that with more realistic atomic models, only a very small fraction of Cerenkov radiation escapes for solids, although significant escape is possible for gases.

By measuring the angle of emission of Cerenkov light it is possible to determine the projectile velocity as shown by eq. VI.19. Litt and Mennier (1973) describe this technique in some detail. By integrating the total light collection, projectile charge and velocity can be measured as indicated by eq. VI.20. Various experimental aspects of this approach are elaborated on by Ahlen et al. (1976). A discussion of background light sources, including Cerenkov emitting delta rays and low level scintillation can be found in this work. The effects of slowing are also considered and experimental data are compared with theory. In Fig. VI.4 we plot a typical integrated light curve. In this case the Cerenkov radiation was a piece of 1.27 cm sandblasted Pilot 425. The incident radiation was ^{20}Ne. More detailed information can be found in Ahlen et al. (1976). Note that scintillation and Cerenkov emitting delta rays contribute a sizable fraction of the emitted light. Note also that the index of refraction as obtained by extrapolating the Cerenkov curve gives a value

of n = 1.508 which is lower than the fitted value of 1.518. This is a consequence of the slowing of the ions in the radiator.

Tompkins (1965) has adopted Fermi's (1940) approach to calculate the Cerenkov radiation for magnetic monopoles. He finds that for magnetic charges, as for electric charges, there is no Cerenkov radiation for $\beta^2\varepsilon < 1$. For $\beta^2\varepsilon > 1$ the result, analogous to eq. VI.20, is:

$$\left(\frac{dN}{d\lambda dx}\right)_m = 2\pi\alpha\left(\frac{ng}{e}\right)^2\left[1 - \frac{1}{n^2\beta^2}\right]/\lambda^2 \qquad \text{VI.22}$$

For a given velocity, the monopole Cerenkov radiation is a factor $[(ng)/Z_1e)]^2$ stronger than for an electrically charged particle. In addition to having a different intensity of Cerenkov radiation, the radiation is polarized differently for a monopole than for an electric charge. Rather than being polarized in the plane of the projectile and photon motion, the electric field is perpendicular to this plane. Hagstrom (1975) has suggested a means of identifying magnetic monopoles by exploiting this property.

Finally, we note that fluctuations in the number of Cerenkov photons emitted per unit length are determined solely by the Poisson statistics implied by eq. VI.21. This is due to the fact that the number of atoms participating in the Cerenkov process is so large as to preclude energy loss fluctuations of the type considered by Bohr, Landau, Symon and Vavilov.

2. Scintillation Counters

The introduction of the use of ZnS screens by Crookes and Regener in 1908 for visual scintillation counting and of ionization

chambers by Rutherford and Geiger (1908) marked the beginning of modern experimental physics. Birks (1964) provides an interesting historical account of the development of scintillation counters which, along with the development of photomultiplier tubes, has enabled them to remain useful tools in experimental physics even up to the present time. The scintillation mechanism is quite simple to understand in its most elementary form. Some type of radiation (anything from ultraviolet light to relativistic uranium nuclei) impinges on a material, causing excitation and ionization. Some fraction of the excited constituents radiatively de-excite resulting in the emission of light. Everything scintillates to a certain extent. What characterizes those materials used for scintillation counters is an unusually large efficiency for converting high energy radiation into visible, or nearly visible light. Aside from gases (most of which are efficient scintillators with the notable exception of oxygen), which are not subject to severe collisional de-excitation, the only known efficient scintillators fall into two classes: 1) various inorganic crystalline solids and 2) organic solids composed to a large extent of benzene rings. It will not be our purpose here to delve into the chemical physics or solid state physics aspects of scintillation. This is an extensive subject and the interested reader would do well to consult Birks (1964), Birks (1967), Windsor (1967), Birks (1970), Williams (1972), Birks (1973) or Birks (1975). We will be primarily concerned with experimental aspects of scintillation counters. In our brief discussion that follows we will draw heavily from the excellent monograph by Birks (1964).

Virtually every type of scintillator in practical usage consists of a bulk material doped with a small concentration of one or more impurities. This is true of inorganic crystals, liquid organic scintillators and plastic scintillators. This is not to say that pure substances cannot scintillate. Examples are anthracene crystals, diamonds and pure NaI and CsI. The luminescence of anthracene reflects its molecular structure. Most other pure substances which scintillate, do so as a result of crystalline properties. In diamond, lattice defects serve as impurity centers and NaI and CsI need to be cooled to liquid nitrogen temperatures for efficient operation. The purpose of impurity centers in inorganic systems or added primary and secondary fluors in organic systems is to provide traps for migrating energy which subsequently emit radiation to which the bulk material is transparent. The energy transfer processes can be any one of or several of the following: 1) exciton migration; 2) long range resonant interactions; 3) radiative emission and reabsorption, etc. Birks provides numerous references to work concerned with energy transfer.

It has long been recognized that scintillators saturate: dL/dE, the light output per unit energy deposited in the scintillator, declines as a function of dE/dx. For anthracene crystals, 1 MeV electrons result in 4.6 times as much light as 1 MeV protons and 15 times as much light as 1 MeV alpha particles (Brooks, 1956). Similar behavior is observed with organic liquid and plastic scintillators. Inorganic crystals are also subject to saturation, although to a more limited extent. The α/β conversion efficienty ratio (i.e. the ratio of conversion efficiency for the response to alpha particles and beta

particles) is roughly 60% for CsI(Tl) (Gwin, 1962) as compared to 7% for organic scintillators.

Becchetti et al. (1976) have recently presented data for the response of NE102, NE110 and NE111 plastic scintillators to heavy ions with Z_o = 1 to 35 and with energies from several MeV to just under 200 MeV. They observe that different types of scintillators prepared under similar conditions produced relative light outputs which are equal to within 10% for ions Z_o = 1 to 16. Ahlen and Salamon (1978) have observed that relative scintillation efficiencies of NE110, Pilot B, Pilot F and Pilot Y are the same to within 4% in response to atmospheric muons, 600 MeV/amu ^{20}Ne, ^{40}Ar and ^{56}Fe ions. It seems safe to conclude that previously reported variations of scintillator saturation reflected experimental effects or differential aging or radiation degradation effects.

Early data with α particles (Birks, 1964) indicated that the specific luminescence per unit length, dL/dx, approaches a constant level, independent of dE/dx, for very high rates of energy loss. This was inferred from the observed proportionality of light output to α particle range. The low velocity data of Becchetti et al. (1976) extend this result. They find that:

$$L \propto Z_o^{1.22}(R-0.04Z_o) \qquad \text{VI.23}$$

where R is the ion range in mg/cm^2. Ahlen et al. (1977) have shown that this strong saturation (i.e. constant dL/dx) does not apply in the high velocity regime. By using ^{20}Ne ions from 100-600 MeV/amu they have shown that simplified ionization quenching models used to explain low velocity data do not work. They present supporting evi-

dence, and supply earlier references, for the conclusion that the scintillation process in the relativistic, heavily ionizing regime is characterized by two effects: 1) the production of copious quantities of high energy delta rays ($w > 1.5$ keV) which transport their energy far from the central track "core" of ionization and excitation into the "halo" regions which are otherwise unaffected by the passage of the primary ion; and 2) the dominance of ionization quenching in the core over depletion of luminescence centers as the cause of non-linear response. Saturation is associated with the quenching, or "turning off" of the track core. Models of scintillation mechanisms by Meyer and Murray (1962) and by Voltz et al. (1966) include these features. The Voltz expression is particularly simple:

$$\frac{dL}{dx} = A\{(1-F_s)\ \exp[-B_s(1-F_s)\frac{dE}{dx}] + F_s\}\ \frac{dE}{dx} \qquad \text{VI.24}$$

where A, B_s and T_o are parameters of the model and F_s is the fraction of delta rays which escape from the core:

$$F_s = \frac{1}{2}\ \frac{\ln(\frac{2mc^2\beta^2\gamma^2}{T_o}) - \beta^2}{\ln(\frac{2mc^2\beta^2\gamma^2}{I}) - \beta^2} \qquad \text{VI.25}$$

Typical values for B_s and T_o are in Table VI.2. They are taken from Ahlen et al. (1977) and Buffington et al. (1978). The latter group do not see any difference between their scintillator response for different scintillators. The difference between their B_s parameter for Pilot Y and that of Ahlen et al. (1977) can be reconciled with the fact that the scintillator used by Ahlen et al. (1977) was very old and severely crazed. Also different photomultiplier tubes are

used by different groups which can confuse inter-group comparisons. Recent work with cosmic rays has shown that, while the qualitative features of the Voltz model are correct, its validity is restricted to a limited domain of charge and velocity (Buffington et al., 1978 and Tarlé et al., 1978). Analysis of the experiment reported by Ahlen and Salamon (1978) should help to clarify some issues of scintillation mechanisms. Pending this and further developments, it must be concluded that extreme caution should be used in extrapolating scintillator responses, although eq. VI.23 and 24 should serve as useful guides. Furthermore, until a proper understanding of scintillation mechanisms is achieved, it will not be possible to evaluate detector resolution a priori. If the bulk of the scintillation light is due to high energy delta rays (due to a quenched core) the fractional resolution will be larger by a factor of ~3 than if all types of energy deposition were equally effective in causing scintillation. Furthermore, higher order corrections depend to a large extent on the roles of the distant and close collisions in the response mechanism.

To close this discussion of scintillators we feel that it is important to emphasize that, in spite of the numerous problems associated with them, scintillators still remain competitive with better understood and better behaved ΔE detectors such as ionization chambers and solid state detectors which have excellent linearity properties. It is difficult to match the economy of scintillators, or their ease of fabrication. In addition, over limited domains of charge and velocity, resolution achieved with them is comparable to that attained with

other detectors. The most convincing evidence for this is the direct comparison of charge resolution for iron group nuclei in the cosmic rays obtained by similar techniques with the replacement of plastic scintillators by ionization chambers. Tueller et al. (1977) use ionization chambers plus a Pilot 425 Cerenkov radiator to this end and Meyer and Minagawa (1977) use Pilot Y scintillators plus a Pilot 425 Cerenkov radiator. The former group achieves a resolution of $\sigma = 0.21$ charge units while the latter attains $\sigma = 0.25$ charge units. Thus, there is no significant difference.

3. Particle Track Detectors

There are a variety of particle detectors which, in one way or another, yield a visible record of the passage of the particle. The most notable detectors which fit into this category are the cloud chamber, bubble chamber, nuclear emulsion, spark chamber and dielectric track recorder. A number of other such detectors have been developed and we will not make any attempt to list them here. Cloud chambers have been reviewed by Fretter (1955) and bubble chambers are discussed by Alvarez (1969). Charpak (1970) has summarized recent developments in the use of spark chambers, including a discussion of related devices such as multiwire proportional chambers. The development of the nuclear emulsion for the study of elementary particles is described by Powell et al. (1959) and Barkas (1963, 1973) describes in great detail various techniques, theories and applications of emulsions. Nuclear track detectors are described by Fleischer et al. (1975). Numerous other monographs and papers are available which deal with track detectors. The interested reader is directed to virtually any

issue of Nuclear Instruments and Methods or to any proceedings of the IEEE.

In this section we will restrict ourselves to detectors particularly suited to the study of relativistic heavily ionizing particles. This essentially restricts us to nuclear emulsions and dielectric track detectors, the others being more suitable to either high energy accelerator work (and singly charged particles) or fully saturated applications for which hodoscopic and trajectory information is the primary goal. Nuclear emulsions have the advantage (or in some instances the disadvantage) of being sensitive to minimum ionizing particles. In this regime the ionization rate is low enough so that the probability of grain sensitization along the particle trajectory is less than unity. Linear grain densities serve as a measure of the ionization rate and the restricted energy loss (REL) is useful in describing this density (Messel and Ritson, 1950). For heavy ions, the core of the emulsion track is fully saturated and information related to particle properties is contained in the halo region as described in the previous section. It has been seen that emulsion response in this regime has been compared with theoretical models of energy deposition by delta rays and that good agreement has been obtained. This indicates that the response of emulsions can be most simply understood in terms of the model of Katz et al. (1972) wherein the sensitization of an emulsion grain is a one hit Poisson process with a minimum energy deposition per grain characterizing one hit.[41] Track structure for arbitrary charged particles should then be calculable within the framework of a Monte Carlo program of the type

promised by Hagstrom (1977). Unfortunately, the understanding of the track formation process in dielectrics is not on so firm a footing as for its emulsion counterpart. We will devote the remainder of this sub-section to a discussion of this process.

It was discovered by Silk and Barnes (1959) that fission fragments leave permanent observable tracks in mica. With an electron microscope they observed diffraction contrast images of the damaged regions which were ≈100 Å in diameter. Fleischer, Price and Walker (1965, 1975) and Price and Fleischer (1971) describe the various theoretical conjectures for track formation mechanisms and the numerous applications of particle tracks in solids. A major contribution of these workers to the field of particle identification lies in their discovery that the primary localized track is particularly subject to chemical etching by caustic solutions. This enables the damaged region to be expanded sufficiently so as to be observable with visible light through optical microscopes. To date, the most commonly used material for particle identification with this technique is Lexan polycarbonate. This is a commercial plastic which is characterized by good large scale uniformity and considerable resistance to radiation.

To date, a large number of models have been advanced to account for the formation of particle tracks and for the subsequent chemical etching process. See Fleischer et al. (1975) and Benton (1970). None of the models advanced so far can be regarded as successful. Since the detailed shape of the etched particle track must depend on complicated processes involving diffusion and chemical kinetics and dynamics it will probably be some time before particle properties can be directly

related to the final observed track. However, it is not unreasonable to expect to find some particular property of the particle which characterizes a given track. This has been the main thrust of work which utilizes Lexan for particle identification. At present the two most popular semi-empirical formalisms used for the analysis of charged particle data in Lexan are the Z_1/β characterization and the REL characterization.

In the restricted energy loss or REL model (Benton, 1970), it is assumed that knockon electrons with energy greater than w_o are ineffective in causing the permanent radiation damage which is the primary track. This hypothesis is supported by the observation that fission fragment primary track diameters are less than 100 Å in plastic (Fleischer et al., 1975). Since high energy delta rays deposit most of their energy quite far from the particle track it is reasonable to suspect that they do not contribute significantly to the primary track. w_o is usually assumed to have a value between 300 and 1000 eV (Benton and Henke, 1972, have chosen 350 eV).

Shirk and Price (1978) and Fowler et al. (1977) have used the primary ionization model described by Price and Fleischer (1965) with constant K set to infinity to analyze ultraheavy cosmic ray data. This approach is equivalent to assuming that a particle track property is determined solely by the ratio Z_1/β. Most experimental data taken in a controlled environment with known particle parameters have lacked sufficient dynamical range to distinguish between the above two approaches. Furthermore, it is well known that successful particle identification over a limited dynamic range is insensitive to the

response function used in the analysis (witness the good charge resolution obtained with plastic scintillators which was referred to in the previous sub-section). However, the data presented by O'Sullivan et. al. (1971) are sufficiently good to rule out the REL model. These workers used accelerator ^{20}Ne and ^{28}Si ions and cosmic ray ^{56}Fe ions.[42] We plot the data of O'Sullivan et al. (1971) in Fig. VI.5 and 6. In Fig. VI.5 we plot log $[V_T/(\mu/h)]$ vs log $[REL/(GeVcm^2/g)]$ where V_T is the etch rate of the tracks and w_o was chosen to be 350 eV. In Fig. VI.6 the parameter log (Z_1/β) has been substituted for log (REL). There is little doubt on the basis of these data that Z_1/β is to be preferred as a universal parameter over REL. This is supported by the quite reasonable ultraheavy cosmic ray compositions obtained by Shirk and Price (1978) and Fowler et al. (1977) which, if an REL model were chosen as a calibration basis, would have to be shifted by ~10 charge units, resulting in peculiar abundance distributions. We might note that higher order corrections to the stopping power come into analysis of ultraheavy cosmic ray data to second order due to the predominance of the distant collisions in influencing track structure. The corrections only mildly affect charge assignments insofar as the rate of change of velocity is affected.

Katz and Kobetich (1968) have proposed a track formation mechanism in which the secondary dose at a radial distance of 17 Å characterizes the threshold criterion for track registration in Lexan. By using available data, their model predicts a critical dose of ~10 Mrad at this critical radius. Considerably larger doses are required to alter bulk properties of Lexan (Golden and Hazell, 1963) so it seems that

this mechanism is not viable. However, the primary dose at ~10 Å is adequate to account for sufficient energy deposition to match macroscopic observations (see Fig. VI.2). Since the characteristic size of a Lexan monomer is ~12 Å, it is tempting to ascribe the total prompt dose at a radius of ~10 Å as the parameter which determines the etch rate. This will not account for the O'Sullivan et al. (1971) data however. It is found that the effect of the adiabatic roll off of prompt primary dose is sufficient to cause the doses at 10 Å of the overlapping iron and neon points of Fig. VII.6 to differ by nearly 100% (the slower ^{20}Ne ion is less efficient at exciting inner shells than the faster ^{56}Fe ion). If, on the other hand, one merely considers the prompt dose which goes toward exciting bonds with energies $\lesssim$10 eV, then etch rates are predicted to be a function of (Z_1/β) for velocities greater than 0.1 c. At lower velocities, reduced etch rates should be expected. Since both of these features are observed for Lexan, this scenario seems to be quite valid. It is difficult to see, however, how the primary track region can be unaffected by the rather violent inner shell excitation and de-excitation processes. It may be that x-ray fluorescence and Auger electron emission dilute this part of the energy deposition so that the efficiency for molecular bond ruptures is reduced relative to direct bond breaking interactions.

If it is true that Lexan responds to only the distant collisions, as the above comments suggest, then its intrinsic resolution may very well exceed that of any other particle detector.[43] By considering the distant collisions, it can be shown (Fano, 1963) that the variance of the total energy loss is:

$$\sigma^2 = 4\pi N Z_1^2 e^4 x[\frac{1-\beta^2/2}{1-\beta^2} + \frac{4}{3}\frac{<K>}{mv^2} \ln \frac{2mv^2}{I_1}] \qquad \text{VI.26}$$

where <K> is the mean kinetic energy of an atomic electron in the ground state of the absorbing atom and

$$\ln I_1 = (\sum_n E_n f_n \ln E_n)/(\sum_n E_n f_n) \qquad \text{VI.27}$$

For $v >> v_o$ one obtains the previously discussed result, eq. III.47. As is true of the Bethe stopping power formula, eq. VI.26 is valid only for rather large velocities so that in this regime, total energy straggling is characterized by the relativistic Bohr formula to quite good accuracy. The second term is useful in determining the distant collision fluctuations however. The free electron approximation predicts that the straggling of energy loss due to collisions with energy transfer between w_{min} and w_{max} is:

$$\sigma^2(w_{max},w_{min}) = \frac{2\pi N Z_1^2 e^4 x}{mv^2} x[1 - \frac{\beta^2}{2}\frac{(w_{max}+w_{min})}{2mc^2\beta^2\gamma^2}](w_{max}-w_{min}) \qquad \text{VI.28}$$

If the response of Lexan is insensitive to collisions with energy transfer greater than w_o, then the relevant fluctuations are given by $\sigma^2 - \sigma^2(2mc^2\beta^2\gamma^2, w_o) = \sigma^2(\text{Lexan})$:

$$\sigma^2(\text{Lexan}) = 4\pi N Z_1^2 e^4 x[\frac{4}{3}\frac{<K>}{mv^2} \ln \frac{2mv^2}{I_1} + \frac{w_o}{2mv^2} - \frac{1}{2}(\frac{w_o}{2mc^2\beta\gamma})^2] \qquad \text{VI.29}$$

From the chemical composition of Lexan ($C_{16}H_{14}O_3$) and the approximate

values for E_n, f_n from Sternheimer (1956) one finds that <K> = 123 eV and that I_1 = 323 eV. These numbers should not be trusted to better than 50%. If w_o = 350 eV then:

$$\sigma^2(\text{Lexan}) = 4\pi N Z_1^2 e^4 x[16.4+3.2\ell n\beta]\frac{10^{-4}}{\beta^2} \qquad \text{VI.30a}$$

The uncertainty in w_o, <K>, I_1 and the non-relativistic approximations required for the derivation of the distant collision part of eq. VI.26 render eq. VI.30a suitable only for a rough estimation of fluctuations.

We can compare eq. VI.30a to resolutions expected for other types of particle detectors. In the relativistic heavily ionizing regime we have seen that emulsions and scintillators are predominantly sensitive to high energy delta rays ($\gtrsim$1500 eV). Hence:

$$\sigma^2(\text{scint.,emulsion}) = 4\pi N Z_1^2 e^4 x[\frac{1-\beta^2/2}{1-\beta^2}] \qquad \text{VI.30b}$$

where we have neglected 1500 eV in comparison to $w_{max} = 2mc^2\beta^2\gamma^2$. Since solid state detectors and ionization chambers are sensitive to all classes of collisions eq. VI.30b applies to them as well.

Suppose that the above detectors respond to a particular class of energy losses so that the detector response is given by some function F of ΔE where:

$$\Delta E = \frac{2\pi N Z_1^2 e^4 x}{mv^2}\ \ell n\frac{w_{max}}{w_{min}} \qquad \text{VI.31}$$

For Lexan track detectors, w_{max} = 350 eV, $w_{min} = I^2/(2mc^2\beta^2\gamma^2)$; for scintillators and emulsions, $w_{max} = 2mc^2\beta^2\gamma^2$, w_{min} = 1500 eV; for

ionization chambers and solid state detectors $w_{max} = 2mc^2\beta^2\gamma^2$ and $w_{min} = I^2/(2mc^2\beta^2\gamma^2)$. Aside from the binomial statistics associated with the production of scintillation photons, sensitized emulsion grains and electron-hole or ion pairs, the quality of a detector of penetrating radiation is measured by the size of the separation of two signals (for different values of ΔE) in units of the intrinsic fluctuation in F due to fluctuations in ΔE. Since this quantity is independent of the functional form of F, a true measure of detector resolution is given by the ratio $\sigma/\Delta E$. In Table VI.3 we give this ratio for the detectors named above. It is seen that for $\beta\gamma \sim 1$, and for given values of Nx, Z_1 and β, track detectors are about 10 times as good as the total ΔE detectors which in turn are about 3 times as good as scintillators and emulsions. Of course, there is considerable variation in practicable sizes for the different detectors. This should always be considered in any application.

4. Ionization Chambers and Solid State Detectors

To conclude this section on charged particle detectors we will discuss the most reliable instruments for the measurement of energy loss. These include the gaseous ionization chamber which detects the number of electron-ion pairs produced by the passage of a charged particle and the solid state or semi-conductor radiation detector which detects the number of electron hole pairs. The use of ionization chambers of one form or another (and this includes the classical electroscopes) dates back to the beginning of this century. The solid state detector is a more recent development. Reviews on their properties and performance can be found by Goulding and Stone (1970), Tavendale (1967) and Miller et al. (1962).

It has been recognized for a long time (see Bethe, 1930 and Mott and Massey, 1965) that the ionization cross section has virtually an identical form to that of the total stopping power. It is not surprising therefore that a measure of the number of liberated electrons should correspond to the amount of energy lost. What is somewhat surprising, however, is the broad range of charge and velocity over which the response of these detectors is accurately represented as a linear function in the total energy loss. One is reminded of the situation for scintillators. For large values of Z_1 and β the response is roughly linear to total energy loss but only because the close collision energy loss is nearly a constant fraction of the total loss. The insensitivity of the scintillator response to distant collisions is reflected by saturation characteristics involving a comparison of data taken over a large span of charge and velocities. The key parameter in the application and theory of ionization counters and solid state detectors is W, which is equal to the amount of total dissipated energy required to liberate one electron-ion or electron-hole pair. In Table VI.4 we present results taken from Fano (1963) for values of W (in eV per pair) for various gases and semi-conductors and for different kinds of radiation sources. References are given by Fano. The remarkable constancy of W over a large range of velocity (β = 0.05 to $\beta \sim 1$) indicates that all types of collisions partake equally in the detection mechanism. For example, the fraction of energy loss which goes toward producing energetic electrons (>1500 eV) in silicon ranges from 0.39 at β = 0.95 to 0.32 at β = 0.05. Any preferential sensitivity to the high energy delta rays is not indicated by the data in Table VI.4.

It may seem that direct ionization, i.e. close collisions, should be more effective in producing ion pairs than the relatively inefficient distant collisions which, as we have previously mentioned, are as likely to be excited as ionized. However, the number of these close collisions is vastly exceeded by the number of distant collisions. Any deficiency in distant collision ionization efficiency can be more than compensated for by this numerical advantage.[44] Subsequent secondary ionization and excitation is essentially the same as the primary process, and the ratio of excitation to ionization events is unaltered. The similarity of the ionization cross section to the stopping power suggests the correspondence of the energy lost in a particle track to the number of primary ion-pairs via the relation $N = \Delta E/\varepsilon$ where ΔE is the energy lost by the projectile. Since roughly half of the energy is lost to the close collisions, $\frac{1}{2}\Delta E/\varepsilon$ is the number of secondary ion pairs. Proceeding with the same argument $(\frac{1}{2})^2\ \Delta E/\varepsilon$ is the number of tertiary ion pairs, $(\frac{1}{2})^3\ \Delta E/\varepsilon$ the number of quaternary pairs, etc. since $\frac{1}{2} + \frac{1}{4} + \frac{1}{8} + \ldots = 1$ we see that the close collisions result in the same number of ion pairs as the distant collisions. Externally applied electric fields separate the charge sufficiently to prevent recombination. It can be seen that $W = \varepsilon/2$. Fano (1963) gives additional arguments and references regarding the excellent linearity of these ionization detectors.[45]

In addition to having superior linearity, ionization detectors have the favorable properties of enhanced counting statistics and excellent temperature stability over scintillation counters. The statistics governing charge production and collection are not totally

understood (see Fano, 1947, van Roosbroeck, 1965 for a theoretical treatment). However, the fractional standard deviation of collected charge is well represented by $\sqrt{F/\bar{N}}$ where F is the Fano factor and $\bar{N}$ is the mean number of electron-ion or hole pairs. F is of the order 0.1 for solid state detectors. In order to produce one photoelectron in typical scintillation counters, 1000 eV or more of deposited energy is required. This is about 300 times more than that required to produce one electron-hole pair in silicon. The enhanced resolution is therefore $\sim\sqrt{300/F} \sim 50$ times as good in semi-conductors as in scintillators. Bichsel (1972) reports that in going from 300° K to 90° K, W increases by 4% for silicon. This is a much smaller temperature coefficient than is possible with any phototube-scintillator combination. Temporal drifts can be expected to be reduced by the same order of magnitude. It should be mentioned that the one disadvantage solid state detectors have in relation to scintillators is expense and size limitation of fabrication. They are also much more prone to radiation damage. These factors should always be considered in the design and analysis of experiments.

Acknowledgements

The successful completion of this Review article would not have been possible without the support, encouragement and advice of Prof. P. Buford Price. Much of the work referenced in this paper was brought to the attention of the author by the participants of the Informal Workshop on Current Stopping Power Problems (New York University, January 1978) and they are gratefully acknowledged. I would like to express my appreciation to M. Inokuti for his interest in this project and for several valuable discussions. Thanks are due to Prof. Price, G. Tarlé and especially M. Salamon for a critical reading of the manuscript and to Judy Blair for a fine typing job. This work was supported by DOE Contract At(04-3)-34.

Footnotes

1. In this Review stopping power will be defined to be the energy loss of the projectile per unit distance traveled by the projectile due exclusively to electronic excitation and ionization.
2. Exceptions to this are found in some of the work by Bohr (1913, 1915) and Bloch (1933a) where an extra charge dependence is introduced in the connection of the close and distant collision results.
3. At the present time there is one such accelerator in the world. The Bevalac at the Lawrence Berkeley Laboratory is capable of accelerating ions up to ^{56}Fe to approximately 2 GeV/amu. In the early 1970's the Princeton Particle Accelerator achieved the capability of accelerating ^{14}N to a total energy of 7.4 GeV before being forced to shut down due to lack of funding.
4. By successful we mean an experiment which yields either negative or positive results at a highly significant level.
5. It was not realized that it was necessary to separately calibrate different batches of the same type of plastic, namely Lexan polycarbonate; within this single category are several types of plastic with different kinds of additives used to enhance commercially valuable properties, such as clarity, resistance to ultraviolet radiation damage, etc. In addition, it was not known very accurately how this particle detector would respond to a magnetic monopole. In fact, the answer to this question is still not known. Similarly, the lack of an accurate predictive track model for nuclear emulsions hindered interpretation of data from these

detectors.

6. By mass and charge, whether it be electric or magnetic, we will mean those quantities which are observed, or renormalized. It may seem unnecessary to explicitly state this but it is advantageous to keep it in mind, particularly when we consider the radiative corrections.

7. The fractional error in stopping power due to this approximation is $-(m/M)/\ell n(2mv^2/I)$ where $M = M_1M_2/(M_1+M_2)$. This is always much less than 0.1% as long as $v > v_o$, the characteristic atomic velocity. This proviso also applies to the above discussion regarding elastic and inelastic collisions. If $v < v_o$, ionization becomes inefficient and elastic collisions dominate the energy loss process.

8. By atom we mean the smallest aggregate of matter which can be treated as an independent unit.

9. Equation III.6 will be referred to as the Bohr formula even though this relativistic expression did not appear in Bohr's early publications. It has been noted that $\Delta E(b)$ as used for close collisions is strictly valid for small CM angles and it reduces to the proper limit for large CM angles. The correct classical relativistic expression is quite complicated and is undoubtedly invalid in any case since quantum mechanical effects are important for these close collisions. However, eq. III.6 will serve as a standard classical expression for comparison with other results.

10. $\psi(z)$ is commonly referred to as the digamma function. See Abramowitz and Stegun, 1970 for a discussion of its properties.

11. Bohr and Bloch present some results which are relativistically valid; however they do not obtain self-consistent expressions for the stopping power of a relativistic projectile.

12. This assumption is contained in assumption 13; we have explicitly stated it here to emphasize that this assumption was not required by Bloch.

13. This is also seen to be the case if one examines the First Born Mott cross section; the $\beta^2 w/w_m$ term in eq. III.46 is a consequence of the electron spin and this is quite negligible for distant collision values of w which are of the order 100 eV.

14. The gas under consideration has been cold, in the sense that atoms are assumed to be in their ground state.

15. This assumption is often made incorrectly for low energy stopping power measurements. This accounts, at least in part, for the large spread (much more than 1%) of these measurements performed by different groups at energies less than 1 MeV/amu (Ziegler, 1978).

16. The concept of an adiabatically limited impact parameter is equally valid in a quantal treatment as in Bohr's classical treatment. This is because eq. III.1 is identical to that obtained in a quantal calculation via time dependent perturbation theory with the understanding that a sum over the excitation energies $\hbar\omega$ of the atom must be made, weighted by the oscillator strengths of the transitions. In a more general sense the limiting impact parameter is a consequence of the Adiabatic Theorem, discussed in most Quantum Mechanics textbooks, which requires that a system

disturbed more slowly than its relaxation time reverts to its initial state after the perturbation returns to zero.

17. Sternheimer and Peierls, 1971 show that the distinction between conductors and non-conductors is of no practical concern. Low velocity determinations of I are assumed to contain the slowly varying low velocity density effect correction for conductors.

18. $\Delta E = S\Delta x$ only in the limit of very thin absorbers and for values of Z_1, β and Δx such that the energy loss distribution is symmetric. If this is not the case one must be careful about the experimental and theoretical modes of the distribution which are being compared (see Ahlen, 1977).

19. See, for example, Table III.3 which is a reproduction of that appearing in Dalton and Turner (1968) and is the set of experiments analyzed by these authors in order to obtain values of I.

20. Bloch's (1933b) contribution to the theory of the mean ionization potential is often acknowledged by pairing him with Bethe in reference to eq. III.38. In view of Bloch's (1933a) correction to Bethe's formula (eq. III.17) this reference can be misleading. Hence we will not use the expression "Bethe-Bloch formula" in this Review.

21. See Dehmer et al. for references.

22. This is slightly higher than 13.6 eV, the ionization potential of the hydrogen atom in the ground state. This is due to the contributions of the continuum states. Although the dipole oscillator strengths for these states decrease rapidly with energy, they are sufficiently large to account for Bethe's result.

The near equality of I with the photo-ionization potential accounts for the success of Sternheimer's (1952) semi-classical calculation of the density effect correction.

23. Note that we always interpret I as the logarithmic mean ionization potential per electron. In this convention then, $I(H_2) = I(H)$ in the absence of chemical binding effects.

24. In actuality, eq. III.43 should be written as a double sum over excitation levels and momentum transfers in such a way that w_{min} depends on the level. Fano (1963) discusses this in greater detail. It is shown that $w_{min}(E_n) = E_n^2/(2mv^2) \sim (v_o/v)^4 w_{max}$. Hence, $w_{min} << w_{max}$ except for small velocities, where shell corrections start being important.

25. According to the Lindhard, Scharff theory, $\sigma^2 = \sigma_B^2$ if $\beta^2 > 3\alpha^2/Z_2$ and $\sigma^2 = \sigma_B^2 L/2$ for lower velocities than this where L is defined according to eq. III.19

26. It might be noted that this transition velocity depends on the charge of the target and of the projectile; for $Z_1 = 92$, electron capture and loss fluctuations become important for $T >> 1$ MeV/amu. Also, lead absorbers are more subject to the restriction $v >> v_o$ than lighter absorbers. These factors should be considered in any practical application.

27. Although it is not mathematically rigorous to do so, one usually introduces no significant errors in convolving a Gaussian distribution with an asymmetric one of the nature of the Landau or Vavilov distributions by requiring the total $(FWHM)^2$ be given by the sum of the squares of the contributing FWHM's.

28. Ahlen (1977) has pointed out a minor error in eq. 4 of Sellers and Hanser (1972). This does not affect any of the subsequent discussion.

29. For the second integral in eq. IV.1, w is defined by eq. IV.3 and has no simple physical interpretation.

30. This is strictly correct only for large momentum transfer; for low momentum transfer the effect of the anomalous magnetic moment of the electron depends on $A_\mu(\vec{q})$; however, since the radiative corrections become negligible for small momentum transfer this distinction is not important.

31. Jackson and McCarthy, 1972 emphasize that only for an infinitely massive scattering center can one make separate expansions in the strength of the external potential and in the coupling of the electron to the electromagnetic field; this is well verified by the calculations of radiative corrections to muon-electron scattering by Eriksson et al., 1963; the close collision energy loss fractional correction due to interference of these two effects can be shown to be $\frac{4\alpha}{\pi}(\ell n \frac{mc^2\gamma}{\Delta E})(\frac{m\gamma}{m_p})/\ell n(w_m/w_o)$ if $Z_1 \sim A_1/2$.

32. This distance corresponds to the minimum non-zero angular momentum allowed by quantum mechanics.

33. Ashley et al., 1972 claim that their expansion in powers of the electron displacement to separation ratio restricts its validity to the outside of the atomic volume. However, one can show that this ratio has a maximum value of the order $Z_1e^2/(mv^2b)$ where b is the impact parameter. For $Z_1\alpha/\beta < 1$ and $b > \hbar/(mv)$ this ratio is less than one. Hence it is not unreasonable to adopt

Bohr's classical treatment for impact parameters well within the atomic volume.

34. The Bohr criterion is that orbital electrons of the ion are stripped if their orbital velocity is less than the ion velocity while they are attached if the opposite case maintains. See Betz, 1972.

35. In particular, Fig. 3.6 of Fleischer et al. (1975) shows that Steward and Wallace calculate the range of ^{56}Fe at 1 MeV/amu in Lexan to be ~30% larger than the measured value.

36. Jones (1977) summarizes experimental results of monopole searches.

37. The cylindrical symmetry of the electric field of the monopole precludes the existence of a net polarization of the absorbing medium.

38. Garcia et al. (1973) review inner shell ionization phenomena and they point out that: "The emission of an Auger electron subsequent to K-shell vacancy production is more probable than x-ray emission for all target Z_2 values less than about 30 and several orders of magnitude more probable for $Z_2 \leq 15$. For higher shells, the range of Z_2 over which Auger emission predominates becomes even larger." For carbon, the K-shell fluorescence yield is only 0.24%, and for oxygen it is 0.77%. Hence, for CH or H_2O, one would expect that ~20% of the distant collision dose involves inner shells for which de-excitation leads predominantly to Auger emission. A carbon Auger electron will have a kinetic energy of the order 200 eV and will execute a random walk with a mean displacement from the origin of the order 15 Å in water or plastic. Hence, the prompt dose profile should differ from the delayed electronic dose by about 20%, which

will be distributed throughout a cylinder of radius ~15 Å.

39. Sternheimer (1953a) has shown that Cerenkov radiation can account for only a very small fraction of energy transfer for silver bromide grains. The effect is undoubtedly enhanced on a smaller scale.

40. Transition radiators produce x-rays which are useful in measuring ultra-relativistic energies. This effect involves the action on the particle fields by the discontinuous absorber boundaries. In this Review we are concerned primarily with bulk effects, and hence we will not discuss transition radiation.

41. Jensen et al. (1976) find that the critical energy deposition per grain is roughly 100 eV. This should be compared to the sensitivity to visible light. Only several optical quanta are required to sensitize a grain which corresponds to ~10 eV.

42. Until very recently it was not known to what extent the isotope spread could affect the interpretation of data like these. However, Tarlé et al. (1978) have shown that the iron isotopes consist primarily of ^{56}Fe.

43. This feature, if true, has thus far been obscured by a ~3% etch rate scatter due to spatial non-uniformities of the plastic itself. Current research on an improved plastic, CR-39 (Cartwright et al., 1978) indicates that the intrinsic resolution is indeed much better than this.

44. By examining Bethe's (1930) derivation, it can be seen that the distant collision ionization cross section is about 5 times as large as the close collision ionization cross section.

45. Recent calibrations with relativistic ^{56}Fe ions (Greiner, 1978) have indicated that for incident angles within ~3° of the electric field lines, charge recombination effects occur which distort the charge collection spectrum of solid state detectors. This could be regarded as a form of saturation. It is easily corrected for however by rotating the detector at an angle greater than 3°.

References

Abramowitz, M. and I.A. Stegun, 1970, Handbook of Mathematical Functions, NBS Appl. Math Series 55.

Ahlen, S.P., 1976, Phys. Rev. D 14, 2935.

Ahlen, S.P., B.G. Cartwright and G. Tarlé, 1976, Nucl. Instr. and Meth. 136, 235.

Ahlen, S.P., 1977, Phys. Rev. Lett. 39, 1398.

Ahlen, S.P., B.G. Cartwright and G. Tarlé, 1977, Nucl. Instr. and Meth. 147, 321.

Ahlen, S.P., 1978a, Phys. Rev. A 17, 1236.

Ahlen, S.P., 1978b, Phys. Rev. D 17, 229.

Ahlen, S.P. and M.H. Salamon, 1978, in Abstracts of Papers for the 26th Annual Meeting of the Radiation Research Society (Academic Press, Inc., New York, N.Y.) p. 28.

Allison, S.K. and S.D. Warshaw, 1953, Rev. Mod. Phys. 25, 779.

Alvarez, L.W., 1969, Science 165, 1071.

Andersen, H.H., A.F. Garfinkel, C.C. Hanke and H. Sørensen, 1966, Kgl. Danske Videnskab. Selskab. Mat.-Fys. Medd. 35, No. 4.

Andersen, H.H., C.C. Hanke, H. Sørensen and P. Vajda, 1967, Phys. Rev. 153, 338.

Andersen, H.H., J.F. Bak, H. Knudsen and B.R. Nielsen, 1977, Phys. Rev. A 16, 1929.

Andersen, H.H. and J.F. Ziegler, 1977, Hydrogen Stopping Powers and Ranges in All Elements (Pergamon Press, New York, N.Y.).

Ashley, J.C., R.H. Ritchie and W. Brandt, 1972, Phys. Rev. B 5, 2393.

Ashley, J.C., R.H. Ritchie and W. Brandt, 1973, Phys. Rev. A 8, 2402.

Baglin, J.E.E. and J.F. Ziegler, 1974, J. Appl. Phys. 45, 1413.

Bakker, C.J. and E. Segré, 1951, Phys. Rev. 81, 489.

Ball, J.A., J.A. Wheeler and E.L. Fireman, 1973, Rev. Mod. Phys. 45, 333.

Bangerter, R.O., W.B. Herrmannsfeldt, D.L. Judd and L. Smith, Eds., 1976, Final Report of the ERDA Summer Study of Heavy Ions for Inertial Fusion, LBL Report 5543 and (National Technical Information Service, U.S. Dept. of Commerce, Springfield, Va.).

Barkas, W.H., W. Birnbaum and F.M. Smith, 1956, Phys. Rev. 101, 778.

Barkas, W.H. and S. von Friesen, 1961, Nuovo Cimento Suppl., Ser. 10, 19, 41.

Barkas, W.H., 1963, Nuclear Research Emulsions: Techniques and Theory (Academic Press, New York, N.Y.).

Barkas, W.H. and M.J. Berger, 1967, in Penetration of Charged Particles in Matter, 2nd printing, (U. Fano, Ed., Natl. Acad. Sci.-Natl. Res. Council Publ. 1133), Paper 7.

Barkas, W.H., 1973, Nuclear Research Emulsions: Particle Behavior and Emulsion Applications (Academic Press, New York, N.Y.).

Bauer, E., 1951, Proc. Cambr. Phil. Soc. 47, 777.

Becchetti, F.D., C.E. Thorn and M.J. Levine, 1976, Nucl. Instr. and Meth. 138, 93.

Bednyukov, A.A., U.V. Bulgakov, V.S. Nikolaev, V.P. Sobakin and V.L. Chernov, 1977, Phys. Lett. 62A, 183.

Benton, E.V. and R.P. Henke, 1969, Nucl. Instr. and Meth. 67, 87.

Benton, E.V., 1970, Rad. Eff. 2, 273.

Benton, E.V. and R.P. Henke, 1972, Univ. of San Francisco, Technical Report No. 19.

Besenbacher, F., J. Heinemeier, P. Hvelplund and H. Knudsen, 1977, Phys. Lett. 61A, 75.

Bethe, H., 1930, Ann. Physik 5, 325.

Bethe, H., 1932, Z. Physik 76, 293.

Bethe, H.A., 1933, in Handbuch der Physik 24/1, 2nd ed., (H. Geiger and K. Scheel, Ed., Julius Springer, Berlin, Germany), p. 273.

Bethe, H. and J. Ashkin, 1953, in Experimental Nuclear Physics 1, (E. Segré, Ed., John Wiley and Sons, Inc., New York, N.Y.), Chap. 2.

Betz, H.D. and L. Grodzins, 1970, Phys. Rev. Lett. 25, 903.

Betz, H.D., 1972, Rev. Mod. Phys. 44, 465.

Bhabha, H.J., 1935, Proc. Cambr. Phil. Soc. 31, 394.

Bichsel, H., R.F. Mozley and W.A. Aron, 1957, Phys. Rev. 105, 1788.

Bichsel, H., 1968, in Radiation Dosimetry 1, (F.H. Attix and W.C. Roesch, Ed., Academic Press, New York, N.Y.), p. 157.

Bichsel, H., 1970, Phys. Rev. V 1, 2854.

Bichsel, H., 1972, in A.I.P. Handbook, (D.E. Gray, Ed., McGraw Hill, New York, N.Y.), p. 8-142.

Bichsel, H. and S. Yu, 1972, IEEE Trans. Nucl. Sci. 19, 172.

Birks, J.B., 1964, The Theory and Practice of Scintillation Counting (Pergamon Press, New York).

Birks, J.B., 1967, in Physics and Chemistry of the Organic Solid State 2, (D. Fox, M.M. Labes and A. Weissberger, Ed., John Wiley and Sons, Inc., New York, N.Y.), Chap. 5.

Birks, J.B., 1970, Photophysics of Aromatic Molecules (John Wiley and Sons, Inc., New York, N.Y.).

Birks, J.B., 1973, Organic Molecular Photophysics 1, (John Wiley and Sons, Inc., New York, N.Y.).

Birks, J.B., 1975, Organic Molecular Photophysics 2, (John Wiley and Sons, Inc., New York, N.Y.).

Bizzeti, P.G. and M. Della Corte, 1959, Nuovo Cimento 11, 317.

Bjorken, J.D. and S.D. Drell, 1964, Relativistic Quantum Mechanics (McGraw Hill, New York, N.Y.).

Bleehen, N.M., 1972, in Recent Advances in Cancer and Radiotherapeutics: Clinical Oncology (K.E. Halnan, Ed., The Williams and Wilkins Company, Baltimore, Md.), Chap. 8.

Bloch, F., 1933a, Ann. Phys. (Leipzig) 16, 285.

Bloch, F., 1933b, Z. Physik 81, 363.

Blunck, O. and S. Leisegang, 1950, Z. Physik 128, 500.

Bohr, N., 1913, Phil. Mag. 25, 10.

Bohr, N., 1915, Phil. Mag. 30, 581.

Bohr, N., 1941, Phys. Rev. 59, 270.

Bohr, N., 1948a, Kgl. Danske Videnskab. Selskab. Mat.-Fys. Medd. 18, (8).

Bohr, A., 1948b, Kgl. Danske Videnskab. Selskab. Mat.-Fys. Medd. 24, (19).

Bonderup, E., 1967, Kgl. Danske Videnskab. Selskab. Mat.-Fys. Medd. 35, (17).

Bonderup, E. and P. Hvelplund, 1971, Phys. Rev. A 4, 562.

Born, M., 1926, Z. Physik 38, 803.

Box, H.C., 1972, Ann. Rev. Nucl. Sci. 22, 355.

Bradt, H.L. and B. Peters, 1948, Phys. Rev. 74, 1828.

Bragg, W.H. and R. Kleeman, 1905, Phil. Mag. 10, S318.

Brandt. W., 1956, Phys. Rev. 104, 691.

Brolley, J.E. and R.L. Ribe, 1955, Phys. Rev. 98, 1112.

Brooks, F.D., 1956, in Progress in Nuclear Physics 5 (O.R. Frisch, Ed., Pergamon Press, London) p. 284.

Buffington, A., C.D. Orth and T.S. Mast, 1978, submitted to Astrophys. J. (LBL Report 7551).

Burkig, V.C. and K.R. MacKenzie, 19-7, Phys. Rev. 106, 848.

Cameron, J.F. et al., 1962, Nuclear Electronics (IAEA), 1, 95.

Carrigan, R.A., 1977, Fermilab Report 77/42.

Cartwright, B.G., E.K. Shirk and P.B. Price, 1978, Nucle. Instr. and Meth., in press.

Cerenkov, P.A., 1934, Dokl. Akad. Nauk SSSR 2, 451.

Chan, E.K.L., R.B. Brown, A.S. Lodhi, D. Powers, S. Matteson and S.R. Eisenbarth, 1977, Phys. Rev. A 16, 1407.

Charpak, G., 1970, Ann. Rev. Nucl. Sci. 20, 195.

Chatterjee, A., H.D. Maccabbee and C.A. Tobias, 1973, Radiat. Res. 54, 479.

Chatterjee, A. and H.J. Schaefer, 1976, Rad. and Environm. Biophys. 13, 215.

Chu, W.K. and D. Powers, 1972, Phys. Lett. 40A, 23.

Chu, W.K., 1976, Phys. Rev. A 13, 2057.

Cole, H.J.D., 1951, Proc. Cambr. Phil. Soc. 47, 196.

CRC, 1968, Handbook of Chemistry and Physics, 49th ed., (R.C. Weast, Ed., The Chemical Rubber Co., Cleveland, Ohio), p. F-158.

Crispin, A. and G.N. Fowler, 1970, Rev. Mod. Phys. 42, 290.

Curr, R.M., 1955, Proc. Phys. Soc. (London) A68, 156.

Dalton, P. and J.E. Turner, 1968, Health Phys. 15, 257.

Darwin, C.G., 1912, Phil. Mag. 23, 901.

Datz, S., C. Erginsoy, G. Leibfried and H.O. Lutz, 1967, Ann. Rev. Nucl. Sci. 17, 129.

Datz, S., 1977, private communication.

Datz, S., J. Gomez del Campo, P.F. Dittner, P.N. Miller and J.A. Biggerstaff, 1977, Phys. Rev. Lett. 38, 1145.

Dehmer, J.L., M. Inokuti and R.P. Saxon, 1975, Phys. Rev. A 12, 102.

Dirac, P.A.M., 1931, Proc. Roy. Soc. A133, 60.

Doggett, J.A. and L.V. Spencer, 1956, Phys. Rev. 103, 1597.

Eby, P.B. and S.H. Morgan, 1972, Phys. Rev. A 5, 2536.

Eriksson, K.E., B. Larsson and G.A. Rinander, 1963, Nuovo Cimento 30, 1434.

Esbensen, H., O. Fich, J.A. Golovchenko, K.O. Nielsen, E. Uggerhøj, C. Vraast-Thomsen, G. Charpak, S. Majewski, F. Sauli and J.P. Ponpon, 1977, Nucl. Phys. B127, 281.

Esbensen, H., 1977, Ph.D. Thesis (University of Aarhus).

Esbensen, H., O. Fich, J.A. Golovchenko, S. Madsen, H. Nielsen, H.E. Schiøtt, E. Uggerhøj, C. Vraast-Thomsen, G. Charpak, S. Majewski, G. Odyniec, G. Petersen, F. Saulo, J.P. Ponpon and D. Siffert, 1978, Phys. Rev. B 18, 1039.

Fano, U., 1947, Phys. Rev. 72, 26.

Fano, U., 1956a, Phys. Rev. 102, 385.

Fano, U., 1956b, Phys. Rev. 103, 1202.

Fano, U., 1963, Ann. Rev. Nucl. Sci. 13, 1.

Fano, U., 1970, in Charged Particle Tracks in Solids and Liquids (G.E. Adams, D.K. Bewley and J.W. Boag, Eds., The Institute of Physics and the Physical Society, London, 1970)

Feller, W., 1968, An Introduction to Probability Theory and Its Applications Vol. 1, 3rd ed. (John Wiley and Sons, Inc., New York, N.Y.), Chap. 10.

Feng, J.S.-Y., W.K. Chu and M.A. Nicolet, 1974, Phys. Rev. B 10, 3781.

Fermi, E., 1940, Phys. Rev. 57, 485.

Fleischer, R.L., P.B. Price and R.M. Walker, 1965, Ann. Rev. Nucl. Sci. 15, 1.

Fleischer, R.L., P.B. Price and R.M. Walker, 1975, Nuclear Tracks in Solids: Principles and Applications (Berkeley: University of California Press).

Fowler, P.H., 1965, Proc. Phys. Soc. London 85, 1051.

Fowler, P.H., V.M. Clapman, V.G. Cowen, J.M. Kidd and R.T. Moses, 1970, Proc. Roy. Soc. (London) A318, 1.

Fowler, P.H., 1977, Nucl. Instr. and Meth. 147, 183.

Fowler, P.H., C. Alexandre, V.M. Clapham, D.L. Henshaw, C.O. Ceallaigh, D. Sullivan and A. Thompson, 1977, Nucl. Instr. and Meth. 147, 195.

Fretter, W.B., 1955, Ann. Rev. Nucl. Sci. 5, 145.

Garcia, J.D., R.J. Fortner and T.M. Kavanagh, 1973, Rev. Mod. Phys. 45, 111.

Gaunt, I.A., 1927, Proc. Cambr. Phil. Soc. 23, 732.

Gemmel, D.S., 1974, Rev. Mod. Phys. 46, 129.

Ginoza, W., 1967, Ann. Rev. Nucl. Sci. 17, 469.

Ginsberg, E.S. and R.H. Pratt, 1964, Phys. Rev. 134, B773.

Ginsburg, V.L., 1940, Zh. Eksperim, Teor. Fiz. 10, 589.

Golden, J.H. and E.A. Hazell, 1963, J. Polymer Sci. A1, 1671.

Goulding, F.S. and Y. Stone, 1970, Science 170, 280.

Gnedin, Yu.N., A.Z. Dolginov and A.I. Tsygan, 1968, Soviet Phys. JETP 27, 267.

Greiner, D.E., P.J. Lindstrom, H.H. Heckman, B. Cork and F.S. Bieser, 1975, Phys. Rev. Lett. 35, 152.

Greiner, D., 1978, private communication.

Grunder, H.A., W.D. Hartsough and E.J. Lofgren, 1971, Science 174, 1128.

Grunder, H.A. and F.B. Selph, 1977, Ann. Rev. Nucl. Sci. 27, 353.

Gwin, R., 1962, Oak Ridge National Lab. Report ORNL 3354.

Hagstrom, R., 1975, Phys. Rev. Lett. 35, 1677.

Hagstrom, R., 1977, Phys. Rev. Lett. 38, 729.

Hahn, B.D., D.G. Ravenhall and R. Hofstadter, 1956, Phys. Rev. 101, 1131.

Hanke, C.C. and H. Bichsel, 1975, unpublished results.

Hart, E.J., 1965, Ann. Rev. Nucl. Sci. 15, 125.

Heckman, H.H. and P.J. Lindstrom, 1969, Phys. Rev. Lett. 22, 871.

Hemmer, P.C. and I.E. Farquhar, 1968, Phys. Rev. 168, 294.

Henderson, G.H., 1922, Phil. Mag. 44, 680.

Herman, R. and R. Hofstadter, 1960, High Energy Electron Scattering Tables (Standord University Press, Stanford, California).

Hill, K.W. and E. Merzbacher, 1974, Phys. Rev. A 9, 156.

Hoffman, G.E. and D. Powers, 1976, Phys. Rev. A 13, 2042.

Hvelplund, P., 1978, private communication.

Inokuti, M., 1978, private communication.

Inokuti, M., Y. Itikawa and J.E. Turner, 1978, Rev. Mod. Phys. 50, 23.

Israel, M.H., P.B. Price and C.J. Waddington, 1975, Physics Today 28, 23.

Jackson, J.D. and R.L. McCarthy, 1972, Phys. Rev. B 6, 4131.

Jackson, J.D., 1975, Classical Electrodynamics, 2nd ed., (John Wiley and Sons, Inc., New York, N.Y.), Chap. 13,15.

Jacobsson, L. and R. Rosander, 1974, Rad. Eff. 22, 123.

Jankus, V.Z., 1953, Phys. Rev. 90, 4.

Jauch, J.M., 1952, Phys. Rev. 85, 951.

Jensen, M., L. Larsson, O. Mathiesen and R. Rosander, 1976, Physica Scripta 13, 65.

Jones, L.W., 1977, Rev. Mod. Phys. 49, 717.

Karol, P.J., 1975, Phys. Rev. C 11, 1203.

Katz, R. and J.J. Butts, 1965, Phys. Rev. 137, B198.

Katz, R. and E.J. Kobetich, 1968, Phys. Rev. 170, 401.

Katz, R. and E.J. Kobetich, 1969, Phys. Rev. 186, 344.

Katz, R., S.C. Sharma and M. Homayoonfar, 1972, Nucl. Instr. and Meth. 100, 13.

Kazama, Y., C.N. Yang and A.S. Goldhaber, 1977, Phys. Rev. D 15, 2287.

Kobetich, E.J. and R. Katz, 1968, Phys. Rev. 170, 391.

Landau, L., 1944, J. Phys. (USSR) 8, 201.

Landau, L.M. and E.M. Lifshitz, 1960, Electrodynamics of Continuous Media (Addison Wesley, Reading, Mass.), Chap. 12.

Langley, R.A. and R.S. Blewer, 1976, Nucl. Instr. and Meth. 132, 109.

Lapidus, R. and J.L. Pieterpol, 1960, Am. J. Phys. 28, 17.

Laulainen, N. and H. Bichsel, 1972, Nucl. Instr. and Meth. 104, 531.

Lindhard, J. and M. Scharff, 1953, Kgl. Danske Videnskab. Selskab. Mat.-Fys. Medd. 27, (15).

Lindhard, J., 1964, Phys. Lett. 12, 126.

Lindhard, J., 1976, Nucl. Instr. and Meth. 132, 1.

Litt, J. and R. Meunier, 1973, Ann. Rev. Nucl. Sci. 23, 1.

Livingston, M.S. and H.A. Bethe, 1937, Rev. Mod. Phys. 9, 282.

Lodhi, A.S. and D. Powers, 1974, Phys. Rev. A 10, 2131.

Lutz, H. and R. Sizmann, 1963, Phys. Lett. 5, 113.

Maccabee, H.D. and D.G. Papworth, 1969, Phys. Lett. 30A, 241.

Marion, J.B. and B.A. Zimmerman, 1967, Nucl. Instr. and Meth. 51, 93.

Martem'yanov, V.P. and S.Kh. Khakimov, 1972, Zh. Eksperim Teor, Fiz. 62, 35 [Engl. transl. Sov. Phys. JETP 35, 20].

Mather, R. and E. Segré, 1951, Phys. Rev. 84, 191.

McKinely, W.A. and H. Feshbach, 1948, Phys. Rev. 74, 1759.

McNulty, P.J. and R.C. Filz, 1977, Nucl. Instr. and Meth. 147, 41.

Menefee, J. and Y. Cho, 1966, IEEE Trans. Nucl. Sci. 13 (3), 159.

Merzbacher, E., 1970, Quantum Mechanics (John Wiley and Sons, New York, N.Y.), Chap. 18.

Merzbacher, E., 1972, in Proceedings of Heavy Ion Summer Study, Oak Ridge National Laboratory, p. 465.

Messel, H. and D.M. Ritson, 1950, Phil. Mag. 41, 1129.

Meyer, A. and R.B. Murray, 1962, Phys. Rev. 128, 98.

Meyer, P. and G. Minagawa, 1977, Proc. 15th Inter. Cosmic Ray Conf. (Plovdiv),)G-68.

Miller, G.L., W.M. Gibson and P.F. Donovan, 1962, Ann. Rev. Nucl. Sci. 12, 189.

Mole, R.H., 1965, Ann. Rev. Nucl. Sci. 15, 207.

Moliere, G., 1948, Z. Naturforsch 3A, 78.

Moliere, G., 1955, Z. Naturforsch 10A, 177.

Møller, C., 1932, Ann. Physik 14, 531.

Morgan, K.Z. and J.E. Turner, 1972, in A.I.P. Handbook (D.E. Gray, Ed., McGraw Hill, New York, N.Y.), p. 8-291.

Morgan, S.H. and P.B. Eby, 1973, Nucl. Instr. and Meth. 106, 429.

Mott, N.F., 1929, Proc. Roy. Soc. (London) A124, 426.

Mott, N.F., 1931, Proc. Cambr. Phil. Soc. 27, 553.

Mott, N.F., 1932, Proc. Roy. Soc. (London) A135, 429.

Mott, N.F. and H.S.W. Massey, 1965, The Theory of Atomic Collisions Oxford University Press, London), p. 110.

Motz, J.W., H. Olsen and H.W. Koch, 1964, Rev. Mod. Phys. 36, 881.

Nakano, G.H., K.R. MacKenzie and H. Bichsel, 1963, Phys. Rev. 132, 291.

NCRP, 1961, National Committee on Radiation Protection, "Stopping powers for use with cavity chambers," Natl. Bur. Stds. (U.S.), Handbook 79.

Neamtan, S.M., 1953, Phys. Rev. 92, 1362.

Nielsen, L.P., 1961, Kgl. Danske Videnskab. Selskab. Mat.-Fys. Medd. 33, (6)

Nikolaev, V.S. and I.S. Dmitriev, 1968, Phys. Letters 28A, 277.

Northcliffe, L.C., 1963, Ann. Rev. Nucl. Sci. 13, 67.

Northcliffe, L.C. and R.F. Schilling, 1970, Nuclear Data Tables A7, 233.

O'Sullivan, D., P.B. Price, E.K. Shirk, P.H. Fowler, J.M. Kidd, E.J. Kobetich and R. Thorne, 1971, Phys. Rev. Lett. 26, 463.

Paretzke, H.G., 1977, Rad. Eff. 34, 3.

Pierce, T.E. and M. Blann, 1968, Phys. Rev. 173, 390.

Piercy, G.R., F. Brown, J.A. Davies and M. McCargo, 1963, Phys. Rev. Lett. 10, 399.

Platzman, R.L., 1952, Symp. Radiobiol., Oberlin Coll., 1950.

Polyakov, A.M., 1974, Zh. ETF Dis. Red. 20, 430 [Engl. transl. in JETP Lett. 20, 194].

Powell, C.F., P.H. Fowler and D.H. Perkins, 1959, The Study of Elementary Particles by the Photographic Method (Pergamon Press, New York, N.Y.).

Price, P.B. and R.L. Fleischer, 1971, Ann. Rev. Nucl. Sci. 21, 295.

Price, P.B., E.K. Shirk, W.Z. Osborne and L.S. Pinsky, 1975, Phys. Rev. Lett. 35, 487.

Price, P.B., E.K. Shirk, W.Z. Osborne and L.S. Pinsky, 1978, submitted to Phys. Rev. D.

PT, 1978, Physics Today 31, 17.

Raisbeck, G.M., H.J. Crawford, P.J. Lindstrom, D.E. Greiner, F.S. Bieser and H.H. Heckman, 1977, Proc. 15th Inter. Cosmic Ray Conf. (Plovdiv) 2, 1977.

RCA, 1970, Photomultiplier Manual, RCA Technical Series PT-61, Harrison, N.J.

Reames, D.V., 1974, in High Energy Particles and Quanta in Astrophysics, eds. F.B. McDonald and C.E. Fichtel (Cambridge; MIT Press), p. 54.

Rossi, B., 1952, High Energy Particles (Prentice Hall, Englewood Cliffs, N.J.), Chap. 2.

Rutherford, E. and H. Geiger, 1908, Proc. Roy. Soc. A81, 141.

Rutherford, E., 1911, Phil. Mag. 21, 669.

Sachs, D.C. and J.R. Richardson, 1951, Phys. Rev. 83, 834.

Sachs, D.C. and J.R. Richardson, 1953, Phys. Rev. 89, 1163.

Sakuraii, J.J., 1967, Advanced Quantum Mechanics (Addison Wesley, Reading, Mass.), Chap. 2 and Appendix A.

Schimmerling, W., K.G. Vosburgh and P.W. Todd, 1973, Phys. Rev. B 7, 2895.

Schwinger, J., 1966, Phys. Rev. 151, 1048.

Schwinger, J., 1975, Phys. Rev. D 12, 3105.

Scott, W.T., 1963, Rev. Mod. Phys. 35, 231.

Sellers, B. and F.A. Hanser, 1972, Nucl. Instr. and Meth. 104, 233.

Shirk, E.K. and P.B. Price, 1978, Astrophys. J. 220, 719.

Shulek, P., B.M. Golovin, L.A. Kulyukina, S.V. Medved and P. Pavlovich, 1967, Sov. J. Nucl. Phys. 4, 400.

Sigmund, P., 1976, Phys. Rev. A 14, 996.

Silberberg, R. and C.H. Tsao, 1973, Astrophys. J. Suppl. 25, 315.

Silk, E.C. and R.S. Barnes, 1959, Phil. Mag. 4, 970.

Stark, J. and G. Wendt, 1912, Ann. Physik 38, 921.

Sternheimer, R.M., 1952, Phys. Rev. 88, 851.

Sternheimer, R.M., 1953a, Phys. Rev. 91, 256.

Sternheimer, R.M., 1953b, Phys. Rev. 93, 351.

Sternheimer, R.M., 1956, Phys. Rev. 103, 511.

Sternheimer, R.M., 1961, in Methods of Experimental Physics, 5A, (L.C.L. Yuan and C.S. Wu, Ed., Academic Press, New York, N.Y.), p. 4.

Sternheimer, R.M., 1963, unpublished results; this formula is used by Barkas and Berger (1967) in their compilations of ranges and energies.

Sternheimer, R.M., 1966, Phys. Rev. 145, 247.

Sternheimer, R.M., 1967, Phys. Rev. 164, 349.

Sternheimer, R.M. and R.F. Peierls, 1971, Phys. Rev. B 3, 3681.

Stevens, D.M., 1973, Virginia Polytechnic Institute Report: VPI-EPP-73-5.

Steward, P.G. and R.W. Wallace, 1970, "Stopping power and range for any nucleus in any nongaseous material - a composite method," UCRL 19428.

Swann, W.F.G., 1938, J. Franklin Inst. 226, 598.

Symon, K., 1948, Fluctuations in Energy Loss by High Energy Charged Particles in Passing Through Matter (Ph.D. Thesis, Harvard Univ., Cambridge, Mass.).

Tamm, I.E. and I.M. Frank, 1937, Dokl. Akad. Nauk SSSR 14, 107.

Tarlé, G., S.P. Ahlen and B.G. Cartwright, 1978, in preparation for Astrophys. J.

Tarlé, G. and M. Solarz, 1978, Phys. Rev. Lett. 41, 483.

Tavendale, A.J., 1967, Ann. Rev. Nucl. Sci. 17, 73.

Thompson, T.J., 1952, "Effect of chemical structure on stopping powers for high energy protons," USAEC Report, UCRL 1910, Ph.D. Thesis.

Thomson, J.J., 1903, Conduction of Electricity Through Gases (University Press, Cambridge, England), p. 370.

Thomson, J.J., 1912, Phil. Mag. 23, 449.

't Hooft, G., 1974, Nucl. Phys. B79, 276.

Tobias, C.A. and P. Todd, 1966, Nat. Cancer Inst. Monogr. 24, 1.

Tobias, C.A., J.T. Lyman, A. Chatterjee, J. Howard, H.D. Maccabee, M.R. Raju, A.R. Smith, J.M. Sperinde and G.P. Welch, 1971, Science 174, 1131.

Todd, P., C.B. Schroy, K.G. Vosburgh and W. Schimmerling, 1971, Science 174, 1127.

Tompkins, D.R., 1965, Phys. Rev. 138, B248.

Tschalär, C., 1967, Ph.D. Thesis (Univ. of Southern Calif., Los Angeles, Calif.).

Tschalär, C., 1968a, Nucl. Instr. and Meth. 61, 141.

Tschalär, C., 1968b, Nucl. Instr. and Meth. 64, 237.

Tueller, J., P. Love, J.W. Epstein, M.H. Israel and J. Klarmann, 1977, Proc. 15th Inter. Cosmic Ray Conf. (Plovdiv),)G-71.

Turner, J.E., V.N. Neelavathi, R.B. Vora, T.S. Subramanian and M.A. Prasad, 1969, Phys. Rev. 183, 453.

Turner, J.E., P.D. Roecklein and R.B. Vora, 1970, Health Phys. 18, 159.

Uehling, E.A., 1954, Ann. Rev. Nucl. Sci. 4, 315.

Upton, A.C., 1968, Ann. Rev. Nucl. Sci. 18, 495.

van Roosbroeck, W., 1965, Phys. Rev. 139, A1702.

Vavilov, P.V., 1957, Zh. Eksperim. Teor. Fiz. 32, 920 [Engl. transl., Sov. Phys. KETP 5, 749].

Vavilov, S.I., 1934, Dokl. Akad. Nauk SSSR 2, 457.

Voltz, R., J. Lopes da Silva, G. Laustriat and A. Coche, 1966, J. Chem. Phys. 45, 3306.

Vora, R.B. and J.E. Turner, 1970, Phys. Rev. B 1, 2011.

Walske, M.C., 1952, Phys. Rev. 88, 1283.

Walske, M.C., 1956, Phys. Rev. 101, 940.

White, M.G., M. Isaila, K. Prelec and H.L. Allen, 1971, Science 174, 1211.

Williams, E.J., 1945, Rev. Mod. Phys. 17, 217.

Williams, F., 1972, in A.I.P. Handbook (D.E. Gray, Ed., McGraw Hill, New York, N.Y.), p. 9-158.

Wilson, L., 1978, Ph.D. Thesis (University of California, Berkeley).

Windsor, M.W., 1967, in Physics and Chemistry of the Organic Solid State 2, (D. Fox, MM. Labes and A. Weissberger, Ed., John Wiley and Sons, Inc., New York, N.Y.), Chap. 4.

Ziegler, J.F., 1978, private communication.

Zrelov, V.P. and G.D. Stoletov, 1959, Soviet Phys. - JETP 9, 461.

Zrelov, V.P., S.P. Kruglov, K.F. Mas, V.D. Savel'ev and P. Sulek, 1974, Sov. J. Nucl. Phys. 19, 653.

Table II.1

Notation Used in this Review

A_1 = mass of projectile in atomic mass units (1 amu = 1.6605×10^{-24} g).

A_2 = mass of absorbing atom in atomic mass units.

a_o = $\hbar^2/(me^2)$ = Bohr radius = 0.5292 Å.

α = $e^2/(\hbar c)$ = fine structure constant = 1/137.036.

β = velocity of the projectile relative to the absorbing medium in units of speed of light in vacuum c = 2.998×10^{10} cm/s.

E = $M_1c^2(\gamma-1)$ = kinetic energy of projectile.

g = renormalized magnetic charge of the projectile if it is a magnetic monopole.

γ = Lorentz factor of the projectile = $1/(1-\beta^2)^{\frac{1}{2}}$.

I = logarithmic mean excitation energy.

λ = αa_o = Compton wavelength of the electron $\div 2\pi$ = 3.862×10^{-11} cm.

M_1 = mass of projectile.

m = rest mass of the electron = 9.110×10^{-28} g.

m_p = rest mass of the proton = 1.672×10^{-24} g = 1.0073 amu.

N = volume density of electrons in the absorber.

r_e = $\alpha^2 a_o$ = classical electron radius = 2.818 F(1 F = 1 Fermi = 10^{-13} cm).

r_o = typical radius of electron orbit in a heavy element.

S = $-dE/dx$ = stopping power of projectile.

T = E/A_1 = 931.5 MeV(γ-1) = energy of projectile per atomic mass unit (often expressed in the unit MeV/amu).

v_o = characteristic electron velocity in a heavy element.

v = βc = projectile velocity.

w = kinetic energy of knockon electron in the laboratory frame.

Table II.1 (cont.)

x = pathlength.

Z_o = number of protons in the projectile if it is an ordinary nucleus.

$Z_1 e$ = renormalized electric charge of the projectile if it is a nucleus or anti-nucleus; $-e$ is the renormalized electric charge of the electron: $e = 4.803 \times 10^{-10}$ esu.

Z_2 = atomic number of the absorbing medium.

Table III.1 Parameters to be used in the general expression for the density effect correction (Sternheimer and Peierls, 1971).

$$C = -2\ell n(I/\hbar\omega_p) - 1$$

$$m = 3.0$$

$$a = -(C + 4.606X_0)/(X_1 - X_0)^m$$

Solids and Liquids

I	$\|C\|$	X_0	X_1
$I < 100$ eV	$\|C\| < 3.681$	0.2	2.0
$I < 100$ eV	$\|C\| \geq 3.681$	$0.326\|C\| - 1.0$	2.0
$I \geq 100$ eV	$\|C\| < 5.215$	0.2	3.0
$I \geq 100$ eV	$\|C\| \geq 5.215$	$0.326\|C\| - 1.5$	3.0

Gases at STP ($T = 0^0$ C and $P = 1$ atm)

$\|C\|$	X_0	X_1
$\|C\| < 10.0$	1.6	4.0
$10.0 \leq \|C\| < 10.5$	1.7	4.0
$10.5 \leq \|C\| < 11.0$	1.8	4.0
$11.0 \leq \|C\| < 11.5$	1.9	4.0
$11.5 \leq \|C\| < 12.25$	2.0	4.0
$12.25 \leq \|C\| < 13.804$	2.0	5.0
$\|C\| \geq 13.804$	$0.326\|C\| - 2.5$	5.0

Gases at density equal to $\eta \times$ density at STP

$$X_0(\eta) = X_0 - \tfrac{1}{2}\ell og_{10}(\eta) \; ; \quad a(\eta) = a$$

$$X_1(\eta) = X_1 - \tfrac{1}{2}\ell og_{10}(\eta) \; ; \quad C(\eta) = C + 2.303\ell og_{10}(\eta)$$

Table III.2 Density and plasma energy for various substances.

Substance	Chemical Formula	ρ (g/cm^3)	$\hbar\omega_p$ (eV)
Beryllium	Be	1.848 (20^{0}C)	26.10
Polyethylene	$(CH_2)_n$	0.93 ± 0.01	21.01
Lucite, Perspex, Plexiglas (polymethyl methacrylate)	$(C_5H_8O_2)_n$	1.19 ± 0.01	23.10
Lexan, Makrofol (polycarbonate of Bisphenol A)	$(C_{16}H_{14}O_3)_n$	1.204	22.92
Polyvinyltoluene	$(C_9H_{10})_n$	1.032	21.56
Anthracene	$C_{14}H_{10}$	1.25	23.40
Water	H_2O	1.000 (4^{0}C)	21.46
Aluminum	Al	2.699 (20^{0}C)	32.86
Silicon	Si	2.33 (25^{0}C)	31.05
Copper	Cu	8.96 (20^{0}C)	58.27
Germanium	Ge	5.323 (25^{0}C)	44.14
Nuclear Emulsion (G5)	0.128Ag+0.128Br+0.001I+0.406H+0.176C+0.040N+0.119Oxygen+0.002S	3.8 ± 0.2	37.87
Silver	Ag	10.50 (20^{0}C)	61.63
Sodium Iodide	NaI	3.67	36.07
Cesium Iodide	CsI	4.51	39.46
Gold	Au	19.32 (20^{0}C)	80.25
Lead	Pb	11.35 (20^{0}C)	61.13
Hydrogen Gas (STP)	H_2	8.96×10^{-5}	0.272
Nitrogen Gas (STP)	N_2	1.246×10^{-3}	0.719
Oxygen Gas (STP)	O_2	1.422×10^{-3}	0.768
Air (STP)	$0.78N_2+0.21O_2+0.01Ar$	1.29×10^{-3}	0.731
Helium Gas (STP)	He	1.779×10^{-4}	0.272
Neon Gas (STP)	Ne	8.97×10^{-4}	0.608
Argon Gas (STP)	Ar	1.774×10^{-3}	0.815
Krypton Gas (STP)	Kr	3.725×10^{-3}	1.153
Xenon Gas (STP)	Xe	5.837×10^{-3}	1.412

Table III.3 Key experiments for determination of I from Dalton and Turner (1968)

Reference	Type of Experiment	Energy (MeV) p = proton d = deuteron	Materials Studied
Bakker and Segré (1951)	Stopping-power relative to aluminum	340 p	CH_2,Li,Be,C,Al,Fe,Cu,Ag,Sn, W,Pb,U
Sachs and Richardson (1951, 1953)	Absolute stopping power	18 p	Al,Ni,Cu,Rh,Ag,Cd,Sn,Ta,Au
Thompson (1952)	Relative stopping-power	270 p	Liquid H,N,O;Solid C; H,C,N, O and Cl in condensed compounds
Brolley and Ribe (1955)	Absolute stopping-power	4.43 p	H,He,C,N,air,O,Ne,Ar,Kr,Xe(gases)
Brolley and Ribe (1955)	Stopping-power relative to air	8.86 d	H,He,C,N,air,O,Ne,Ar,Kr,Xe(gases)
Bichsel, Mozley and Aron (1957)	Range measurement	6 - 18 p	Be,Al,Cu,Ag,Au
Burkig and MacKenzie (1957)	Stopping-power relative to aluminum	19.8 p	Be,Al,Ca,Ti,V,Fe,Ni,Cu,Zn,Nb, Mo,Rh,Pd,Ag,Cd,In,Sn,Ta,W,Ir, Pt,Au,Pb,Th
Zrelov and Stoletov (1959)	Range measurement	658 p	Cu
Zrelov and Stoletov (1959)	Stopping-power relative to copper	635 p	CH_2,Be,C,Fe,Cd,W
Nielsen (1961)	Absolute stopping-power	1 -5 p,d	Be,Al,Ni,Cu,Ag,Au
Barkas and von Friesen (1961)	Range measurement	752.2 p	Al,Cu,Pb,U,emulsion
Nakano, MacKenzie and Bichsel (1963)	Stopping-power relative to aluminum	28.7 p	Be,Al,Ti,V,Co,Ni,Cu,Ag,Ta, W,Ir,Au
Andersen et al. (1966)	Absolute stopping-power	5 - 12 p,d	Al
Andersen et al. (1967)	Absolute stopping-power	5 - 12 p,d	Cu,Be,Ag,Pt,Au

Table III.4 Values of mean ionization potential from various sources. Values are expressed in eV.

Z_2	Material	NCRP 1961	Fano 1963	Bichsel 1968	Turner et al. 1970	Bichsel 1972	Andersen and Ziegler 1977
1	H_2 (Gas)	-	18.3 ± 2.6	18	18.2	19.2	18.8
1	H (Liquid)	20.7	-	-	-	-	-
1	H (Saturated compounds)	17.6	15 - 18	-	-	-	-
1	H (Unsaturated compounds)	14.8	15 - 18	-	-	-	-
2	He (Gas)	-	42 ± 3	42	44.3	41.3	41.7
3	Li (Solid)	38	40, 38	-	37.4	39	47.6
4	Be (Solid)	67	64	64	61.7	64	62.7
5	B (Solid)	-	-	-	-	-	76
6	C (Graphite)	78.4	81	78	81.2	78	77.3
6	C (Saturated compounds)	77.3	77 - 80	-	-	-	-
6	C (Unsaturated compounds)	75.1	77 - 80	-	-	-	-
6	C (Highly chlorinated)	64.8	-	-	-	-	-
7	N_2 (Gas)	-	88	-	-	-	86.7
7	N (Liquid)	85.1	-	-	-	-	-
7	N (Amines, nitrates)	99.5	79 - 102	-	-	-	-
7	N (Ring)	76.8	79 - 102	-	-	-	-
7	N (Unspecified)	-	-	78	89.6	78	-
8	O_2 (Gas)	-	101	100	-	-	97.7
8	O (Liquid)	98.3	-	-	-	-	-
8	O (-O-)	98.5	91 - 101	-	-	-	-
8	O (O=)	88.9	91 - 101	-	-	-	-
8	O (Unspecified)	-	-	-	101	93	-
9	F (Unspecified)	-	-	-	-	-	120
10	Ne (Gas)	-	-	-	132	129	139
11	Na (Unspecified)	-	-	-	-	-	148
12	Mg (Unspecified)	-	-	-	-	-	156
13	Al (Solid)	164	163	164	163	166	162
14	Si (Solid)	-	-	170	-	173	165
15	P (Unspecified)	-	-	-	-	-	172
16	S (Solid)	-	-	-	-	-	180
17	Cl (Liquid)	170	-	-	176	-	-
17	Cl (Unspecified)	-	-	-	-	-	185

Table III.4 continued

18	Ar (Gas)	-	190	184	189	182	194
19	K (Unspecified)	-	-	-	-	-	193
20	Ca (Solid)	-	-	-	187	191	196
21	Sc (Solid)	-	-	-	-	214	218
22	Ti (Solid)	-	-	-	224	230	230
23	V (Solid)	-	-	-	250	238	239
24	Cr (Solid)	-	-	-	-	260	259
25	Mn (Solid)	-	-	-	-	275	270
26	Fe (Solid)	264	273	-	277	282	280
27	Co (Solid)	-	-	-	290	303	296
28	Ni (Solid)	-	-	312	312	306	310
29	Cu (Solid)	306	315	322	316	319	322
30	Zn (Solid)	-	-	-	319	328	320
31	Ga (Unspecified)	-	-	-	-	-	324
32	Ge (Solid)	-	-	350	-	-	330
33	As (Unspecified)	-	-	-	-	-	338
34	Se (Solid)	-	-	-	-	-	340
35	Br (Unspecified)	-	-	-	-	-	349
36	Kr (Gas)	-	360	-	350	358	358
37	Rb (Unspecified)	-	-	-	-	-	358
38	Sr (Unspecified)	-	-	-	-	-	363
39	Y (Unspecified)	-	-	-	-	-	370
40	Zr (Solid)	-	-	-	-	386	378
41	Nb (Solid)	-	-	-	407	-	390
42	Mo (Solid)	-	-	-	422	-	406
43	Tc (Unspecified)	-	-	-	-	-	410
44	Ru (Unspecified)	-	-	-	-	-	423
45	Rh (Solid)	-	-	-	440	-	443
46	Pd (Solid)	-	-	-	456	-	458
47	Ag (Solid)	462	471	475	466	475	466
48	Cd (Solid)	-	-	-	462	-	-
48	Cd (Unspecified)	-	-	-	-	-	471
49	In (Solid)	-	-	-	481	-	480
50	Sn (Solid)	517	-	500	486	500	487
51	Sb (Solid)	-	-	-	-	-	494
52	Te (Unspecified)	-	-	-	-	-	495
53	I (Unspecified)	-	-	-	-	-	498

Table III.4 continued

54	Xe (Gas)	-	-	-	480	-	497
55	Cs (Unspecified)	-	-	-	-	-	490
56	Ba (Unspecified)	-	-	-	-	-	483
57	La (Unspecified)	-	-	-	-	-	480
58	Ce (Solid)	-	-	-	-	-	493
59	Pr (Unspecified)	-	-	-	-	-	507
60	Nd (Unspecified)	-	-	-	-	-	521
61	Pm (Unspecified)	-	-	-	-	-	537
62	Sm (Unspecified)	-	-	-	-	-	548
63	Eu (Unspecified)	-	-	-	-	-	562
64	Gd (Solid)	-	-	-	-	-	564
65	Tb (Unspecified)	-	-	-	-	-	585
66	Dy (Unspecified)	-	-	-	-	-	600
67	Ho (Unspecified)	-	-	-	-	-	623
68	Er (Solid)	-	-	-	-	-	640
69	Tm (Unspecified)	-	-	-	-	-	652
70	Yb (Solid)	-	-	-	-	-	662
71	Lu (Unspecified)	-	-	-	-	-	672
72	Hf (Unspecified)	-	-	-	-	-	682
73	Ta (Solid)	-	-	730	692	707	684
74	W (Solid)	750	-	740	704	-	693
75	Re (Unspecified)	-	-	-	-	-	698
76	Os (Unspecified)	-	-	-	-	-	707
77	Ir (Solid)	-	-	-	-	730	-
77	Ir (Unspecified)	-	-	-	-	-	735
78	Pt (Solid)	-	-	780	711	780	759
79	Au (Solid)	-	761	790	760	784	755
80	Hg (Unspecified)	-	-	-	-	-	756
81	Tl (Unspecified)	-	-	-	-	-	748
82	Pb (Solid)	812	788	820	767	813	759
83	Bi (Solid)	-	-	-	-	-	765
84	Po (Unspecified)	-	-	-	-	-	775
85	At (Unspecified)	-	-	-	-	-	785
86	Rn (Unspecified)	-	-	-	-	-	793
87	Fr (Unspecified)	-	-	-	-	-	796
88	Ra (Unspecified)	-	-	-	-	-	799
89	Ac (Unspecified)	-	-	-	-	-	808

Table III.4 continued

90	Th (Solid)	-	-	-	698	-	-
90	Th (Unspecified)	-	-	-	-	-	825
91	Pa (Unspecified)	-	-	-	-	-	837
92	U (Solid)	945	872	900	856	-	847
	Air (Gas)	85	85	-	-	-	-
	Emulsion (Solid)	-	323	-	-	-	-
	Methane (Gas)	-	45	-	-	-	-

Table III.5 Ratio of mean ionization potential in gas phase to that in condensed phase as given by theoretical models of Sternheimer (1953b) and Brandt (1956) and by comparison of exact calculations of Dehmer et al. (1975) to data.

	I(gas)/I(condensed)		
Material	Sternheimer	Brandt	Dehmer et al.
Li	0.84	0.88	0.88
Be		0.70	0.75 ± 0.16
C	0.90	0.84	0.84
Al	0.97	0.73	0.76
Cl		0.84	0.95

Table III.6. Recommended values of I and values for I_{adj} and I as given by eq. III.40 and eq. III.42 respectively. All values are expressed in eV.

Z_2	Material	Recommended	I_{adj}	I
1	H_2 (Gas)	18.5 ± 0.2	19	23
1	H (Liquid)	20.7	19	23
1	H (Saturated condensed compounds)	17.6	19	23
1	H (Unsaturated condensed compounds)	14.8	19	23
2	He (Gas)	42.3 ± 0.5	31	35
3	Li (Solid)	40.0 ± 1.6	43	46
4	Be (Solid)	63.9 ± 0.7	55	58
5	B (Solid)	76	67	70
6	C (Graphite)	79.0 ± 0.7	79	81
6	C (Saturated condensed compounds)	77.3	79	81
6	C (Unsaturated condensed compounds)	75.1	19	23
6	C (Highly chlorinated condensed compound)	64.8	79	81
7	N_2 (Gas)	82 ± 4	91	93
7	N (Liquid)	85.1	91	93
7	N (Amines, nitrates in condensed compounds)	99.5	91	93
7	N (Rings in condensed compounds)	76.8	91	93
8	O_2 (Gas)	98.5 ± 1.5	103	105
8	O (Liquid)	98.3	103	105
8	O (-O- in condensed compounds)	98.5	103	105
8	O (O= in condensed compounds)	88.9	103	105
9	F_2 (Gas)	120	115	117
10	Ne (Gas)	133 ± 3	127	128
11	Na (Solid)	148	139	140
12	Mg (Solid)	156	151	152
13	Al (Solid)	164 ± 1	163	163
14	Si (Solid)	169 ± 2	172	175
15	P (Solid)	172	182	183
16	S (Solid)	180	191	192
17	Cl (Liquid)	173 ± 3	200	201
18	Ar (Gas)	188 ± 2	210	210
19	K (Solid)	193	219	218
20	Ca (Solid	191 ± 3	228	227
21	Sc (Solid)	216 ± 2	238	236
22	Ti (Solid)	228 ± 2	247	244
23	V (Solid)	242 ± 4	257	253
24	Cr (Solid)	260 ± 1	266	262
25	Mn (Solid)	273 ± 3	276	271
26	Fe (Solid)	275 ± 3	285	279
27	Co (Solid)	296 ± 4	295	288
28	Ni (Solid)	310 ± 2	304	297
29	Cu (Solid)	317 ± 2	314	305

30	Zn (Solid)	322 ± 3	324	314
31	Ga (Solid)	324	333	323
32	Ge (Solid)	340 ± 10	343	332
33	As (Solid)	338	352	340
34	Se (Solid)	340	362	349
35	Br_2 (Liquid)	349	372	358
36	Kr^2 (Gas)	357 ± 2	381	366
37	Rb (Solid)	358	391	375
38	Sr (Solid)	363	400	384
39	Y (Solid)	370	410	392
40	Zr (Solid)	382 ± 4	420	401
41	Nb (Solid)	399 ± 9	429	410
42	Mo (Solid)	414 ± 8	439	419
43	Tc (Solid)	410	448	427
44	Ru (Solid)	423	458	436
45	Rh (Solid)	442 ± 2	468	445
46	Pd (Solid)	457 ± 1	477	453
47	Ag (Solid)	469 ± 2	487	462
48	Cd (Solid)	467 ± 5	497	471
49	In (Solid)	481 ± 1	506	480
50	Sn (Solid)	498 ± 6	516	488
51	Sb (Solid)	494	526	497
52	Te (Solid)	495	535	506
53	I (Solid)	498	545	514
54	Xe (Gas)	489 ± 9	555	523
55	Cs (Solid)	490	564	532
56	Ba (Solid)	483	574	541
57	La (Solid)	480	584	549
58	Ce (Solid)	493	593	558
59	Pr (Solid)	507	603	567
60	Nd (Solid)	521	613	575
61	Pm (Solid)	537	622	584
62	Sm (Solid)	548	632	593
63	Eu (Solid)	562	642	602
64	Gd (Solid)	564	651	610
65	Tb (Solid)	585	661	619
66	Dy (Solid)	600	671	628
67	Ho (Solid)	623	680	636
68	Er (Solid)	640	690	645
69	Tm (Solid)	652	700	654
70	Yb (Solid)	662	709	663
71	Lu (Solid)	672	719	671
72	Hf (Solid)	682	729	680
73	Ta (Solid)	703 ± 10	739	689
74	W (Solid)	722 ± 14	748	697
75	Re (Solid)	698	758	706
76	Os (Solid)	707	768	715
77	Ir (Solid)	733 ± 3	777	723
78	Pt (Solid)	758 ± 16	787	732
79	Au (Solid)	770 ± 7	797	741
80	Hg (Liquid)	756	806	750
81	Tl (Solid)	748	816	758

82	Pb (Solid)	793 ± 11	826	767
83	Bi (Solid)	765	835	776
84	Po (Solid)	775	845	784
85	At (Solid)	785	855	793
86	Rn (Gas)	793	865	802
87	Fr (Solid)	796	874	811
88	Ra (Solid)	799	884	819
89	Ac (Solid)	808	894	828
90	Th (Solid)	762 ± 64	903	837
91	Pa (Solid)	837	913	845
92	U (Solid)	884 ± 18	923	854

Table IV.1. Fractional Radiative correction to the Bethe formula for heavy charged particles in argon gas. $W_o = I = 186$ eV.

	100 x (F+G)/2		
γ	Jankus (1953), Q=m	Jankus, Q=2mγ	Eq. IV.10
10	0.27	0.19	0.32
20	0.45	0.37	0.43
50	0.75	0.66	0.60
100	0.95	0.88	0.73

Table IV.2 Fractional kinematical correction to the Bethe formula for protons in argon gas.

γ	Δ (%)
10	-0.045
20	-0.079
50	-0.17
100	-0.31
200	-0.54
500	-1.08
1000	-1.72

Table IV.3 Fractional form-factor correction to the Bethe formula for nuclei and anti-nuclei in argon gas.

	Δ (%)			
γ	$A_1 = 1$	$A_1 = 10$	$A_1 = 100$	$A_1 = 250$
10	-0.0026	-0.013	-0.058	-0.11
20	-0.0089	-0.041	-0.19	-0.35
50	-0.047	-0.21	-0.93	-1.60
100	-0.16	-0.73	-2.68	-4.02

Table IV.4 Fractional form-factor (complete) plus recoil corrections to the Bethe formula for protons and deuterons in aluminum.

	Δ (%)	
γ	Protons (Turner et al., 1969)	Deuterons (Vora and Turner, 1970)
10	-0.044 (-0.048)	-0.08
50	-0.088 (-0.22)	-0.32
100	-0.30 (-0.47)	-0.71
250	-0.69	-2.57
500	-1.5	-5.05
750	-2.3	-6.77
1000	-3.1	-7.47

Table IV.5 Ratio of bremsstrahlung to collisional energy loss for heavy nuclei in an argon gas.

	Ratio (%)			
γ	$A_1=1,\ Z_1=1$	$A_1=10,\ Z_1=5$	$A_1=100,\ Z_1=50$	$A_1=250,\ Z_1=100$
10	0.029	0.088	1.02	1.72
20	0.053	0.158	1.83	3.10
50	0.116	0.347	4.04	6.82
100	0.213	0.637	7.41	12.5
200	0.394	1.177	13.7	23.1
500	0.895	2.67	31.1	52.6
1000	1.674	5.00	58.2	98.3

Table IV.6 Values for $\cos\chi$ to be used in eq. IV.23.

$\lvert Z_1\alpha/\beta\rvert$	$\cos\chi$
0	1.000
0.05	0.9905
0.10	0.9631
0.15	0.9208
0.20	0.8680
0.30	0.7478
0.40	0.6303
0.50	0.5290
0.60	0.4471
0.80	0.3323
1.00	0.2610
1.20	0.2145
1.50	0.1696
2.00	0.1261

Table IV.7 Value for Z_{eff} as given by eq. IV.28 at the Bohr velocity of $Z_0 c/137$.

Z_0	Z_{eff}(Bohr velocity)
10	8.7
20	18.5
30	28.4
40	38.4
50	48.5
60	58.5
70	68.6
80	78.7
90	88.7

Table IV.8. Values of B from Moliere theory from Bichsel (1972).

Z_2	ρx, $\frac{g}{cm^2}$	$Z_1 = 1$									$Z_1 = 2$		$Z_1 = 6$	
		$\beta^2=0$	0.005	0.01	0.02	0.05	0.1	0.2	0.5	1.0	0.1	1.0	0.1	1.0
3	10^{-3}	10.5	8.8	8.3	7.6	6.6	5.7	4.9	3.8	2.8	7.4	4.6		
	10^{-2}	13.0	11.5	16.8	10.2	9.2	8.5	7.7	6.6	5.7	16.0	7.4		
	10^{-1}	15.4	14.0	13.3	12.8	11.7	11.0	10.3	9.2	8.5	12.5	10.0		
	1	17.9	16.4	15.8	15.2	14.2	13.5	12.8	11.8	11.0	14.9	12.6		
10	10^{-3}	8.2	8.0	7.7	7.4	6.7	6.0	5.2	4.2	3.2	7.2	4.9	8.1	7.2
	10^{-2}	10.7	10.5	10.3	9.9	9.3	8.7	8.0	7.0	6.2	9.8	7.7	10.6	9.7
	10^{-1}	13.3	13.0	12.8	12.4	11.8	11.2	10.5	9.6	8.8	12.3	10.3	13.1	12.3
	1	15.7	15.4	15.2	14.8	14.3	13.7	13.1	12.1	11.4	14.8	12.8	15.5	14.7
20	10^{-3}	6.8	6.7	6.6	6.5	6.2	5.8	5.2	4.2	3.5	6.5	5.0	6.8	6.4
	10^{-2}	9.4	9.3	9.3	9.2	8.9	8.5	7.9	7.1	6.4	9.2	7.8	9.4	9.1
	10^{-1}	12.0	11.9	11.8	11.7	11.4	11.0	10.5	9.7	9.0	11.7	10.3	11.9	11.6
	1	14.4	14.4	14.3	14.2	13.9	13.5	13.1	12.2	11.5	14.2	12.8	14.4	14.2
50	10^{-3}	4.7	4.7	4.7	4.6	4.6	4.5	4.3	3.7	3.2	4.6	4.1	4.7	4.6
	10^{-2}	7.5	7.5	7.5	7.4	7.4	7.3	7.2	6.6	6.0	7.5	7.0	7.5	7.4
	10^{-1}	10.0	10.0	10.0	10.0	10.0	9.9	9.7	9.2	8.8	10.0	9.6	10.1	10.0
	1	12.5	12.5	12.5	12.5	12.5	12.4	12.2	11.8	11.3	12.6	12.1	12.5	12.5
100	10^{-3}	3.1	3.1	3.1	3.1	3.0	3.0	3.0	2.8	2.5	3.1	2.9	3.1	3.1
	10^{-2}	6.0	6.0	6.0	6.0	6.0	5.9	5.9	5.7	5.4	6.0	5.8	6.0	6.0
	10^{-1}	8.7	8.7	8.7	8.7	8.7	8.6	8.6	8.4	8.2	8.7	8.5	8.7	8.7
	1	11.2	11.2	11.2	11.2	11.2	11.1	11.1	10.9	10.7	11.2	11.0	11.2	11.2

Table IV.9. Multiple scattering integral distribution function from Bichsel (1972).

x	B = 4	6	8	10	12
0.2	0.04617	0.04320	0.04195	0.04123	0.04078
0.4	0.16893	0.15993	0.15616	0.15393	0.15253
0.6	0.33004	0.31815	0.31316	0.31008	0.30814
0.8	0.48890	0.48156	0.47856	0.47637	0.47496
1.0	0.61973	0.62359	0.62554	0.62592	0.62614
1.2	0.71612	0.73300	0.74088	0.74449	0.74676
1.4	0.78446	0.81102	0.82357	0.82981	0.83380
1.6	0.83429	0.86473	0.87948	0.88704	0.89194
1.8	0.87231	0.90159	0.91620	0.92378	0.92875
2.0	0.90166	0.92709	0.94016	0.94690	0.95136
3.0	0.96607	0.97697	0.98244	0.98447	0.98575
4.0	0.98398	0.98934	0.99189	0.99212	0.99224
5.0	0.99152	0.99429	0.99557	0.99504	0.99503
6.0	0.99530	0.99676	0.99741	0.99651	0.99655
7.0	0.99655	0.99762	0.99810	0.99744	0.99747
8.0	0.99736	0.99818	0.99854	0.99804	0.99806
9.0	0.99791	0.99856	0.99885	0.99845	0.99847
10.0	0.99831	0.99883	0.9907	0.99874	0.99876

Table IV.10. Mean free paths for inelastic nuclear reactions in units of Range at 1 GeV/amu.

Projectile/Target	Air	Aluminum	Copper	Lead
^{1}H	0.192	0.206	0.229	0.254
^{12}C	0.234	0.290	0.386	0.507
^{20}Ne	0.314	0.401	0.548	0.756
^{40}Ar	0.363	0.482	0.698	1.02
^{56}Fe	0.456	0.620	0.920	1.37
^{195}Pt	0.606	0.874	1.39	2.30

Table VI.1. Energy removed from "thick" aluminum absorber by delta rays produced by passing proton.

T(MeV)	δ(eq.VI.16)(keV)	δ(Laulainen & Bichsel)
10	0.62	0.59
20	1.05	1.05
30	1.47	1.41
40	1.87	1.79
50	2.27	2.18

Table VI.2. Parameters of Voltz model obtained by several groups.

Source	Scintillator Type	B_S(g/cm^2/MeV)	T_o(keV)
Ahlen et al. (1977)	Pilot F	6.29×10^{-3}	1.37
Ahlen et al. (1977)	Pilot Y	1.02×10^{-2}	1.78
Buffington et al. (1978)	NE 110	4.5×10^{-3}	1.5
Buffington et al. (1978)	Pilot Y	4.5×10^{-3}	1.5

Table VI.3. Detector resolution $\sigma/\Delta E$ in units of $(\frac{2\pi N Z_1^2 e^4 x}{mv^2})^{-\frac{1}{2}} (\ell n \frac{2mc^2\beta^2\gamma^2}{I})^{-1}$.

Detector	$\sigma/\Delta E$
Lexan track detector	$10^{-2}\sqrt{2mc^2}(16.4+3.2\ell n\beta)^{\frac{1}{2}}(\frac{9.6+2\ell n\beta\gamma}{11.2+2\ell n\beta\gamma})$
Scintillator and Emulsion	$\beta\gamma\sqrt{2mc^2}(1-\frac{\beta^2}{2})^{\frac{1}{2}}(\frac{9.7+2\ell n\beta\gamma}{6.5+2\ell n\beta\gamma})$
Ionization Chamber and Solid State Detector	$\frac{1}{2}\beta\gamma\sqrt{2mc^2}(1-\frac{\beta^2}{2})^{\frac{1}{2}}$

Table VI.4. Values of W(eV/ion pair) for various substances.

	Substance	α particles	340 MeV protons	β particles
Gases	He	42.7,46.0		42.3
	Ne	36.8		36.6
	Ar	26.4,26.25		26.4
	Kr	24.1		24.2
	Xe	21.9		22.0
	H_2	36.3,37.0,36.0	36.5	36.3
	N_2	36.4,36.5	34.7	34.9
	O_2	32.2,32.5	32.6	30.9
	Air	35.0	34.4	30.9
	CO_2	34.0,34.3		32.9
	CH_4	29.0,29.2,29.4		27.3
Solids	Si	3.55		3.55
	Ge	2.9		
	Se	3.9		
	InSb	0.6		
	AgCl			7.6

Figure Captions

Figure III.1. Non-relativistic forms of eqs. III.20a,b and c. Note that L_{BETHE} is independent of Z_1 and that $L_{BOHR} = L_{BLOCH}$ for $Z_1 = 92$, $L_{BETHE} = L_{BLOCH}$ for $Z_1 = 1$ and that $L_{BLOCH} \rightarrow L_{BOHR}$ at small velocities and $L_{BLOCH} \rightarrow L_{BETHE}$ at large velocities for $Z_1 = 10$.

Figure III.2a. Shell corrections for protons as given by Bichsel (1972).

Figure III.2b. Shell corrections for protons as given by Fano (1963).

Figure III.2c. Theoretical and experimental shell corrections for aluminum for Andersen et al. (1977). $(C/Z_2)_{th}$ is calculated by Bonderup (1967); $(C/Z_2)'$ is the semi-empirical proton shell correction such as that given by Fano (1963) and Bichsel (1972) which includes higher order Born terms; (C/Z_2) is the pure shell correction (which is only a function of velocity and not of Z_1) as obtained by subtracting the Bloch and Lindhard corrections.

Figure III.2d. Theoretical and experimental shell corrections for copper from Andersen et al. (1977).

Figure III.2e. Theoretical and experimental shell corrections for silver from Andersen et al. (1977).

Figure III.2f. Theoretical and experimental shell corrections for gold from Andersen et al. (1977).

Figure III.3a. Density effect corrections for various solids obtained with parameters of Table III.1.

Figure III.3b. Density effect corrections for various gases.

Figure III.4. Comparison of theoretical and experimental values for the mean ionization potential. See text for a discussion.

Figure III.5. Plot of I/Z_2 as given by experiments. The expressions for I/Z_2 as given by Dalton and Turner (1968) and for I_{adj}/Z_2 as given by Sternheimer (1963) are also displayed. The scatter at low atomic number is due to variations of chemical and solid state structure. The scatter at large atomic number is due to experimental errors.

Figure III.6. Sensitivity of the stopping-power to the value used for I for several values of I and β.

Figure III.7. $(\bar{\Delta} - \Delta_{mp})/\eta$ as a function of $1/a$ as given by Sellers and Hanser (1972). See text for a definition of these variables.

Figure III.8. Range straggling for protons in various substances obtained from Bichsel (1972).

Figure IV.1. Distant collision polarization correction of Jackson and McCarthy (1972), C_1 being the fractional correction to total energy loss.

Figure IV.2. Theoretical and experimental Z_1^3 and Z_1^4 corrections to stopping-power from Andersen et al. (1977). The data are consistent with the validity of the Bloch correction while the polarization correction of Jackson and McCarthy (1972) is about a factor of two too small.

Figure IV.3. Scaled polarization corrections of Andersen et al. (1977) compared with those of Heckman and Lindstrom (1969). The former were obtained with heavy ions and

the latter were obtained with positive and negative pions.

Figure IV.4. Corrections to the Bethe formula for an aluminum absorber as a function of atomic number Z_0 (from which Z_1 was derived) and velocity. See text for a discussion of these corrections.

Figure V.1. Stopping-power of $|g| = 137e$ magnetic monopole in water as calculated by Ahlen (1976) and Ahlen (1978b). The separation of the curves at low velocities is due primarily to the Bloch correction which was not considered in the earlier calculation. The curves join at large energies due to the different manner in which the density effect was calculated.

Figure VI.1. Parameters used in the calculation of prompt dose. $F(\xi) = \xi^2 K_1^2(\xi)$ and $G(\xi) = \xi^2 K_0^2(\xi)$ where K_1 and K_0 are modified Bessel functions.

Figure VI.2. Prompt dose profiles for a water absorber divided by Z_1^2 (higher order contributions are neglected). Curves A and B are primary doses from eq. VI.5 for $\beta = 0.1$ and 0.9 respectively. Curves C and D are secondary doses from Kobetich and Katz (1968) for $\beta = 0.1$ and 0.9 respectively. The dashed lines are the small and large radius limits. 1 Mrad = 10^8 ergs/g.

Figure VI.3. First and next higher order Feynman diagrams representing Cerenkov radiation.

Figure VI.4. Typical Cerenkov counter integrated response with the

delta ray Cerenkov tail and the scintillation component indicated. Taken from Ahlen et al. (1976). The Cerenkov radiator was Pilot 425.

Figure VI.5. Etch rate dependence for Lexan on restricted energy loss (REL) as a function of particle type. Data from O'Sullivan et al. (1971).

Figure VI.6. Etch rate dependence on Z_1/β as a function of particle type. Note that all particle species fall on the same line. The data are the same for Fig. VI.5.

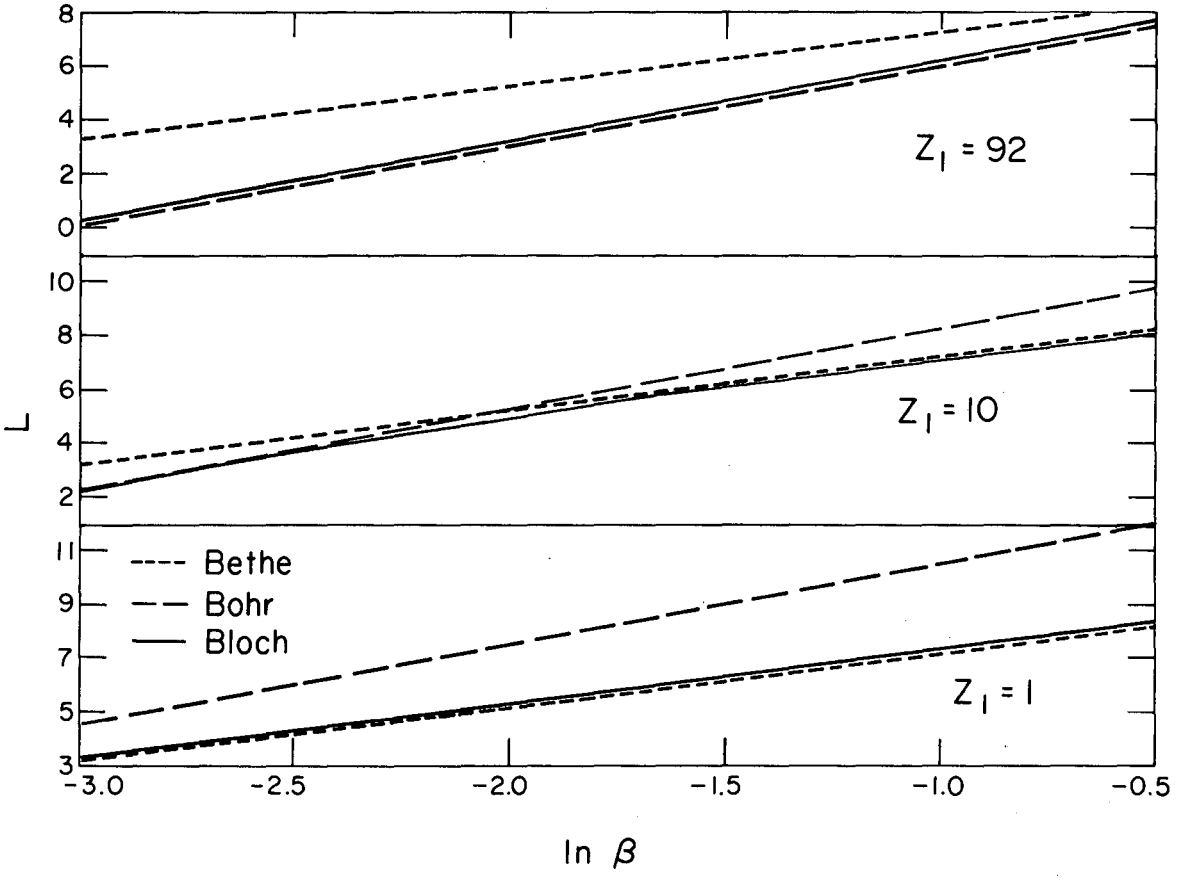

XBL 793-698

Figure III.1

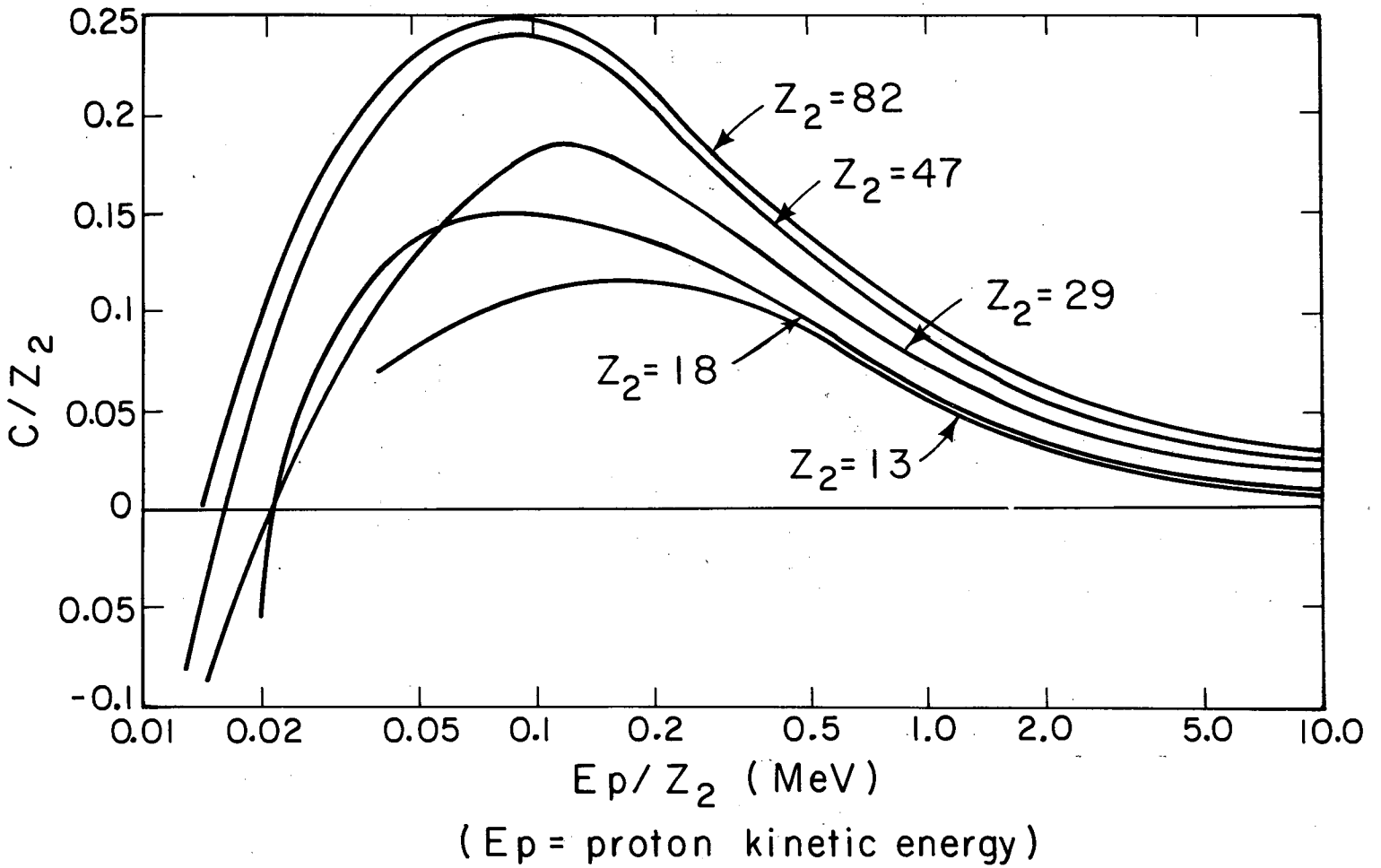

XBL788-1432

Figure III.2a

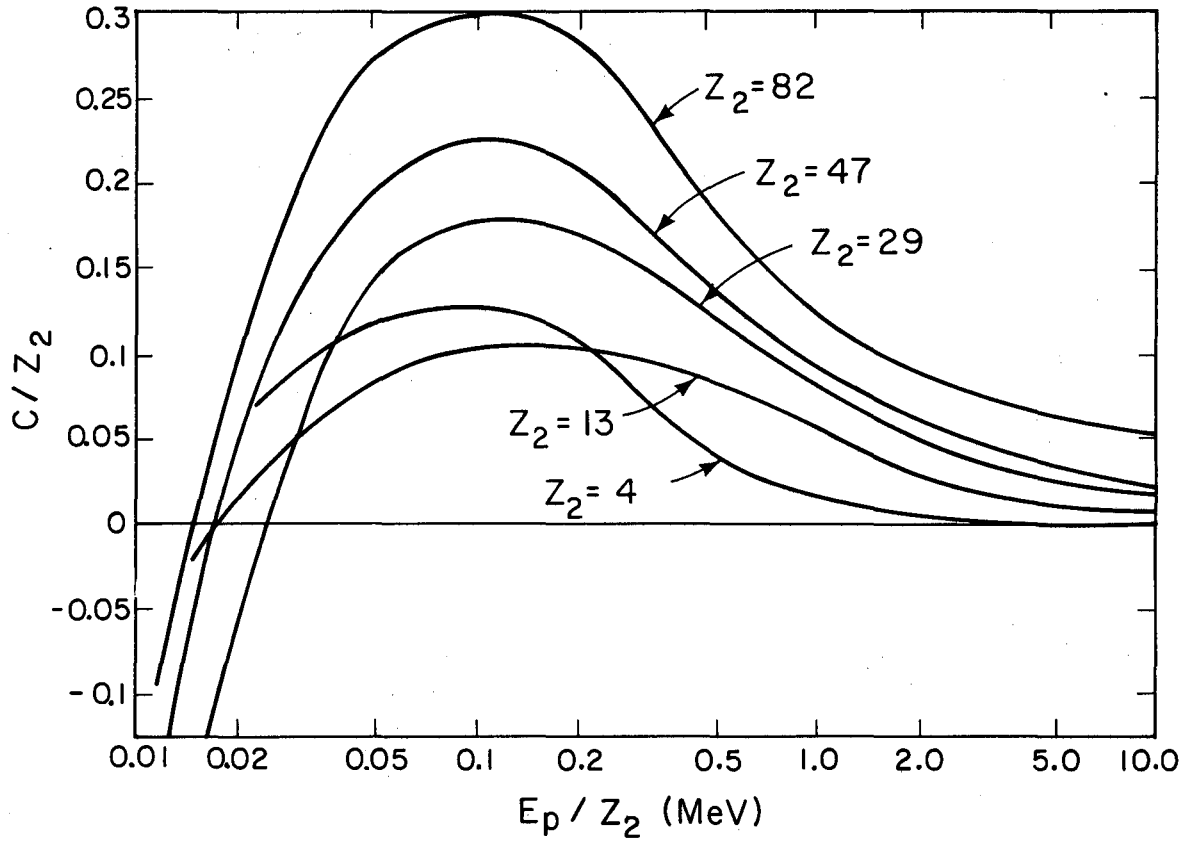

XBL788-1429

Figure III.2b

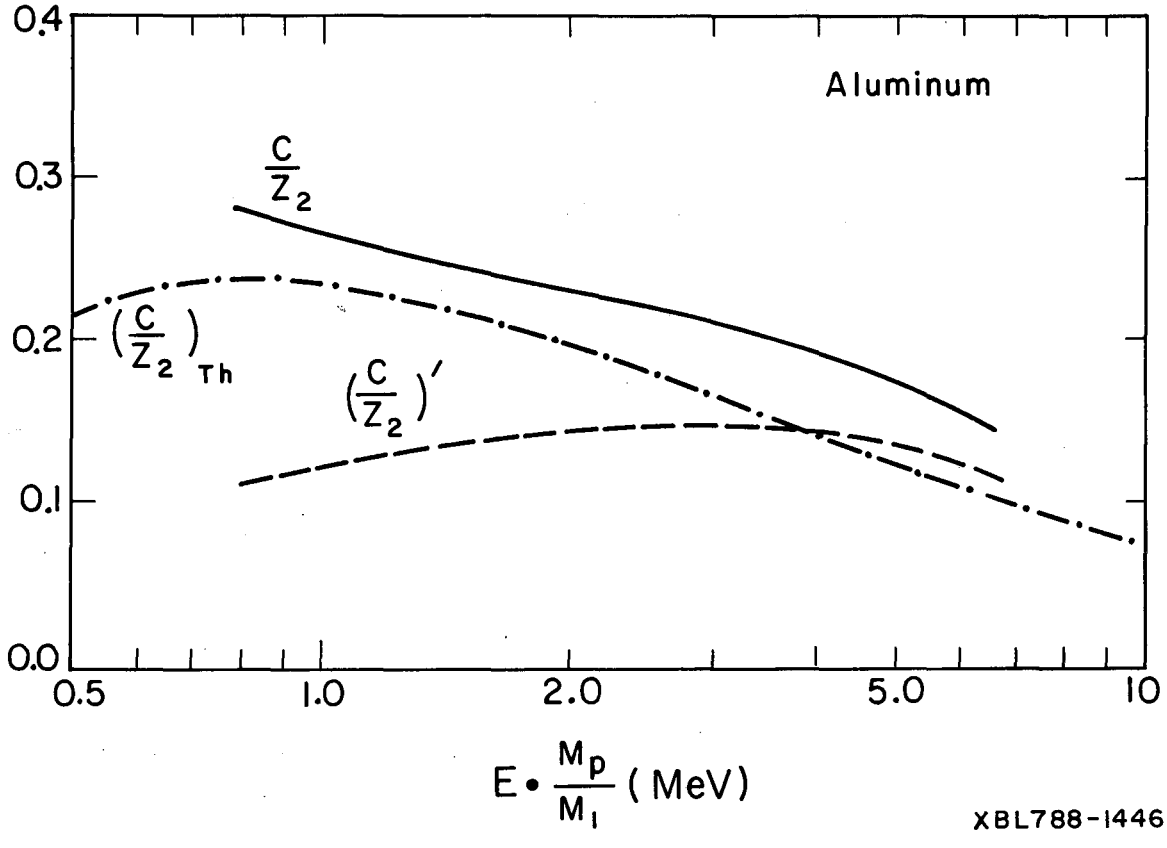

Figure III.2c

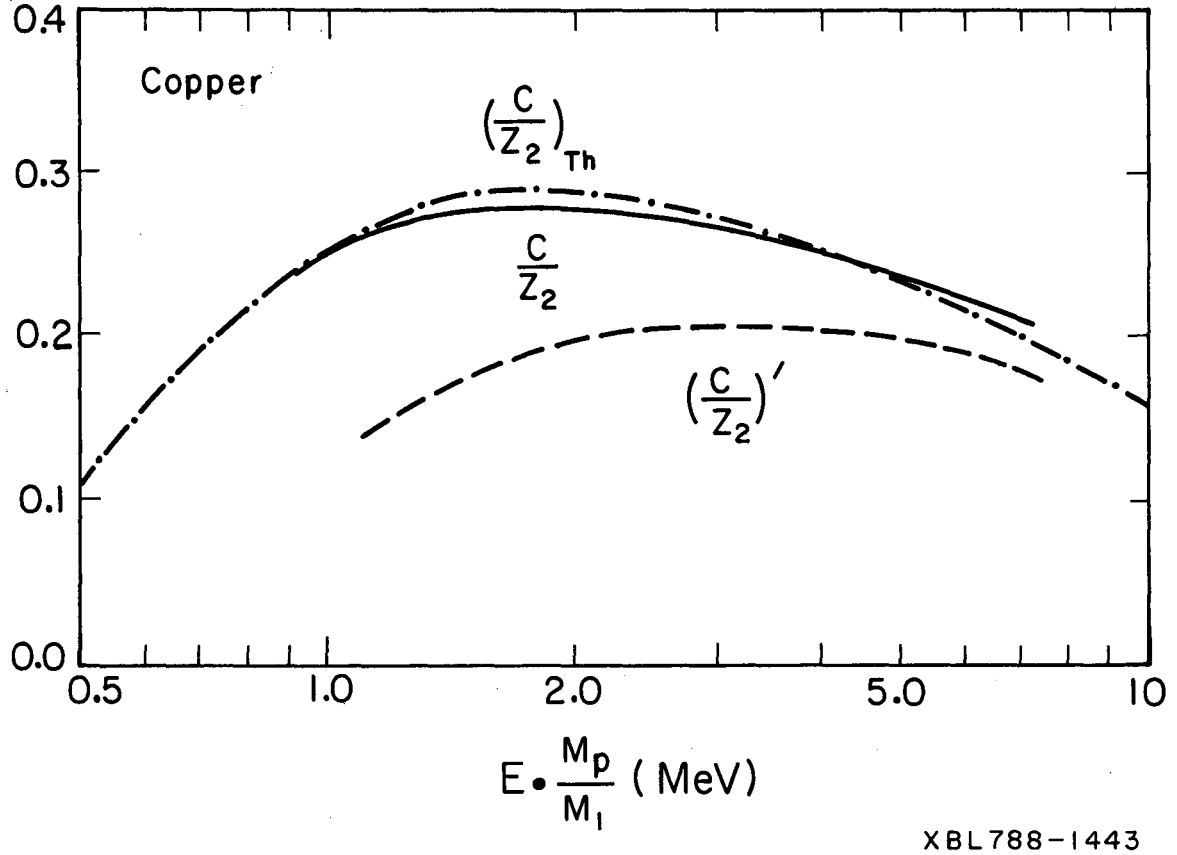

Figure III.2d

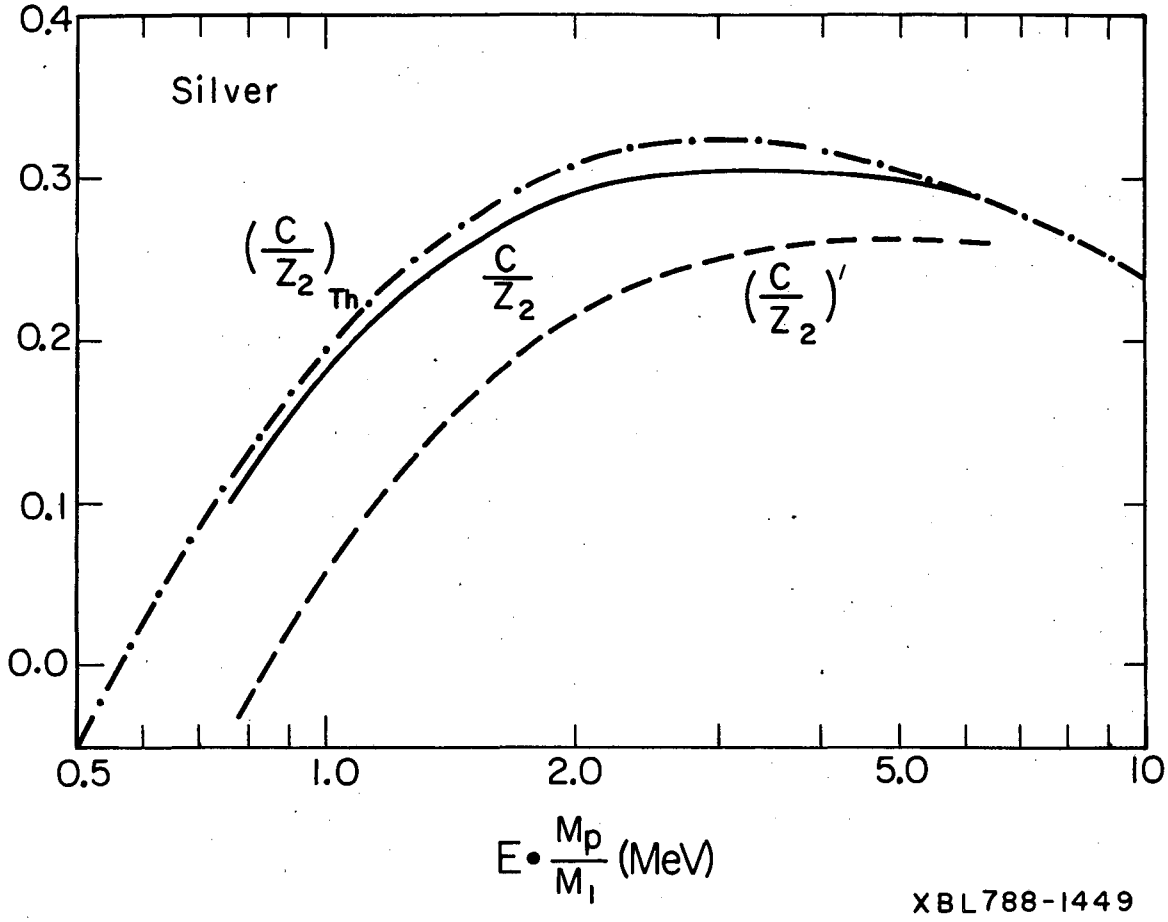

Figure III.2e

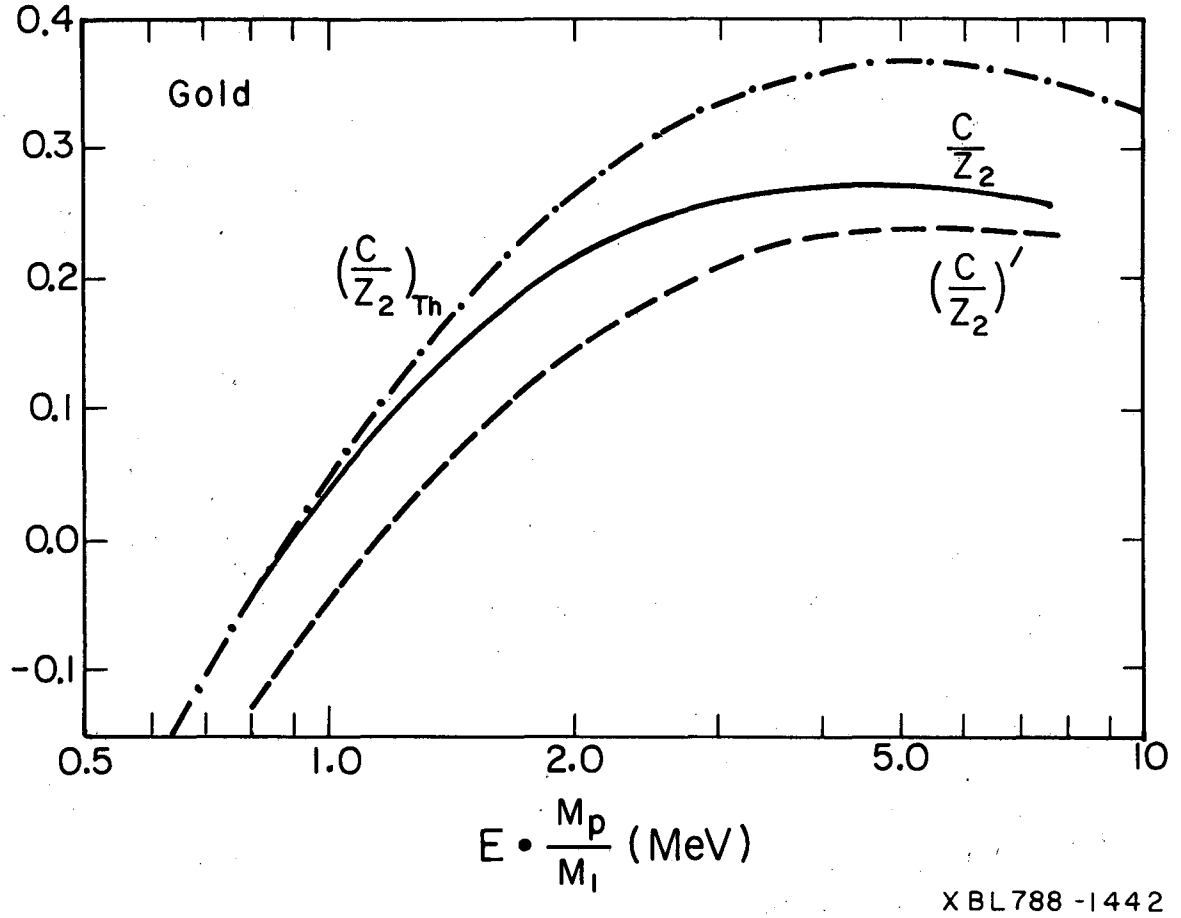

Figure III.2f

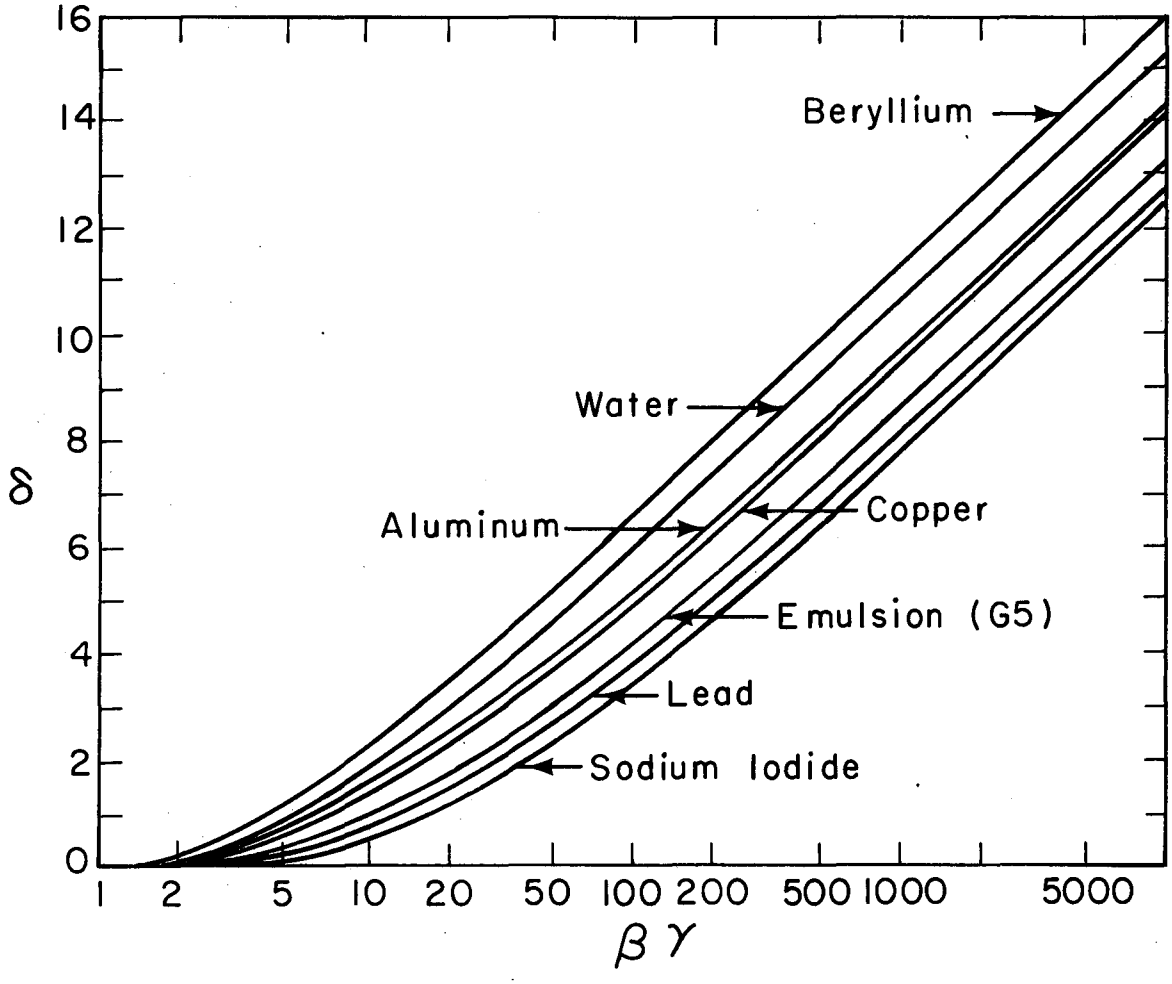

XBL788-1451

Figure III.3a

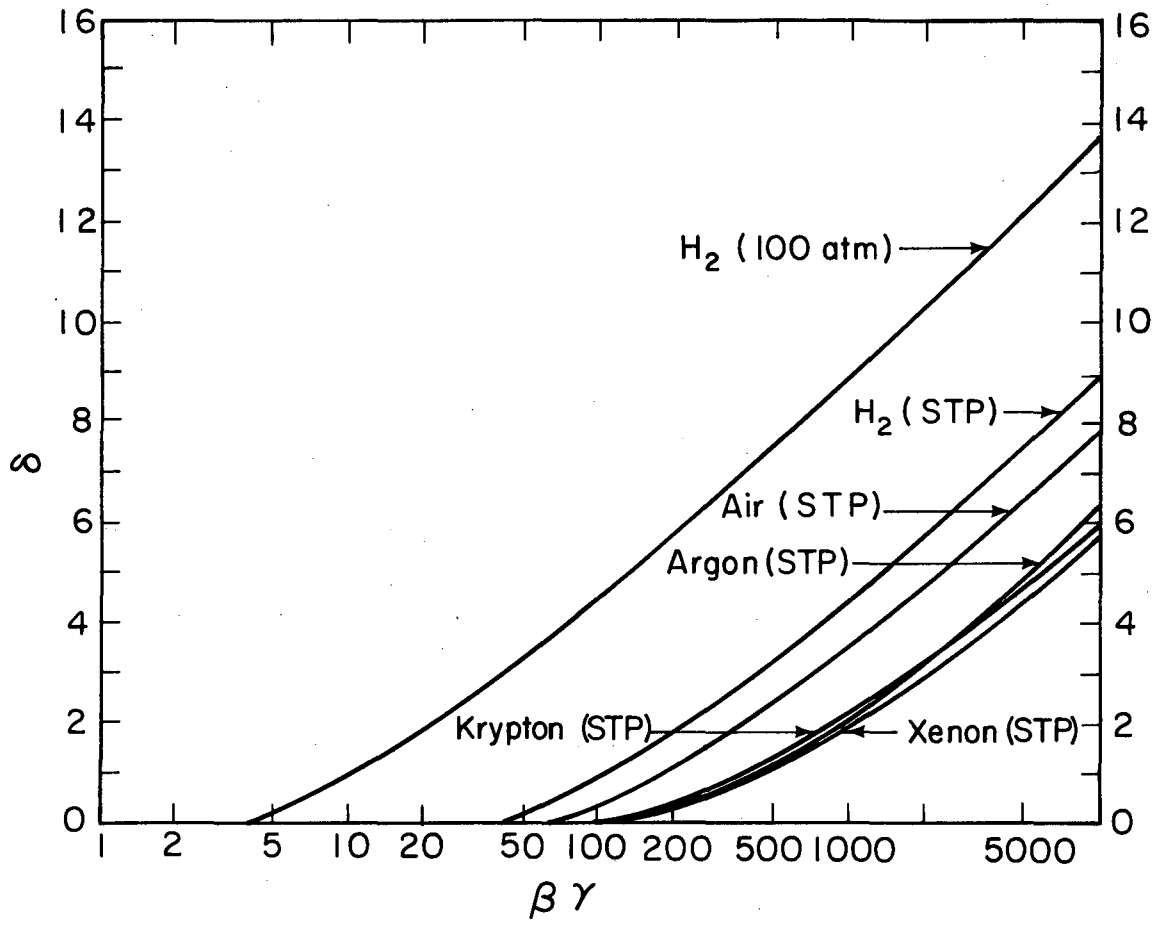

XBL788-1434

Figure III.3b

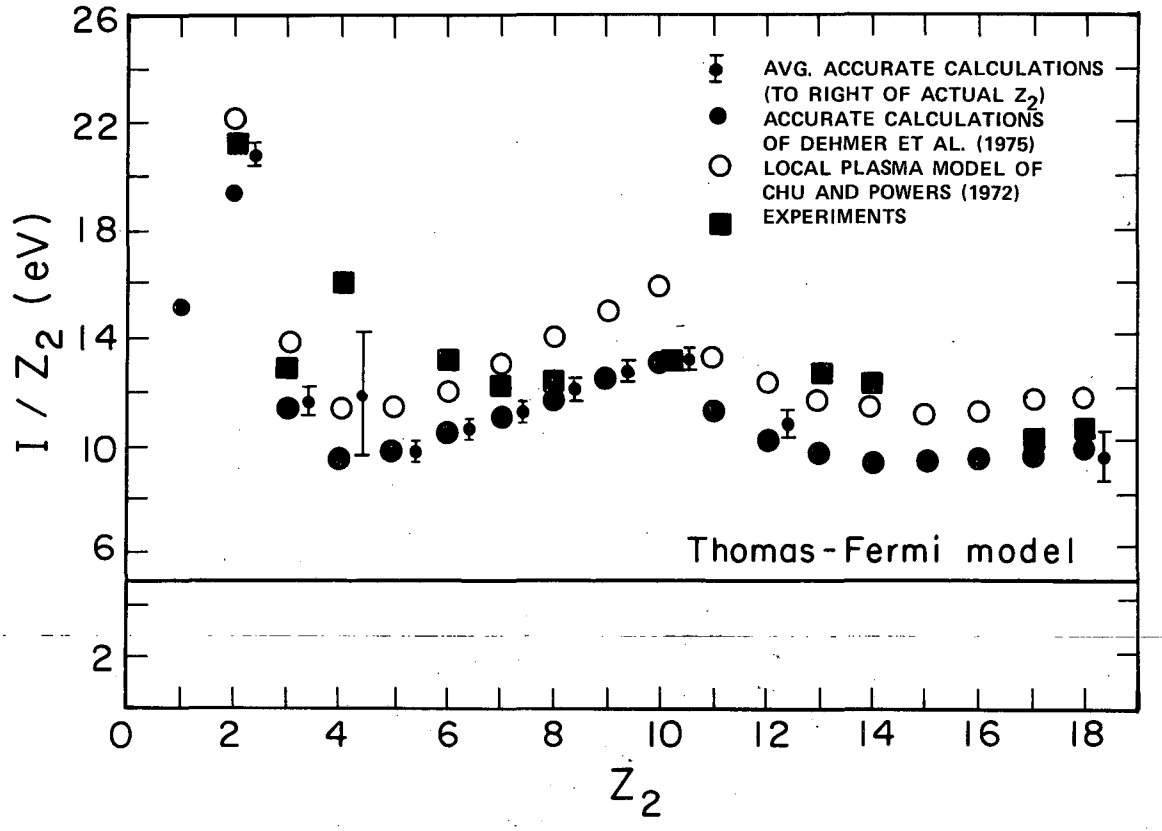

XBL 788-1431

Figure III.4

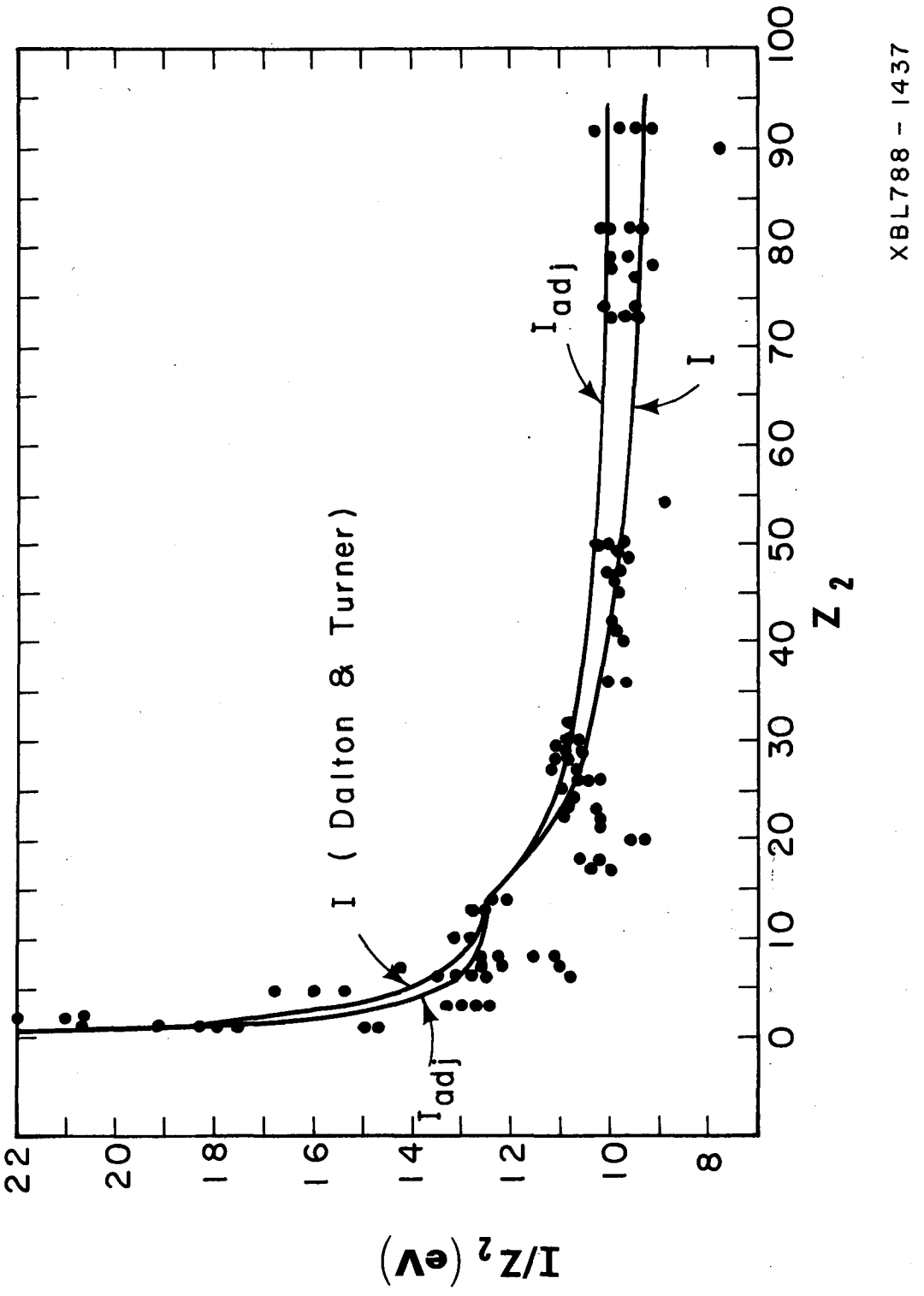

Figure III.5

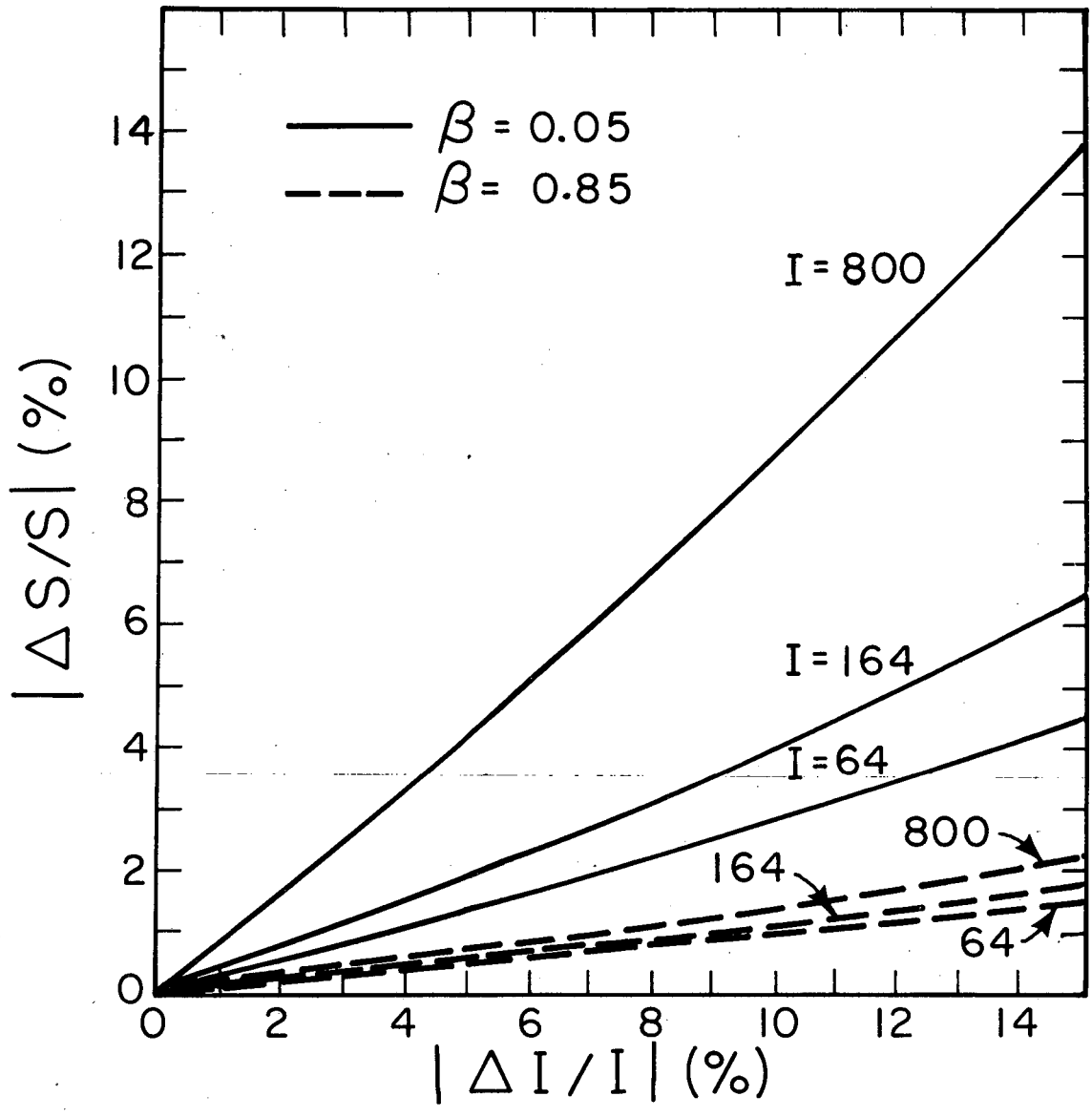
β = 0.05
β = 0.85
I = 800
I = 164
I = 64
800
164
64
|ΔS/S| (%)
|ΔI/I| (%)
0
2
4
6
8
10
12
14
XBL788 - 1450

Figure III.6

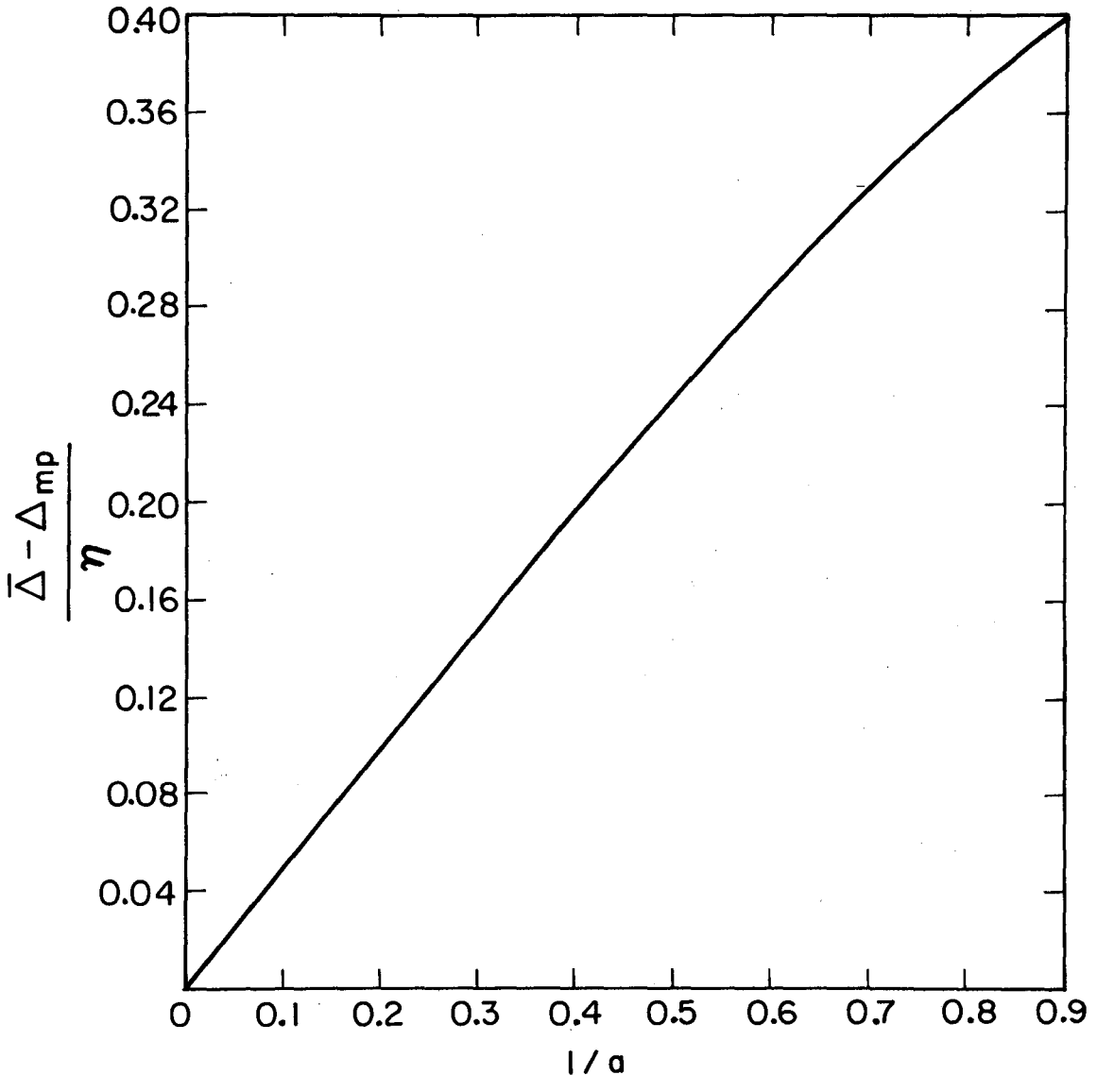

XBL788-1444

Figure III.7

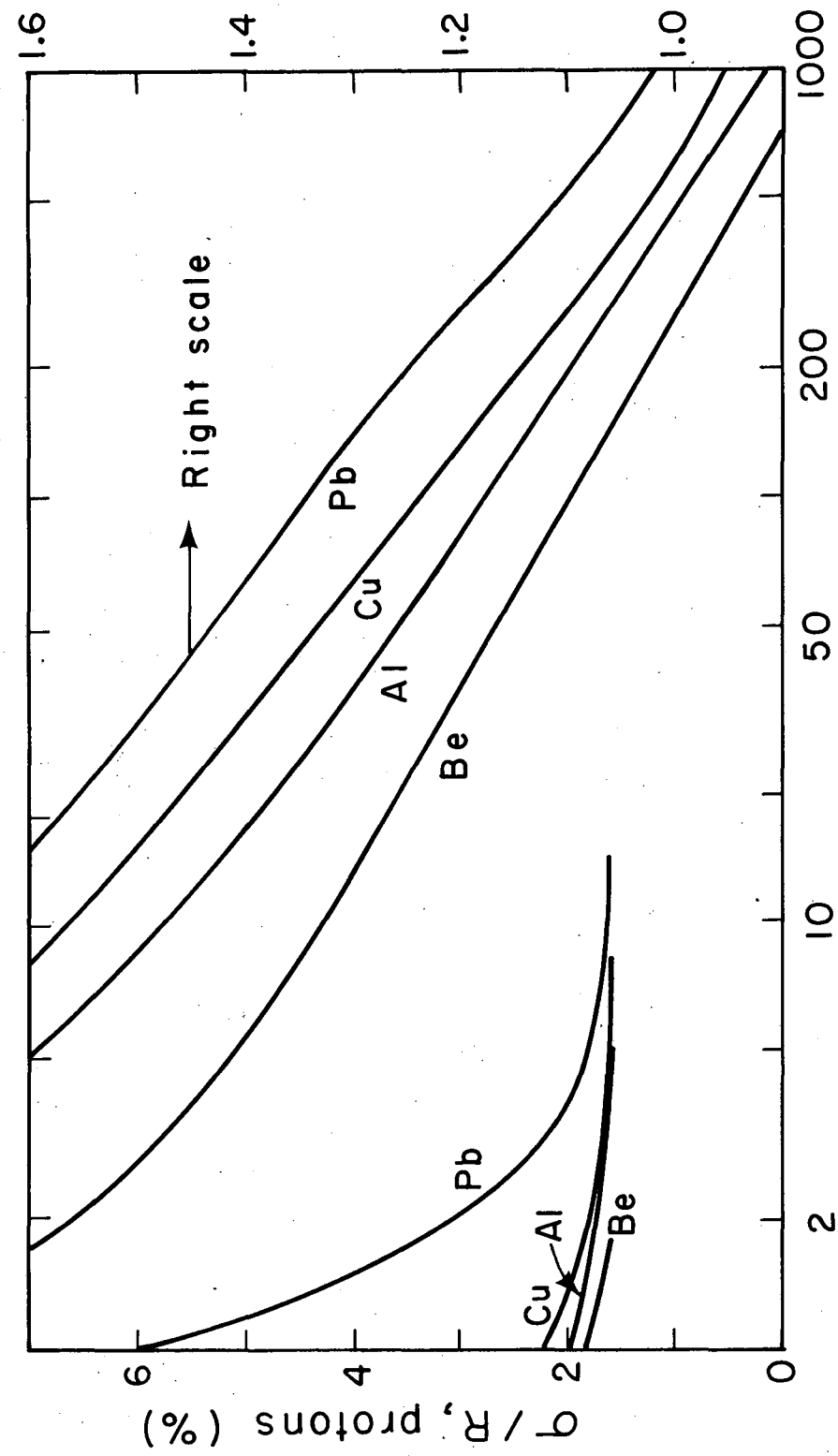

XBL 788-1440

Figure III.8

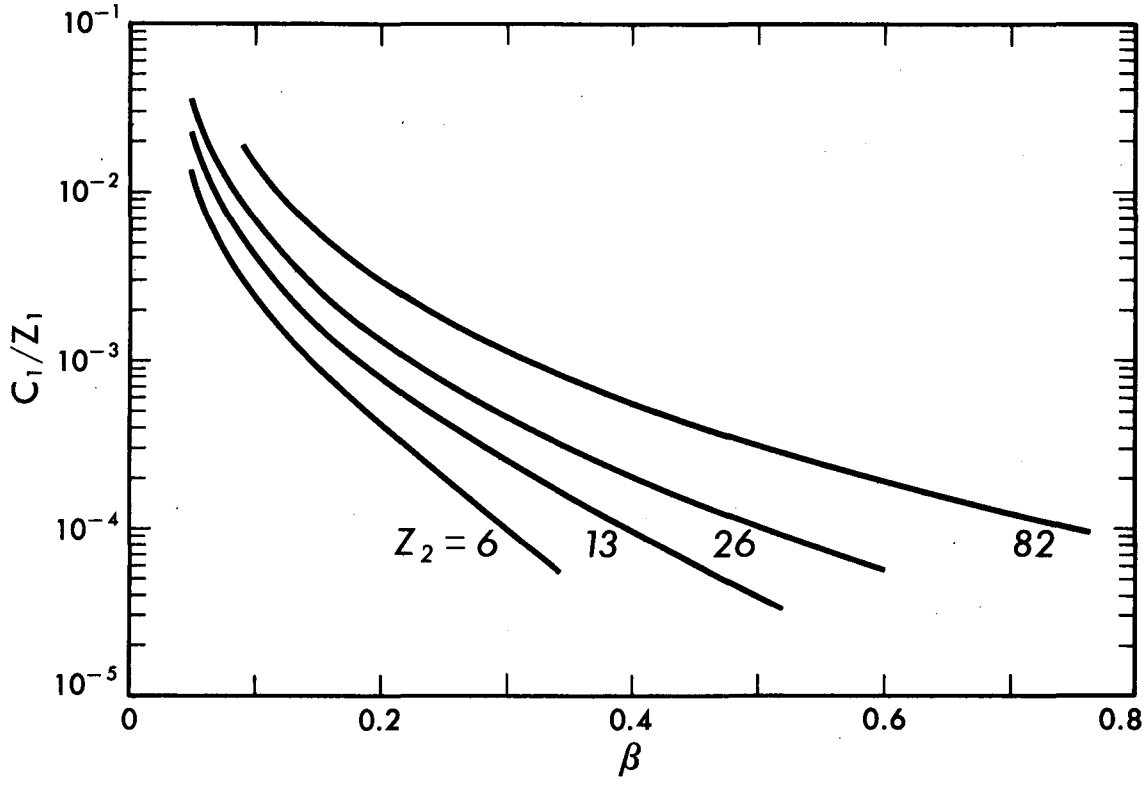

XBL 794-9281

Figure IV.1

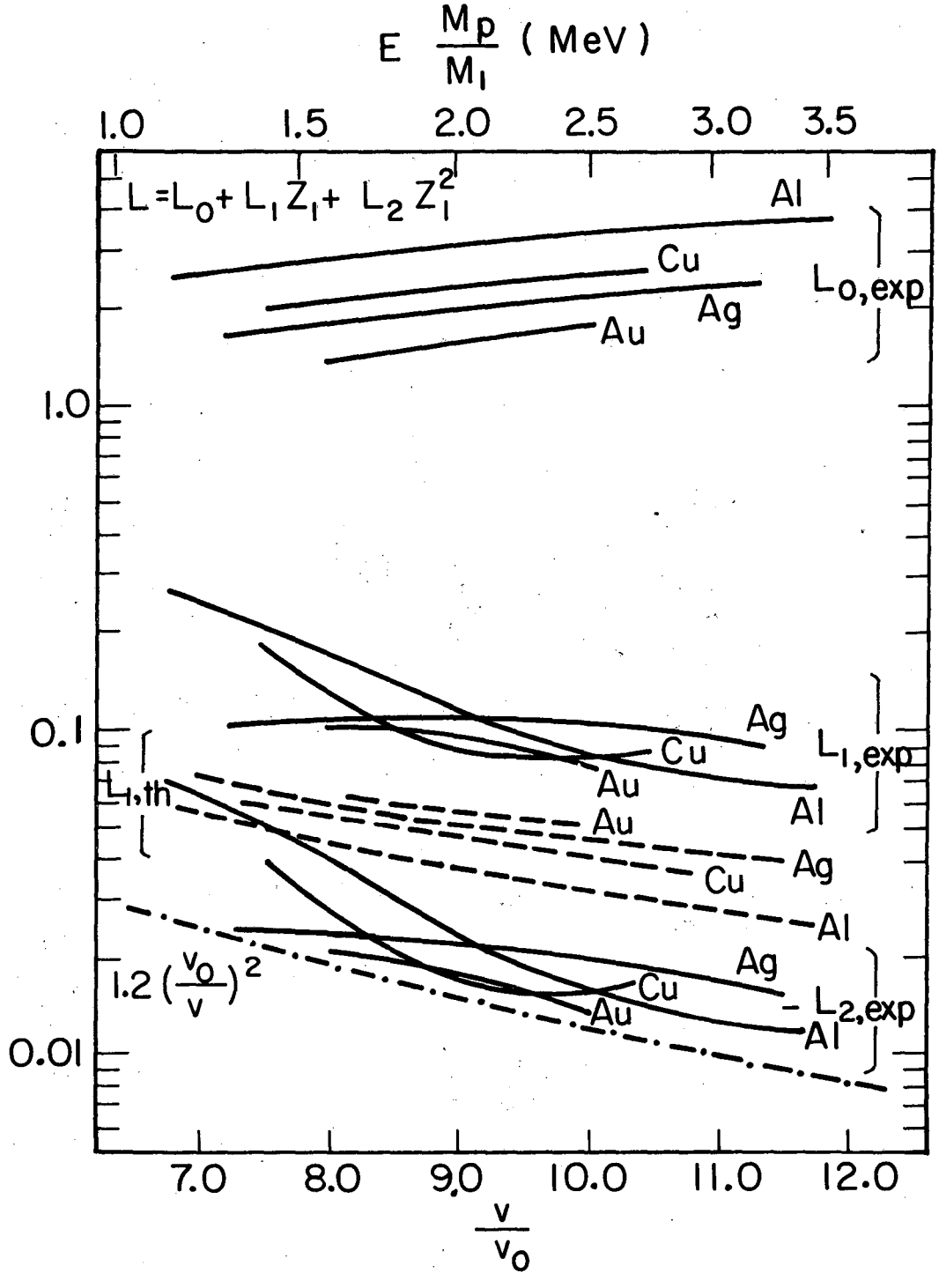

X B L 788-1430

Figure IV.2

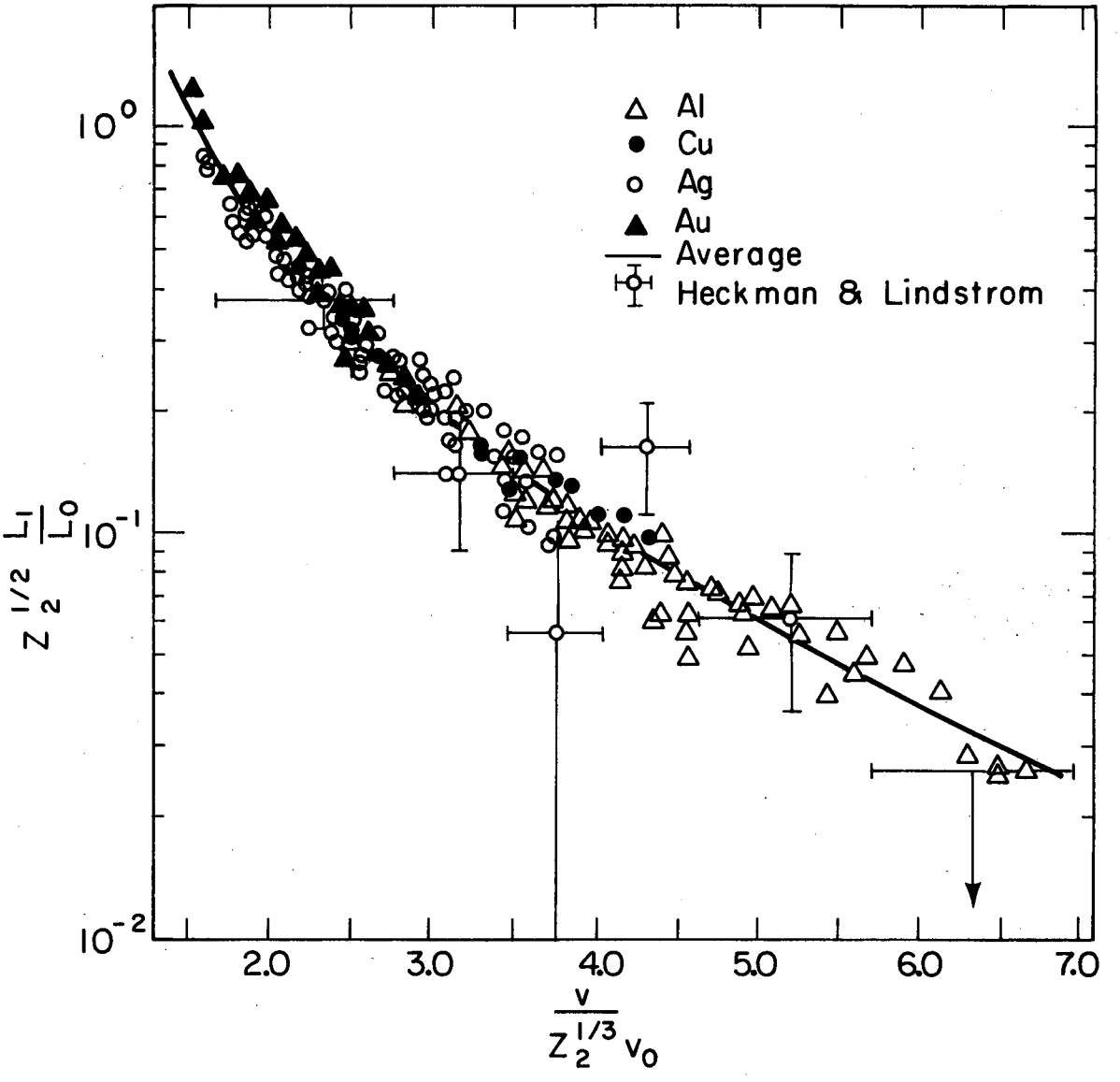

XBL788-1428

Figure IV.3

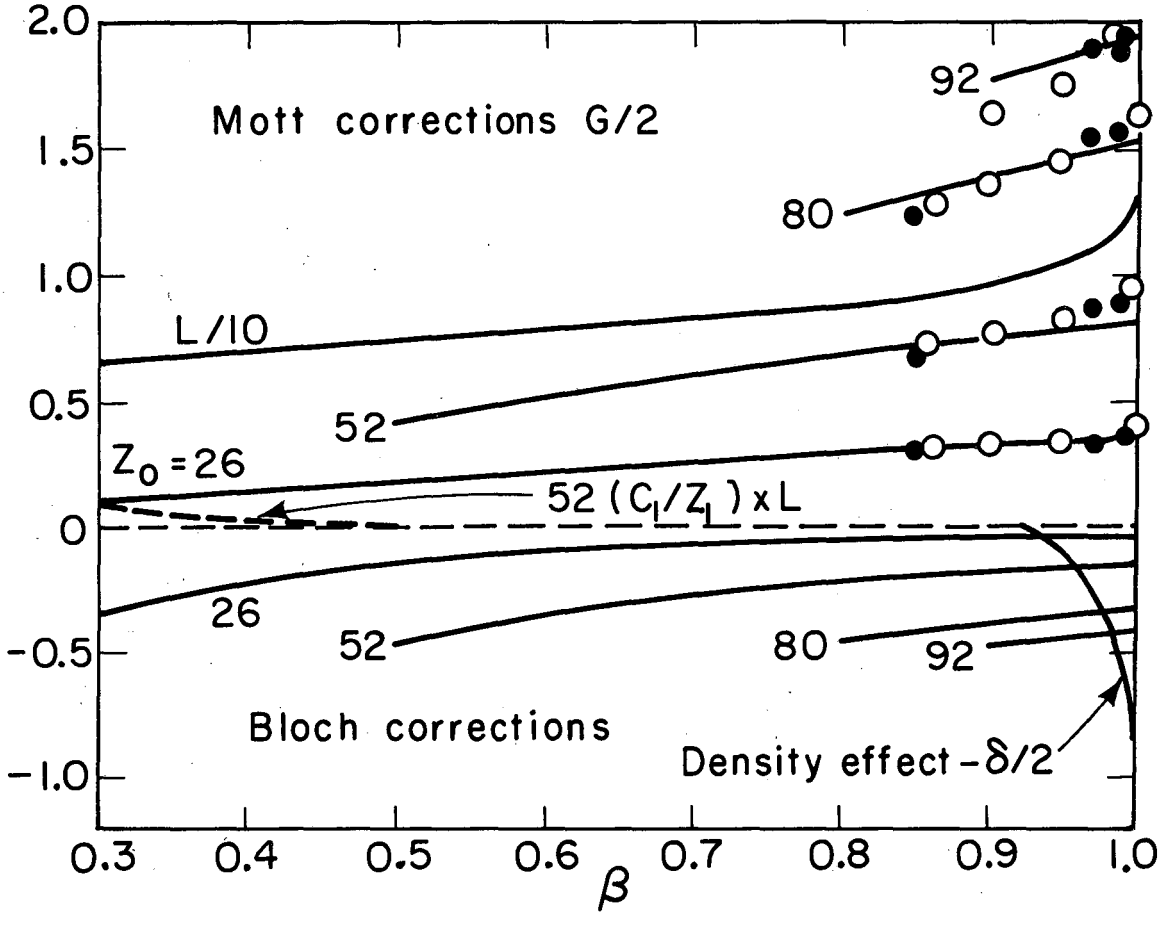

XBL 788-1433

Figure IV.4

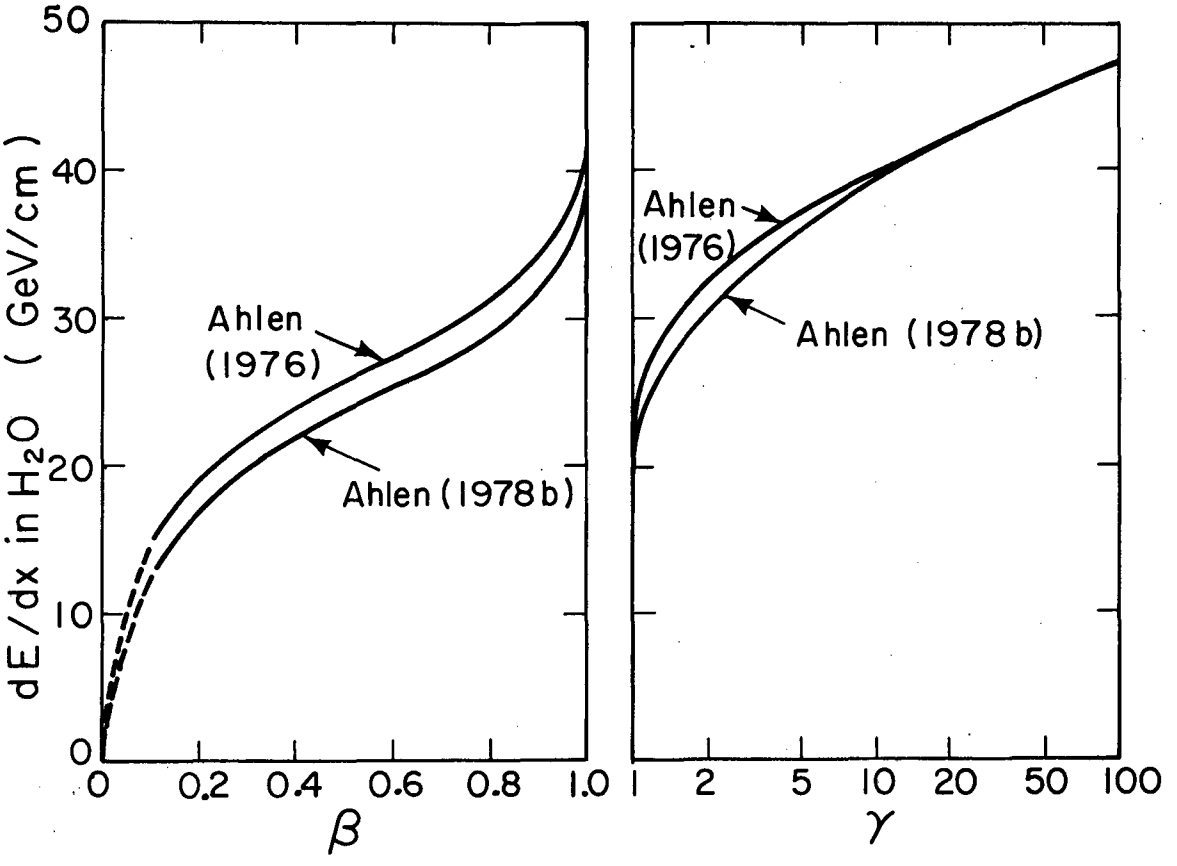

XBL788-1441

Figure V.1

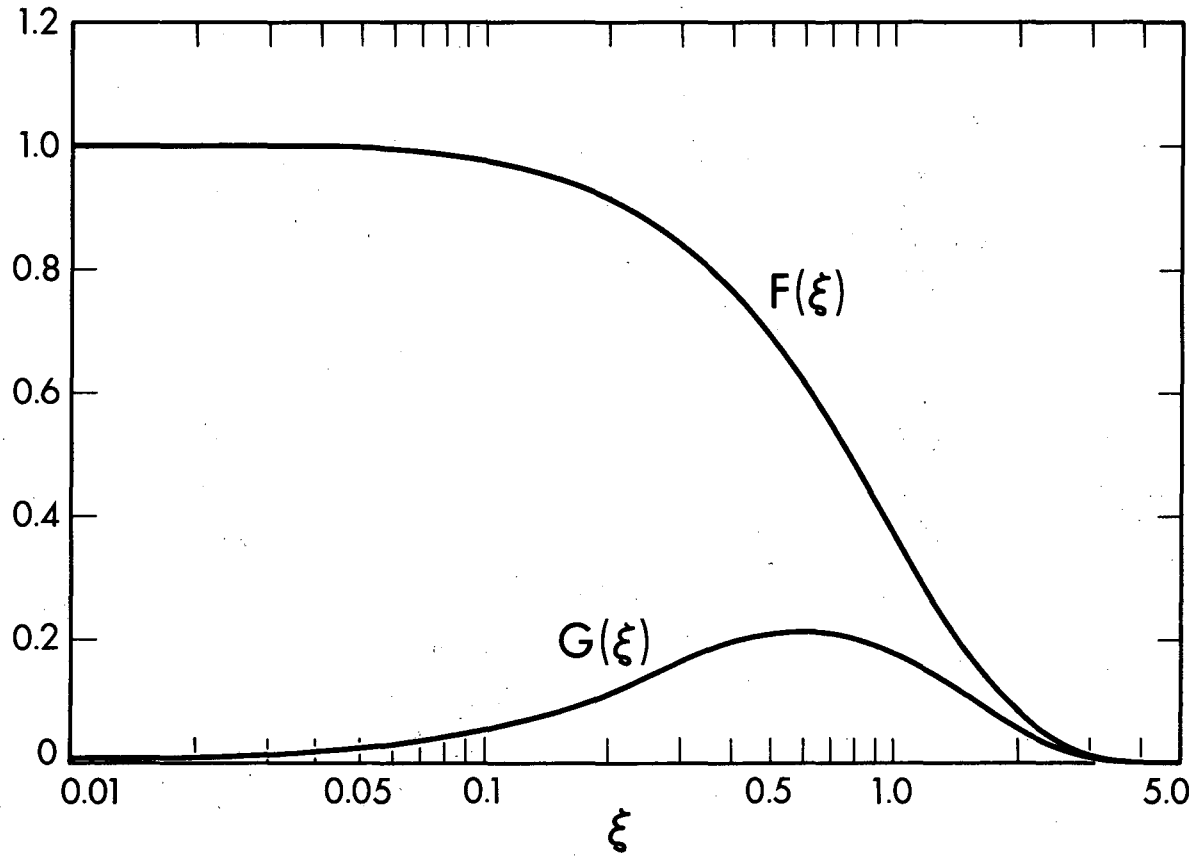

XBL 794-9280

Figure VI.1

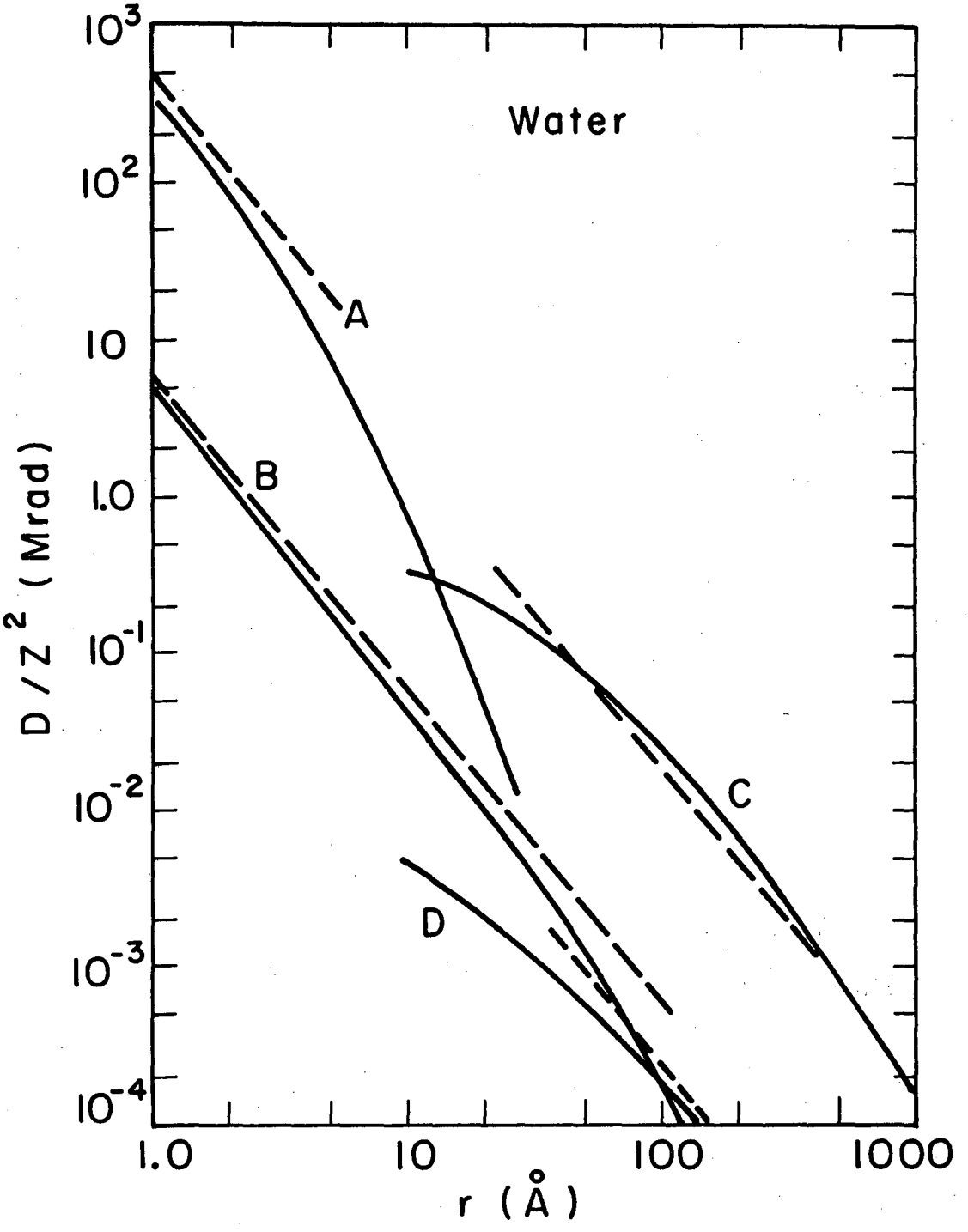

XBL788-1447

Figure VI.2

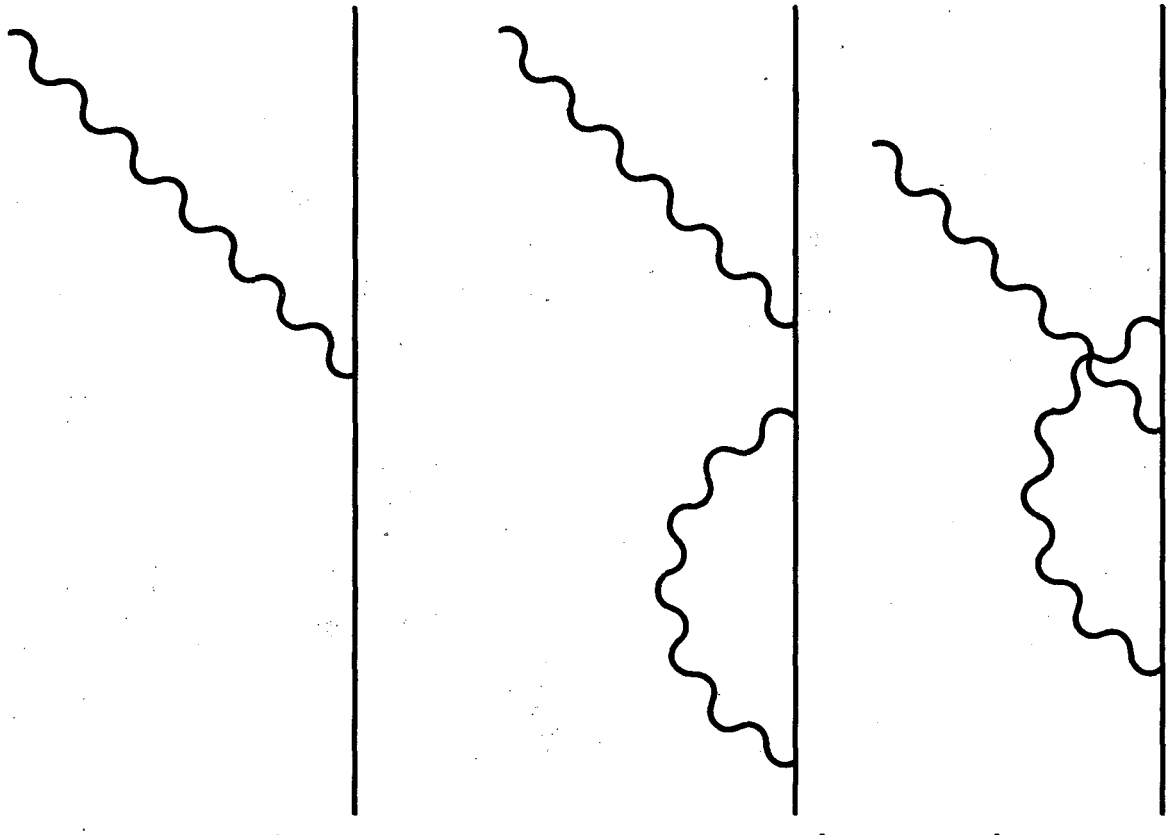

XBL 794-9279

Figure VI.3

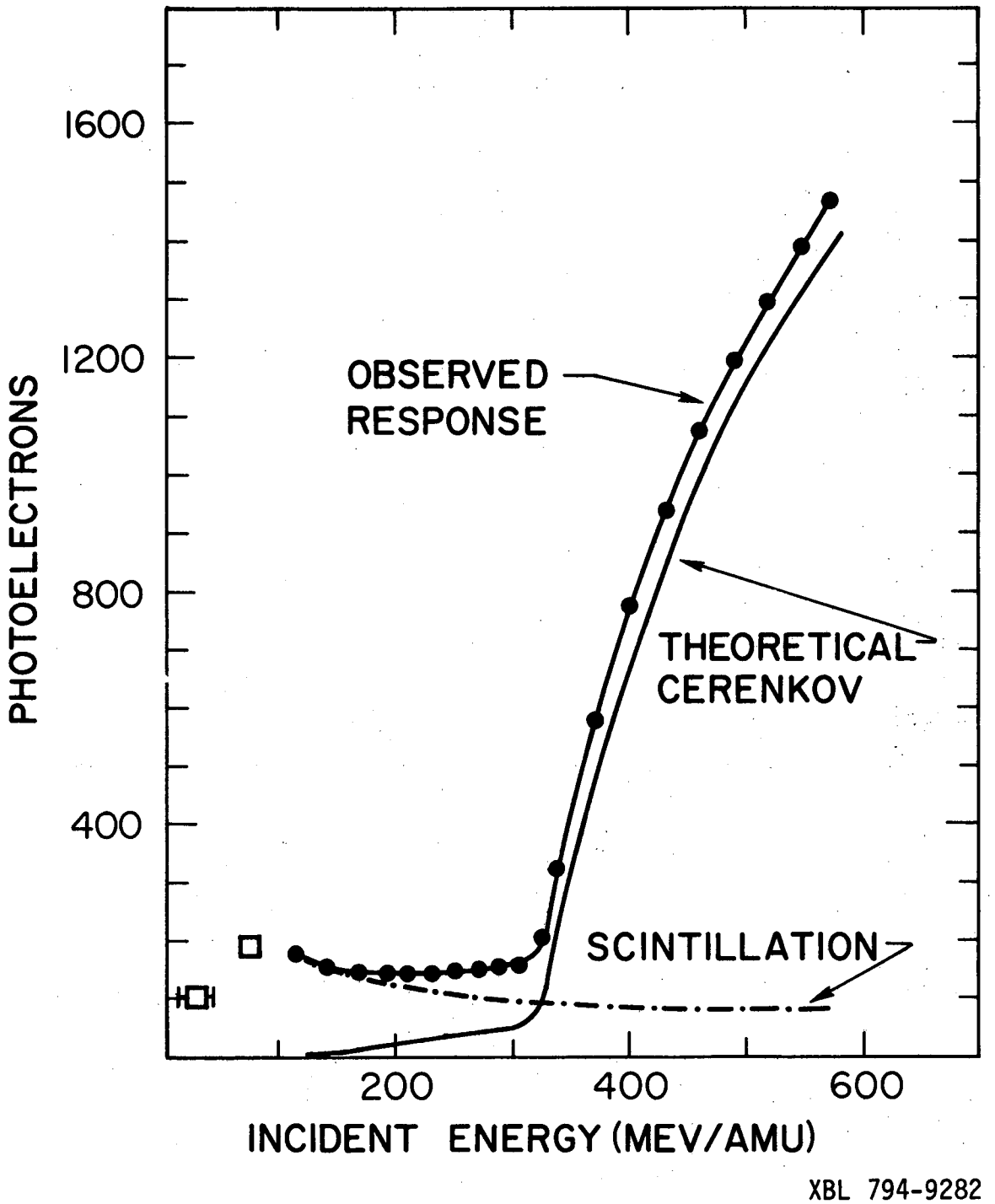
1600
1200
800
400
PHOTOELECTRONS
OBSERVED
RESPONSE
THEORETICAL
CERENKOV
SCINTILLATION
200
400
600
INCIDENT ENERGY (MEV/AMU)
XBL 794-9282

Figure VI.4

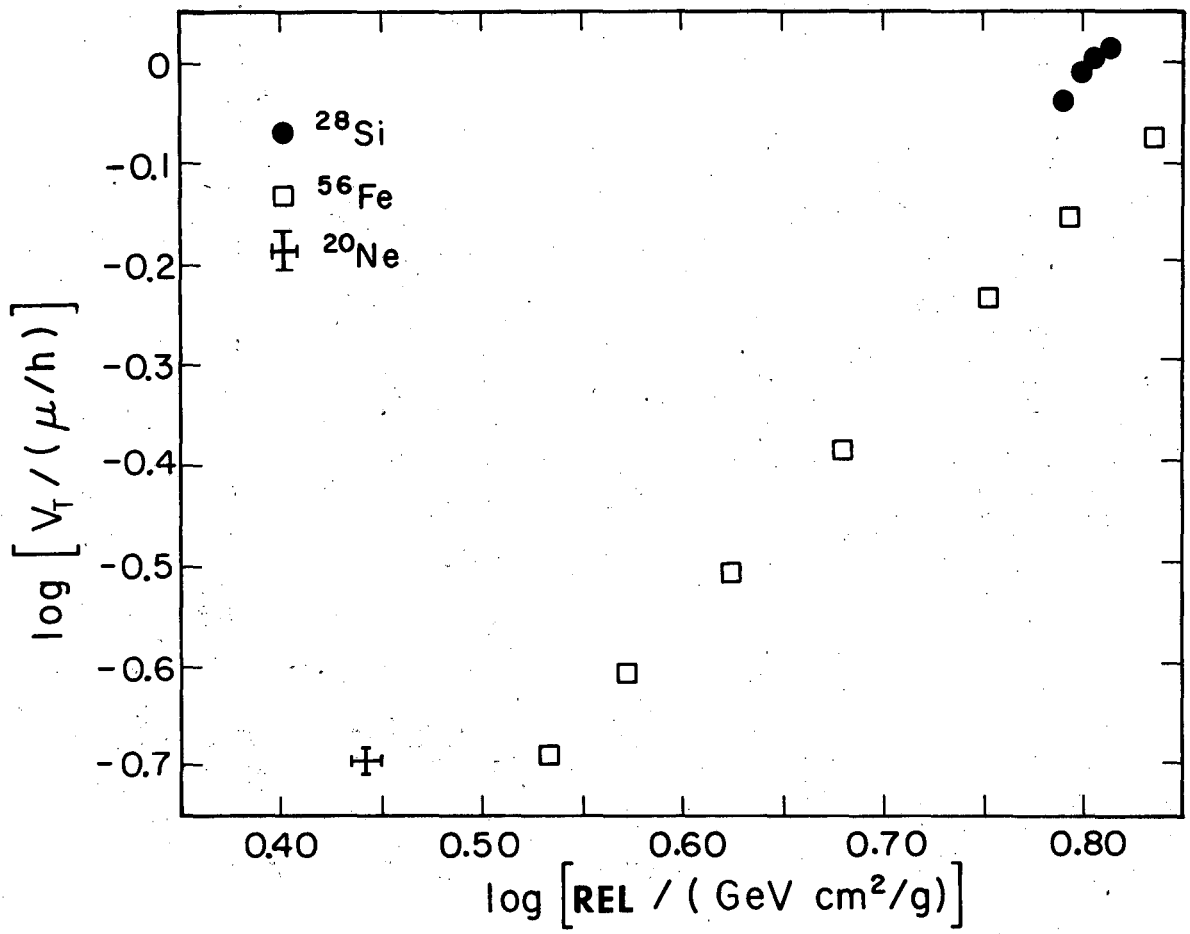
0
-0.1
-0.2
-0.3
-0.4
-0.5
-0.6
-0.7
^{28}Si
^{56}Fe
^{20}Ne
log [V_T / (μ/h)]
0.40
0.50
0.60
0.70
0.80
log [REL / (GeV cm^2/g)]
XBL788-1448

Figure VI.5

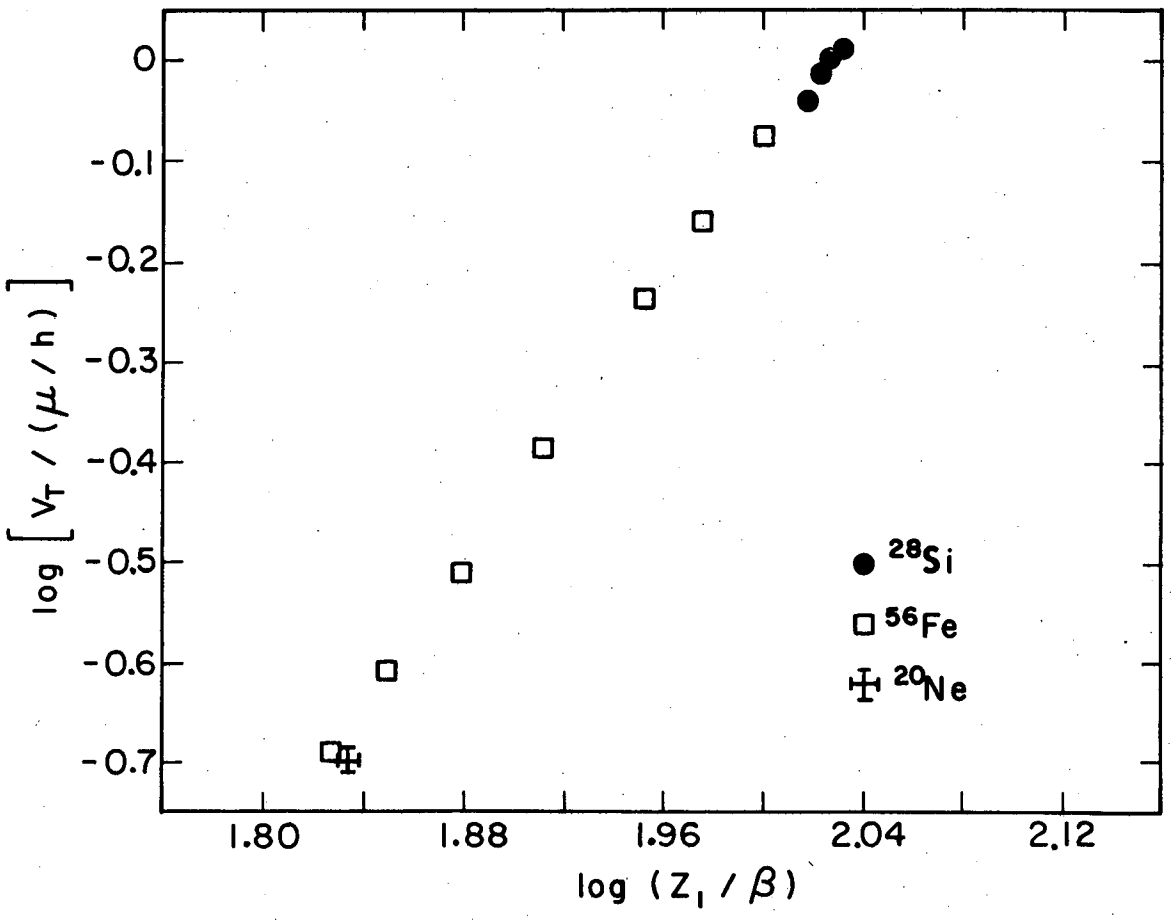

XBL788-1436

Figure VI.6

TECHNICAL INFORMATION DEPARTMENT
LAWRENCE BERKELEY LABORATORY
UNIVERSITY OF CALIFORNIA
BERKELEY, CALIFORNIA 94720